THE ROLE OF MATRIX METALLOPROTEINASES IN INFLUENCING STEM CELL BEHAVIOR AND SKELETAL MUSCLE HEALING

by

Ian Heath Bellayr

B.S. in Biomedical Engineering, University of Virginia, 2005

Submitted to the Graduate Faculty of

Swanson School of Engineering in partial fulfillment

of the requirements for the degree of

Doctor of Philosophy

University of Pittsburgh

2011

UNIVERSITY OF PITTSBURGH

SWANSON SCHOOL OF ENGINEERING

This dissertation was presented

by

Ian Heath Bellayr

It was defended on

June 22nd, 2011

and approved by

Dr. Stephen Strom, PhD, Professor, Department of Pathology

Dr. Partha Roy, PhD, Associate Professor, Department of Bioengineering

Dr. Johnny Huard, PhD, Professor, Department of Orthopaedic Surgery, Molecular Genetics, Biochemistry & Bioengineering

Dr. Sanjeev Shroff, PhD, Professor, Department of Bioengineering

Dissertation Director: Dr. Yong Li, MD, PhD, Assistant Professor, Department of Orthopaedic Surgery, Pathology and Bioengineering

THE ROLE OF MATRIX METALLOPROTEINASES IN INFLUENCING STEM CELL BEHAVIOR AND SKELETAL MUSCLE HEALING

Ian Heath Bellayr, PhD

University of Pittsburgh, 2011

Stem cells are highly valued for their capacity to aid in the functional recovery of damaged or diseased tissue. They are defined by their remarkable ability to maintain their undifferentiated state through countless cycles of cell division and to differentiate into variable types of specialized cells. Since ethical controversy has hindered funding for embryonic stem cell research and induced pluripotent stem cells are in the initial stages of investigations, much research has been conducted using adult stem cells. The use of adult stem cells in clinical applications is gradually becoming a reality; however, the major limitation is the difficulty to isolate, purify and expand them in culture.

Matrix metalloproteinases (MMPs) have been regarded as a group of zinc-endopeptidases that influence tissue remodeling by degrading constituents of the extracellular matrix to actively promote cell proliferation, migration, apoptosis and differentiation. They have been suggested to play important roles in the regeneration of amputated newt limbs by contributing to a population of undifferentiated stem cells, called a blastema, which is likely formed by cell dedifferentiation.

The research presented here builds on previous work investigating the therapeutic use of MMP1. Investigations have demonstrated the ability of MMP1 to aid in the recovery of skeletal muscle tissue by degrading fibrous scar tissue to facilitate cell migration and differentiation. This work examines the potential of MMP1 in skeletal muscle healing to stimulate stem cell behavior by the expression of certain muscle stem cell markers and its impact on cell differentiation. In

addition, stem cells derived from skeletal muscle tissue were investigated to thoroughly elucidate the effect of blocking MMP signaling. MMP inhibition using GM6001 was observed to negatively impact muscle stem cell migration, stem cell associated markers and their differentiation capacity thus indicating the key role of MMPs in muscle stem cell behavior.

TABLE OF CONTENTS

LIST OF TABLES

LIST OF FIGURES

NOMENCLATURE

ADAM, a disintegrin and a metalloproteinase

AEC, apical epithelial cap

ALP, alkaline phosphatase

ANOVA, analysis of variance

ATCC, American Type Culture Collection

bFGF, basic-fibroblast growth factor

BMP, bone morphogenetic protein

CEE, chick embryo extract

CMV, Cytomeyalovirus

CSL, CBF1/Su(H)/LAG1

$CXMD_J$, canine X-linked muscular dystrophy in Japan

DAPI, 4,6'-diamidine-2-phenylindole

DLL, Delta-like

DMEM, Dulbecco's Modified Eagle Medium

ECM, Extracellular Matrix

EDL, extensor digitorum longus

EdU, 5-ethynyl-2'-deoxyuridine

ESC, Embryonic Stem Cells

FBS, fetal bovine serum

Flk1, fetal liver kinase 1

GM, gastrocnemius

HBSS, Hank's balanced salt solution

HS, horse serum

ICC, immunocytochemistry

IGF-1, insulin growth factor 1

IFN-γ, interferon-gamma

iPS, induced Pluripotent Stem (Cell)

IR, Ischemia Reperfusion

JAG, Jagged

kDa, kilodaltons

LTR, long terminal repeats

MDSC, Muscle-Derived Stem Cell

MHC, myosin heavy chain

MMP, Matrix Metalloproteinase

MRL, Murphy-Roth-Large

mRNA, messenger Ribonucleic Acid

MT, Membrane-Type

NCAM, neural cell adhesion marker

Neo^{r}, neomycin resistant

Oct4, Octamer-binding transcription factor 4

OD, optical density

Pax, Paired box protein

PBS, phosphate-buffered saline

PDT, Population Doubling Time

P/S, pencillin/streptomycin

rgn, regeneration (gene)

rpm, rotations per minute

RT-PCR, Reverse Transcriptase – Polymerase Chain Reaction

Sca1, stem cell antigen 1

siRNA, small interfering RNA

TA, tibialis anterior

TBS, Tris-Buffered Saline

TGF-β, Transforming growth factor-beta

TIMP, Tissue Inhibitor of Metalloproteinase

PREFACE

The work presented here has been made possible by grants to Yong Li from the Research Advisory Committee of the Children's Hospital of Pittsburgh of UPMC, the NIH, and the Department of Defense (W81XWH-09-2-0099). The Department of Bioengineering at the University of Pittsburgh has provided me with a great opportunity to work in such an excellent and collaborative research environment. I am fortunate to have conducted my scientific studies under my adviser, Dr. Yong Li. The past three years were very engaging and I have gained valuable insight and learned numerous techniques that will truly benefit me in my future endeavors.

My sincere thanks go to my dissertation advisory committee of Dr. Partha Roy, Dr. Sanjeev Shroff, Dr. Stephen Strom and Dr. Huard for their comments and suggestions to help me develop my skills as a bioengineer. I genuinely appreciate the advice and support they offered during my tenure at the University of Pittsburgh.

Much of my gratitude goes out to the entire Stem Cell Research Center staff, both past and present, who aided me in my studies. I particularly want to acknowledge Michelle Witt, William Chen, Laurie Meszaros, Joe Vella, Dr. Burhan Gharaibeh, Nick Oyster, Jonathan Proto, Jim Cummins and Dr. Bridget Deasy as well as the administrative staff specifically, Michele Keller, Paul Loedding and Matt Bosco for their assistance. I thank them for their help and for

orchestrating several massive moves to relocate the laboratory as well the animal facilities. Their efforts were critical in allowing me to achieve my academic goals.

The work presented here would have not been possible without the members of the Laboratory of Molecular Pathology, Dr. Xiaodong Mu, Haiying Pan, Kiley Murray, Kyle Holden, Dr. Jianqun Ma and Dr. Xiaoping Chen. All of them have had a tremendous impact on my work and my time here at the University of Pittsburgh. Dr. Xiaodong Mu's influence has been instrumental in my development as a scientist with his knowledge of analytical techniques and methods. The first undergraduate student to work with me, Kyle Holden, notably aided in my research pursuits. Instructing him help me improve my teaching skills.

Last, but not least, I am thankful to all the interesting friends I have made while living in Pittsburgh for the past six years, particularly those I met through the Engineering Graduate Student Organization. I also thank my parents and my fiancée, Jennifer, for their boundless support and encouragement.

1.0 INTRODUCTION

1.1 MATRIX METALLOPROTEINASES

Matrix metalloproteinases (MMP) belong to a superfamily of enzymes known as metazincins, which encompass a number of other endopeptidases including serralysins, asatacins, adamalysins, leishmanolysins, snapalysins and pappalysins (Gomis-Ruth 2003; Huxley-Jones, Clarke et al. 2007). Currently, there are 23 known human MMPs, with other species having slightly variable structures, all of which share similar characteristics (e.g. a zinc ion binding site) and are inhibited by tissue inhibitors of metalloproteinases (TIMPs) (Parsons, Watson et al. 1997; Somerville, Oblander et al. 2003; Page-McCaw, Ewald et al. 2007). Furthermore, these enzymes have similar structures, including a signaling peptide, a propetide domain, a catalytic domain, where the zinc ion binding site resides, and a hinge region that binds to the C-terminal hemoplexin domain (Parsons, Watson et al. 1997; Visse and Nagase 2003). The enzymes can be classified by small differences in structure, such as insertions of vitronectin, cysteine array, fibronectin domains, IgG-like domains and distinct types of transmembrane domains or the deletion of hemoplexin domain. Based on their structural elements, MMPs are categorized into several groups: collagenases, gelatinases, matrilysin, membrane-type (MT) MMPs, metalloelastases, stromelysins and other various types (Table 1).

Table 1.1 Various MMPs, their location and source of activation from a pro-form

Enzyme	MMP	Location	Activation
Collagenases	MMP1	Secreted	MMP3
	MMP8	Secreted	MMP3
	MMP13	Secreted	MMP14/TIMP2/MMP3
	MMP18*	Secreted	Unknown
Gelatinases	MMP2	Secreted	MMP14/TIMP2
	MMP9	Secreted	MMP3/MMP13
Matrilysin	MMP7	Secreted	MMP3
	MMP26	Secreted	Unknown
Membrane-Type MMPs	MMP14	Membrane	Furin
	MMP15	Membrane	Furin
	MMP16	Membrane	Furin
	MMP17	Membrane	Furin
	MMP24	Membrane	Furin
	MMP25	Membrane	Furin
Metalloelastase	MMP12	Secreted	Unknown
Stromelysin	MMP3	Secreted	MMP14/TIMP2
	MMP10	Secreted	Unknown
	MMP11	Secreted	Furin
Others	MMP19	Secreted	Unknown
	MMP20	Secreted	Unknown
	MMP21	Secreted	Unknown
	MMP23	Secreted	Furin
	MMP27	Secreted	Unknown
	MMP28	Secreted	Furin
*MMP18 is only found in Xenopus			

A majority of MMPs are secreted in a latent form known as a pro-MMP and can only become active when the bond between the free thiol of the conserved cysteine residue on the propeptide domain and the zinc ion on the catalytic domain is broken or through complete cleavage of the propeptide domain through the use of other MMPs (Caron, Asselin et al. 1999; Ra and Parks 2007). Other MMPs are activated intracellularly by furin before they are secreted or incorporated into the cell membrane.

Despite these differences in their biomolecular structure, all MMPs are known for their involvement in a number of biological tasks. Generally, they participate to a moderate extent in embryogenic development and are almost undetectable in normal adult resting tissues; however, they become clearly activated when perturbed through injury, disease and during pregnancy (Paul, Sharma et al. 2008; Vu, Yun et al. 2008; Yu, Kamada et al. 2008; Akhavani, Madden et al. 2009; Choi, Jung et al. 2009). While some MMPs are known primarily for their ability to

degrade certain components of the extracellular matrix (ECM), they are not solely limited to this physiological task (McCawley and Matrisian 2001; Chromek, Tullus et al. 2003; Parks, Wilson et al. 2004). When stimulated, MMPs interact with various cytokines and chemokines to become engaged in different roles such as cell proliferation, migration, differentiation, apoptosis and angiogenesis (Menon, Singh et al. 2005; Pereira, Strasberg-Rieber et al. 2005; Shan, Morris et al. 2007; McCawley, Wright et al. 2008; Wang, Pan et al. 2009; Yang, Liu et al. 2009; Zeng, Yao et al. 2009). Overall, these processes serve to facilitate tissue or organ regeneration by actively remodeling it when damage occurs.

Complementary to MMPs are four inhibitors known as TIMPs (Table 2), which serve the purpose of inhibiting MMPs, in addition to closely related members of the adamalysin group, a disintegrin and a metalloproteinase (ADAMs) (Baker, Edwards et al. 2002; Jacobsen, Visse et al. 2008; Melendez-Zajgla, Del Pozo et al. 2008).

Table 1.2 Biological MMP Inhibitors

Inhibitor	Expression	Tissue distribution	Location	Specificity/function
TIMP1	Inducible	Wide distribution	Secreted	Inhibits most MMPs well, except MMP14, 15, 16, 19 and 24; ADAM10
TIMP2	Constituted	Wide distribution	Secreted/Cell Membrane	Inhibits most MMPs; ADAM12; activates MMP2, 3 and 13
TIMP3	Inducible	Wide distribution	ECM	Inhibits all MMPs; ADAM10, 12 and 17;
TIMP4	Highly regulated and restricted	Heart, brain, ovary, kidney, testes, fat, pancreas and colon	Secreted/Cell Membrane	Inhibits all MMPs

Like most MMPs, TIMPs are secreted proteins that regulate degradation of ECM constituents and tissue remodeling through interaction with MMPs. They can limit the extent of MMP participation in the regenerative process by restricting cellular function such as proliferation and migration (Stetler-Stevenson 2008). The typical shape of TIMPs is wedge-like, containing both

an N- and C-terminal domains with a molecular weight ranging from 21-29 kDa (Parsons, Watson et al. 1997; Visse and Nagase 2003). Both terminals consist of six conserved cysteine residues forming three disulfide bonds, however, only the N terminal is responsible for inhibiting MMP activity (Visse and Nagase 2003; Stetler-Stevenson 2008).

1.2 REGENERATION

It is commonly known that, for adult mammals, amputated limbs do not grow back. Adult amphibians, such as newts and salamanders, however, can regenerate fully functional arms and legs over the course of 70 days, a process in which MMPs play a vital role (Brockes 1997; Yokoyama 2008). Regeneration of amputated has been documented in some higher-order mammals during the embryonic and neonatal stages, although this phenomena was only possible when the amputation was restricted to the phalangeal bones (Han, Yang et al. 2008). On other occasions, fingertip regeneration has been observed in children and, if managed properly, could restore the finger's contour, fingerprint and function with minimal scarring, while impairing the full lengthening of the amputated digit (Vidal and Dickson 1993; Alagoz, Uysal et al. 2006). The unique ability of amphibians to regenerate whole limbs demonstrates a greater capacity for regeneration and healing when compared with the wound healing in mammals.

The events that follow immediately after injury are comparable between mammals and amphibians, despite their differences in regenerative ability. The process of wound healing in mammals and regeneration in amphibians use MMPs to guide the remodeling of damaged tissue. The first stage of mammalian wound healing initiated after incidental epithelial damage is inflammation (Shen, Li et al. 2008). During this period, cytokines and growth factors are

released by a combination of cells including platelets, macrophages and neutrophils, as well as epithelial cells and stromal cells (Gill and Parks 2008; Yokoyama 2008). At the same time, MMPs are synthesized by many similar cell types to promote leukocyte migration as well as degradation collagen in close proximity to the damaged site. In the days following inflammation, MMPs play a more active part in re-epithelialization of the wound (Campbell and Crews 2008). By degrading the ECM surrounding the wounded area, they stimulate migration of the cells encompassing the injured region. Upon arrival, these cells proliferate and work in conjunction to direct differentiation and angiogenesis to prevent further fluid loss or bacterial infection by closing the ruptured tissue barrier. In the final stages of wound healing, collagen synthesis is observed. For very severe injuries, excessive collagen synthesis occurs due to the overproduction of transforming growth factor (TGF)-β at the latter stages of healing, which invariably restricts the functional recovery of the tissue (Li, Foster et al. 2004).

In contrast, regeneration for amphibians follows a different course, yet MMP activity is still present. Almost instantly after injuries occur in newts, MMP activity becomes highly elevated in order to rapidly produce an apical epithelial cap (AEC) to cover the wound, minimize additional tissue damage, contamination or inflammatory response (Miyazaki, Uchiyama et al. 1996; Yokoyama 2008). Following AEC formation, peripheral cells at the amputation site undergo dedifferentiation, whereby they are converted into a multipotent state (Satoh, Bryant et al. 2008). This phenomenon results in the formation of a blastema from migrated fibroblasts. Several MMPs have been identified with blastema formation and limb regeneration in newts. One study found sequence homology between MMPs, MMP3/10a and MMP3/10b, expressed in newts and humans only for regenerating limbs and not in healthy resting tissue (Miyazaki, Uchiyama et al. 1996). Both MMPs aided in tissue remodeling by digesting gelatin, casein and

collagen I and IV. Other studies provided evidence that MMP9 contributed to limb regeneration by digesting similar constituents of the ECM to aid in removing damage cartilage tissue (Yang, Gardiner et al. 1999; Vinarsky, Atkinson et al. 2005). MMP3/10a, MMP3/10b and MMP9 were notably upregulated immediately following limb amputation in newts and remained elevated up to 20 days. Furthermore, the administration of an MMP inhibitor, GM6001, demonstrated severely dwarfed and dysfunctional limbs or regeneration impeded at an early stage, resulting in a stump covered by uncharacteristic acellular scar-like tissue.

Under normal circumstances, once the blastema is generated, it continues to grow distally, producing an entire limb, remarkably even when it is grafted to different locations of the body (Crawford and Stocum 1988). Axolotls and newts are not the only creatures known to form a blastema after tissue trauma. Blastema formation in response to MMPs has been identified in several other species including *Drosophila*, mouse and zebrafish (Gourevitch, Clark et al. 2003; Bai, Thummel et al. 2005; McClure, Sustar et al. 2008). In *Drosophila*, two genes, the regeneration (rgn) gene and MMP1 gene, were found to actively take part in leg disc regeneration, but not development. It is believed that both genes become activated in the blastema by wingless signaling and that mutations directed toward rgn or MMP1 will affect the formation of a blastema. Likewise, Murphy-Roth-Large (MRL) mice, which have a greater capacity for regeneration, demonstrated regrowth of lost cartilage and complete closure of through-and-through ear hole punches, with no scar formation in comparison to normal adult mice (Fitzgerald, Rich et al. 2008). Consequently, MRL mice have a greater MMP to TIMP ratio of MMP2 and MMP9 for the purpose of breaking down the ECM and basement membrane prior to blastema formation, while normal B6 mice never display blastema formation (Gourevitch, Clark et al. 2003). Zebrafish expressed MMP2, in addition to MMP14 and TIMP2, during the

formation of the blastema as with MRL mice (Bai, Thummel et al. 2005). Additionally, GM6001 was found to produce a negative effect on blastema formation, thus inhibiting caudal fin regeneration. MMP2 may play a specific role in the regeneration of connective tissue, as confirmed through studies of MRL mice and zebrafish.

1.3 ROLE OF MMPS IN SKELETAL MUSCLE TISSUE

Muscle injuries can occur by a number of ways such as lacerations, strains, ischemia, or neurological dysfunctions. After years of research, a timeline for muscle recovery has been defined in three stages for mammals: muscle degeneration and inflammation; regeneration and scar tissue formation (Huard, Li et al. 2002). The main limitation of muscle regeneration is the period of fibrosis, occurring between the second and third week after the muscle injury (Huard, Li et al. 2002; Nozaki, Li et al. 2008). As previously mentioned, increased TGF-β1 production will trigger secretion of collagen type I and III by myofibroblasts, generating fibrotic scar tissue (Li, Foster et al. 2004; Chan, Li et al. 2005; Alexakis, Partridge et al. 2007). The administration of several remedies, such as basic-fibroblast growth factor (bFGF), insulin growth factor type 1 (IGF-1), suramin, decorin, interferon (IFN)-γ and angiotensin II receptor blocker were used to successfully improve muscle healing by either promoting myoblast proliferation or blocking TGF-β1 expression (Huard, Li et al. 2002; Foster, Li et al. 2003; Sato, Li et al. 2003; Li, Foster et al. 2004; Chan, Li et al. 2005; Alexakis, Partridge et al. 2007; Li, Li et al. 2007; Bedair, Karthikeyan et al. 2008; Nozaki, Li et al. 2008). Unfortunately, these treatments of stimulating myoblast proliferation/migration by inhibiting TGF-β1 are ineffective in regenerating muscle

with pre-existing fibrotic tissue (Huard, Li et al. 2002; Li, Foster et al. 2004; Wang, Pan et al. 2009).

To resolve this dilemma, researchers have begun examining MMPs as a prospect for muscle regeneration. Recent studies performed *in vitro* and *in vivo* have shown the beneficial impact of MMP1 administration on muscle healing (Bedair, Liu et al. 2007; Kaar, Li et al. 2008; Wang, Pan et al. 2009). In vitro experiments illustrated cellular increases in mobility by increased expression of four migration proteins, N-cadherin, β-catenin, pre-MMP2 and TIMP1. Differentiation into myotubes was greater for cells treated with MMP1 compared with nontreated cells based on quantity and the increased expression of myogenin, a checkpoint protein involved in myofiber formation (Wang, Pan et al. 2009). *In vivo* evidence showed that direct injection of C2C12 myoblasts in combination with MMP1 improved cell migration and increased myofiber differentiation from the point of injection in both gastrocnemius (GM) and tibialis anterior (TA) muscle of mice with muscular dystrophy. Furthermore, the injection of MMP1 alone to a site of injury created in mice, improved muscle healing by reducing fibrotic tissue and increasing myofiber formation (Bedair, Liu et al. 2007). Alternative studies have suggested the importance of MMPs in skeletal muscle cell migration. Using two MMP inhibitors at moderate concentrations, MMP inhibitor II (inhibits MMP1, MMP3, MMP7 and MMP9; from Calbiochem) and GM6001 (inhibits MMP1, MMP2, MMP3, MMP8 and MMP9), suppressed C2C12 cell migration (Nishimura, Nakamura et al. 2008). Another experiment used siRNA to specifically target MMP3 because of its importance in activating pro-MMP1, MMP7, MMP8 and MMP9. By inhibiting MMP3, additional MMPs related to cell migration could not become activated, thus impairing the expression of other cell migratory proteins.

Other MMPs explored for their involvement in muscle regeneration are the gelatinases MMP2 and MMP9. The regulation of these two proteins has had a profound impact in the status of MDX mice, an X-linked genetic disease where muscles lack the dystrophin gene, causing an increased rate of degeneration (Sicinski, Geng et al. 1989). In a study using MDX mice (which serves as a model for Duchenne muscle dystrophy in humans), scientists administered L-arginine to decrease the expression of MMP2 and MMP9, which in turn destabilized satellite cell adhesion and myoblast fusion (Hnia, Gayraud et al. 2008). Their principle result was that both MMPs work conjointly to maintain the integrity of the muscle membrane while L-arginine reduces inflammation. A similar study determined that elevated MMP9 activity mutually increases the number of stem cell antigen (Sca)-1 positive cells (a stem cell marker for muscle derived stem cells (MDSCs) or muscle satellite cells) to favor cell migration and activation of myogenic precursors (Bani, Lagrota-Candido et al. 2008). An increase in MMP2, on the other hand, corresponded to an increase in the number of neural cell-adhesion molecule (NCAM)-positive cells aiding in regeneration. However, confounding results indicate that their activity may be linked to persistent inflammation and membrane fragility in spite of their regenerative myofiber capacity. Another team of investigators examined the variable expression of MMP2 and MMP9 in two different muscle types. In Soleus, slow-twitch muscle, MMP9 was upregulated for 14 days post-injury, compared with 7 days in extensor digitorum longus (EDL), fast-twitch muscle (Zimowska, Brzoska et al. 2008). MMP2 activity was higher for the EDL muscle than for the Soleus muscle and may be responsible for ECM remodeling during the reconstruction phase, by preventing accumulation of ECM components. The extensive fibrosis resulting in the Soleus muscle could be contributed to insufficient degradation of ECM components. Furthermore MMP2 was found to play a crucial role in cell fusion, whereas MMP9

was involved in all stages of myoblast differentiation (including an active part in cell proliferation). These researchers concluded that the differences in the activity of both MMPs modifying myoblast migration and fusion are the root of the difference in the regenerative response of the two muscle types.

Additional studies have confirmed the role of MMP9 in muscle cell differentiation and MMP2 in myoblast elongation/fusion, working in conjunction to remodel the ECM (Ohtake, Tojo et al. 2006; Fukushima, Nakamura et al. 2007). In a study using canine X-linked muscular dystrophy in Japan ($CXMD_J$), increases in MMP2, MMP9 and MMP14, and TIMP1 and TIMP2 expression were found in comparison to normal wild-type canines. Increased MMP9 expression was found to correspond with degradation of the basal lamina in necrotic tissue of $CXMD_J$ and the promotion of inflammatory cell migration to the site of interest. Following the process of muscle healing, muscle fibers were regenerated based on the expression of MMP2 (Fukushima, Nakamura et al. 2007). The researchers hinted that TIMP1 upregulation most likely followed peak MMP9 levels, while TIMP2 and MMP14 expression might be involved with MMP2 as they are known activators of pro-MMP2. Although some of the results are speculative, they suggested that additional experiments using cardiotoxin injury could clarify whether TIMP1 and 2 activity is dependent on the stage of muscle healing. Another investigation evinced a more defined function of MMP14 in muscle tissue by coming to several conclusions. First, MMP14 serves as a checkpoint for the three stages of morphological differentiation (proliferation, elongation and fusion) and also engages in degrading fibronectin (Ohtake, Tojo et al. 2006). Myotube formation decreased when MMP14 activity was blocked using hairpin RNA and upon observation in MMP14-deficient mice. Inhibiting MMP14 during the proliferative and elongation stages of skeletal muscle development prevents proper activation of MMP2, which in turn blocks myotube

fusion. Furthermore, while TIMP2 has been known to work in combination with MMP14 to activate MMP2, an overexpression of TIMP2 and 1 will have a distinct inhibitory effect on MMP14 and drastically reduce myotube formation (Ohtake, Tojo et al. 2006). These findings demonstrate that the absence of MMP14 causes fibronectin to act as a negative regulator of myogenic differentiation. As fibronectin is degraded during the elongation phase of skeletal muscle development by MMP14, myotube formation will continue with the aid of MMP2. The elevated expression of MMP9, as well as MMP3, by over expressing osteoactivin in skeletal muscle cells was observed to repress denervation-mediated fibrosis (Furochi, Tamura et al. 2007).

1.4 STEM CELLS

Three types of stem cells, embryonic, adult and induced pluripotent (iPS) stem cells are currently under multiple investigations in scientific research. With the potential of these cells to be used in cell therapy to treat debilitating diseases or repair devastating wounds, scientists are challenged with determining which of the three different stem cell types will produce the best outcome for a particular disorder. All three cell types match the classical definitions of a stem cell; that is (1) they can maintain their undifferentiated state through multiple cycles of cell division/proliferation and (2) they are capable of differentiating into various types of specialized cells (Thomson, Itskovitz-Eldor et al. 1998; Pittenger, Mackay et al. 1999; Takahashi and Yamanaka 2006). Fundamentally, the traits and behaviors that distinguish each of the three stem cell types will help researchers choose an appropriate cell for a specific treatment. What separates an embryonic stem cell (ESC) from adult stem cells or iPS cells is their origin. ESCs

are the result of cells harvested from the inner mast cells of a blastocyst, an early-stage embryo, after 5 to 7 days in culture (Stojkovic, Lako et al. 2004). ESCs are defined as pluripotent because they differentiate into all three germ layers: endoderm, ectoderm, and mesoderm. Under defined cell culture conditions with certain growth factors, ESCs can remain pluripotent almost indefinitely. What makes using ESC controversial is their ability to generate human life. Of course, many individuals believe it is wrong to destroy life at any stage of development. Some even fear studies with ESCs will lead to human cloning and embryo farms.

Adult stem cells avoid this ethical dispute, and studies have demonstrated a comparable effectiveness as ESCs. Adult stem cells, unlike ESCs, can be derived from various tissues, such as bone marrow, adipose tissue, and skeletal muscle (Pittenger, Mackay et al. 1999; Huard, Yokoyama et al. 2002; Zuk, Zhu et al. 2002). These cells are considered multipotent because they are capable of giving rise to a number of specialized tissues, including osteogenic, chondrogenic, adipogenic, myogenic, and neurogenic, yet have a reduced ability to differentiate compared to pluripotent cells (ESCs).

The third and newest stem cell option is iPS cells, which are observed to be as pluripotent as ESCs and evade some ethical dispute. Originally, the two approaches used to generate pluripotent adult cells were performed by either directly transferring the nuclear contents of an adult cell into an oocyte or by fusion with an ESC (Cowan, Atienza et al. 2005; Sung, Gao et al. 2006). Then in 2006, Dr. Yamanaka's research team in Japan manufactured adult pluripotent stem cells by transfecting both mouse and human somatic fibroblasts with four embryonic transcription factors: Oct ¾, Sox2, c-Myc, and Klf4 (Takahashi and Yamanaka 2006; Takahashi, Tanabe et al. 2007). Other researchers speculated that transcriptional factors Nanog and Lin28 may play a role in creating iPS cells (Yu, Vodyanik et al. 2007). These iPS cells were

indistinguishable from ESCs based on morphology, gene expression, and even teratoma formation.

Scientific investigators have yet to identify which of the three cells types best suits treatment for wound repair and genetic disorders. At first glance, ESCs appear as the optimal cell therapy for humanity's ailments based on the unique ability to generate every cell type. However, ESCs proved to have negative impacts on health such that transplantation studies revealed the formation of teratomas through uncontrollable differentiation and immunorejection. The discovery of adult stem cell and iPS cells minimized the problem of immune rejection because these cells were acceptable for autologous transplantation. Some researchers, even preferred adult stem cells on the basis of multiple tissue sources for harvesting, which provided several approaches to treat a disease or injury. While animal studies have indicated improvement in patients' health, none demonstrated complete functional recovery of the tissue/organ. A reduced differentiation capacity is not the only limitation of adult stem cells. Some studies have demonstrated erroneous differentiation such as inadequate differentiation of mesenchymal stem cells or the unwanted differentiation of MDSCs into fibrotic cells because of stimuli in the local environment (Li and Huard 2002; Kim, Kim et al. 2008). These factors have contributed to some hesitation in choosing ESCs or adult stem cells as treatment in clinical trials.

In this regard, the creation of iPS cells has been acknowledged as a popular alternative. Cells isolated from a patient can be manipulated to generate iPS cells, which avoid the risk of immune rejection. Because they have a differentiation capability similar to that of ESCs through gene transfer of 4 prime genes (Oct ¾, Sox2, c-Myc, and Klf4), they have also been deemed a potentially useful option for certain treatments. The major drawback of iPS cells is the genome-integrating viruses used to transfect cells, which could cause undesirable effects from improperly

removing harmful viral DNA or disrupting other vital genes in the genome. Other limitations of iPS cells were low efficiency of reprogramming a small population of human primary cells and the formation for teratomas from *in vivo* transplantation by the activation of the c-Myc retrovirus. To resolve the apparent disadvantage of viral integration, researchers have explored several other methods of manufacturing iPS cells. One group tested non-integrating adenoviruses transiently expressing Oct4, Sox2, c-Myc, and Klf4 on mouse fibroblasts and liver cells, while Yamanaka's team tested repeated transfection of two expression plasmids (one with Oct ¾, Sox2, and Klf4 cDNA and the other with c-Myc cDNA) in mouse embryonic fibroblasts (Okita, Nakagawa et al. 2008; Stadtfeld, Nagaya et al. 2008). Different investigators have suggested that iPS cells could be generated with a reduced number of vectors, such as without c-Myc or even Klf4, which are known oncogenes (Huangfu, Osafune et al. 2008; Nakagawa, Koyanagi et al. 2008). Regrettably, removing factors for cell reprogramming has lowered the efficiency with which these genes combine with the host cell; however, with the help of small molecular compounds, valproic acid or BIX01294 and BahK864 used together, reprogramming efficiency has been improved (Huangfu, Osafune et al. 2008; Shi, Desponts et al. 2008). Despite the advances made with iPS cells, questions still remain as to whether there are any differences between iPS cells created from different adult tissue and how similar they are to ESCs.

1.5 MUSCLE DERIVED STEM CELLS

Stem cells isolated from skeletal muscle tissue have been investigated for their impressive multi-lineage differentiation capacity and self-renewal ability (Deasy, Gharaibeh et al. 2005). These cells were isolated from muscle tissue using a modified preplate technique by enzymatic

dissociation from a muscle biopsy and divided into six populations based on adhesion characteristics in collagen coated flasks (Qu-Petersen, Deasy et al. 2002; Gharaibeh, Lu et al. 2008). Later preplates are regarded as MDSCs and are identified by flow cytometry for their expression of stem cell antigen (Sca) 1, CD34, fetal liver kinase 1 (Flk1) and measurable amounts of desmin, but they do not exhibit expression of c-kit or CD45 (Lee, Qu-Petersen et al. 2000; Jankowski, Haluszczak et al. 2001; Deasy, Gharaibeh et al. 2005).

Experimental studies have demonstrated their multipotency where they have been observed to differentiate into cells belonging to all three germ layers. These investigations have revealed positive cell differentiation results when MDSCs were exposed to osteogenic, chondrogenic and adipogenic differentiation assays (Lee, Qu-Petersen et al. 2000; Wright, Peng et al. 2002; Cao, Zheng et al. 2003; Kuroda, Usas et al. 2006). Other studies have demonstrated MDSC differentiation along the ectoderm cell lineages by expressing markers of neuron and glial cells, and even differentiation into the endoderm lineage such as urinary bladder cells and hepatocyte-like cells (Romero-Ramos, Vourc'h et al. 2002; Deasy, Li et al. 2004; Lavasani, Lu et al. 2006; Smaldone and Chancellor 2008; Bellayr, Gharaibeh et al. 2010). The non-invasive isolation procedure and easy accessibility have made these MDSCs advantageous for self-autologous cell transplantation therapies.

1.6 PROJECT OBJECTIVES

My hypothesis for this project is that MMP1 stimulation has the ability to influence stem cell behavior of terminally differentiated cells, while MMP inhibition of stem cells derived from skeletal muscle tissue will negatively impact their stem cell behavior.

1.6.1 Objective #1: Assess the ability of MMP1 to actively promote MDSC behavior.

MMP1 has demonstrated is unique ability to aid in the repair of skeletal muscle tissue by degrading collagens I and III during tissue remodeling. In addition, MMP1 has also been observed to aid skeletal muscle tissue remodeling by directly promoting increased myoblast migration and myogenic differentiation capacity. Several techniques were used to explore the influence of MMP1 administration using different incubation periods and concentrations on the expression of cell markers related to MDSCs at both gene and protein level for primary mouse myoblasts. Stem cell differentiation assays were also employed to assess the affect of MMP1 administration on their ability to undergo multiple differentiation.

1.6.2 Objective #2: Examine whether MMP inhibition negatively impacts adult muscle stem cell behavior.

MDSCs have an incredible ability to regenerate injured or diseased skeletal muscle tissue. Existing literature has indicated the long term capacity for proliferation of MDSCs and their multipotency as the basis for aiding in the repair of skeletal muscle tissue. For this objective, MMP expression was inhibited using GM6001, a broad spectrum MMP inhibitor. GM6001 was administered to MDSCs for different time periods and dosages in several experiments to observe the effects on cell proliferation and migration. In addition, the stem cell characteristics were explored for MDSCs by examining the stem cell marker expression and their multipotency in *in vitro* and *in vivo*.

2.0 MMP1 INFLUENCES STEM CELL BEHAVIOR

2.1 INTRODUCTION

Stem cells are highly regarded for possessing an incredible ability to aid in tissue regeneration, whether they embryonic, adult or iPS cells. Each of these cell types are known for their impressive capacity to maintain their undifferentiated state through numerous cycles of cell division and their characteristic multiple differentiation into a diversified number of specialized cells (Thomson, Itskovitz-Eldor et al. 1998; Takahashi, Tanabe et al. 2007; Marongiu, Gramignoli et al. 2010). While ESCs hold much of the spotlight in the stem cell field with their remarkable totipotent behavior, ultimately adult stem cells are the front runners in stem cell research. Adult stem cells are advantageous for their multiple tissue sources for isolation and their minimal risk with immune rejection for autologous transplantation (Li, Pan et al. 2010; Miki, Marongiu et al. 2010; Rui, Lui et al. 2010; Scott, Nguyen et al. 2011). Despite the substantial amount of literature produced on adult stem cells, they are still limited by their difficulty to isolate, purify and expand in culture (Peister, Mellad et al. 2004). iPS cells have remedied this limitation, where the isolation of terminally differentiated cells that proliferate well in culture are administered several mixture of genes (typically Oct ¾, Sox2, c-Myc and Klf4) using a viral vector (Takahashi, Tanabe et al. 2007). However, one constraint in the therapeutic use of iPS cells is the genome-integrating virus which could cause unwanted harmful effects.

Instead, a more natural method of inducing terminally differentiated cells to exhibit stem cell characteristics would be preferable.

Known as a group of zinc-endopeptidases, MMPs, have garnished much influential support in tissue remodeling through extracellular degradation as well as cell-cell and cell-matrix signaling events (Page-McCaw, Ewald et al. 2007; Ra and Parks 2007). The interactions between MMPs and different cell types have been observed to regulate events such as cell proliferation, death, motility and differentiation. MMPs, in particular, have been suggested to play a crucial role in the regeneration of severed newt limbs whereby they contribute to cell dedifferentiation in the formation of a blastema (Miyazaki, Uchiyama et al. 1996; Vinarsky, Atkinson et al. 2005; Yokoyama 2008). This phenomenon of MMPs influencing blastema formation has also been observed in the other organisms including the Drosophila, zebrafish and MRL mice (Gourevitch, Clark et al. 2003; Bai, Thummel et al. 2005; McClure, Sustar et al. 2008).

One notable MMP is the collagenase MMP1, which is synthesized as a single polypeptide and is known for its ability to degrade collagens I and III (Pardo and Selman 2005). Several animal studies have demonstrated the benefits of administering MMP1 during injuries to improve tissue regeneration by degrading scar tissue (Iimuro, Nishio et al. 2003; Bedair, Liu et al. 2007; Kaar, Li et al. 2008). Furthermore, data have indicated the benefits of MMP1 *in vivo*, by its effects on increase cell migration and myogenic differentiation of myoblasts (Wang, Pan et al. 2009). In this set of experiments, MMP1 was administered to primary mouse myoblasts and markers associated with MDSCS were evaluated. In addition, the effect of MMP1 administration on cell differentiation assays was investigated. The data presented here indicates that MMP1 stimulates stem cell behavior in terminally differentiated myoblasts.

2.2 METHODS

2.2.1 Isolation and Culture of Primary Mouse Myoblasts

Primary mouse myoblasts were isolated from the GM muscle of three-week old C57BL/10J mice using a modified preplate technique (Gharaibeh, Lu et al. 2008; Li, Pan et al. 2010). A detailed description of this method can be found in the Appendix A. These cells were cultured in proliferation media containing phenol red Dulbecco's modified Eagle medium (DMEM, Gibco) supplemented with 10% fetal bovine serum (FBS, Gibco), 10% horse serum (HS, Gibco), 1 % penicillin/streptomycin (P/S, Gibco), and 0.5% chick embryo extract (CEE, Accurate Chemical) at 5% CO_2 and 37^{o}C.

2.2.2 Immunocytochemistry (ICC)

After MMP1 stimulation, primary mouse myoblasts were fixed in 4% formalin for 5 minutes at room temperature with HS used to block unspecific binding for 1 hour. Primary antibodies (Ab) (Sca1 [1:200, BD Pharmingen], CD34 [1:200, BD Pharmingen], desmin [1:200, Sigma], and Oct4 [1:300, Abcam]) were prepared in PBS with 2% HS overnight at 4^{o}C. Cells were incubated with secondary antibodies (Alexa Fluor 488 anti-rabbit Ab [1:350, Invitrogen], Alexa Fluor 594 anti-rat Ab [1:350, Invitrogen]) the following day for 1 hour at room temperature. 4',6-diamindine-2-phenylindole (DAPI) was diluted in PBS (100 ng/mL) and administered for 5 minutes. Between each step, the primary mouse myoblasts were washed with PBS. Alls cells were visualized using a Leica DM IRB fluorescent microscope.

2.2.3 RT-PCR

Primary mouse myoblasts were treated with either 100 ng/mL of MMP1 (Aldevron, LLC) for 0, 3, 6, 12, 18, and 24 hours or received a 10 fold increase dose (0-100 ng/mL) of MMP1 for 6 and 18 hours prior to total RNA isolation using the RNeasy plus mini kit (Qiagen). Complimentary DNA was generated using the iScript cDNA Synthesis Kit (Bio-Rad) as per the manufacturer's instructions. Polymerase chain reaction (PCR) amplifications were performed using specific sense and anti-sense primers for RT-PCR as shown in Appendix B. The cycling parameter used for all primers were as follows: 94^{o}C for 5 minutes; PCR for 30 cycles of: denature for 45 seconds at 95^{o}C, anneal for 30 seconds (53^{o}C – 56^{o}C) and extend for 45 seconds at 72^{o}C. RT-PCR was performed using a Bio-Rad MyiQ thermal cycler.

2.2.4 Western Blot

Primary mouse myoblasts stimulated with 10-fold increases in MMP1 from 0-100 ng/mL for 18 hours were washed twice with PBS and then lysed using cell lysis buffer (95% Laemmli sample buffer [Bio-Rad] and 5% 2-Mercaptoethanol [Sigma]). After 5 minutes in the lysis buffer, the cells are scraped off the flask and transferred to an eppendorf tube where they are centrifuged at 3500 rpm for 5 minutes and the supernatant collected. Equal amounts of the protein extracts were fractioned on 10% or 12% sodium dodecyl sulfate-polyacrimide gels (depending on the protein size) and electroblotted onto transfer paper (Amersham Hybond^{TM}-P). The membranes were incubated in blocking buffer consisting of 5% milk powder in TBS/Tween (0.5% Tween) for 1 hour at room temperature. Primary antibodies (β-actin [1:1000, Sigma], Sca1 [1:500, BD Biosciences], Paired box protein (Pax) 7 [1:1000, DHSB], MMP1 [1:1000, abcam]) were

administered to transfer blots in TBS/Tween overnight at 4^{o}C. Secondary antibodies (anti-rabbit IgG horse-radish peroxidase-linked [1:10000], anti-rat IgG streptavidin [1:4000]) were administered in TBS/Tween at room temperature for 1 hour. If necessary, a third Ab was used (biotin horse-radish peroxidase [1:5000]). The signals on the transfer blots were detected using SuperSignal® West Pico Chemiluminescent Substrate (Pierce).

2.2.5 Primary Mouse Myoblast Proliferation Kinetics

A live cell automated imager captured images of the number of primary mouse myoblasts per field of view at 20 minute intervals for 3 days. The population doubling time (PDT) as represented in the exponential equation $N_i = N_o 2^{(t_i/PDT)}$, was calculated by fitting an exponential trendline to several measurements of N over the 3 day period. The exponential regression method provides a fitted curve in the form of $N_i = N_o e^{kt_i}$, where k = ln2/PDT and PDT = ln2/k (Deasy, Gharaibeh et al. 2005). The Click-iT 5-ethynyl-2'-deoxyuridine (EdU) imaging kit (Invitrogen) was used to evaluate the cell proliferation as per the manufacturer's instructions. Briefly, primary mouse myoblasts were seeded on a 12 multiwell collagen coated plate at 5 x 10^3 cells and grown in proliferation media containing 0.1% EdU. After 12 hours in culture, the cells were fixed and a species specific secondary antibody Alexa Fluor 594 (Invitrogen, 1:400) was used for EdU detection. Hoechst 33342 (Invitrogen) was used as a counter stain to visualize the cell nuclei at a 1:2000 dilution.

2.2.6 Osteogenic Differentiation

Osteogenic differentiation was performed as previously described (Zheng, Cao et al. 2006). Myoblasts were plated in a multiwell dish (3.0×10^3 cells per cm^2) and allowed to attach to the dish for 24 hours. Prior to osteogenic induction, cells were treated with 50 ng/mL of MMP1 in DMEM for 6 and 24 hours. After treatment, cells were cultured in osteogenic differentiation media (DMEM supplemented with β-glycerolephosphate (10mM, Sigma), dexamethasone (0.1 μM, Sigma), ascorbate-2-phosphate (50 μM, Sigma), bone morphogenetic protein (BMP)-4 (100 ng/mL, R&D Systems), 10% FBS and 1% P/S). One group of myoblasts was treated continuously with 25 μM of GM6001 for the duration of osteogenic induction. The medium was changed every 2 days and osteogenesis was assessed by observing alkaline phosphatase (ALP) activity 5 and 7 days after initial osteogenic induction. An alkaline phosphatase kit from Sigma (86C-1KT) was used to detect ALP activity. Calcium deposition was also observed after osteogenic differentiation using Von Kossa and Alizarin red stains.

2.2.7 Adipogenic Differentiation

Adipogenic differentiation was performed as previously described (Zheng, Cao et al. 2006). Myoblasts were plated in a multiwell dish (2.0×10^3 cells per well) and allowed to attach to the dish for 24 hours. Prior to adipogenic differentiation, one group of cells was treated with 100 ng/mL of MMP1. After treatment, cells were cultured in adipogenic differentiation media (DMEM supplemented with insulin (10 μM), dexamethasone (1 μM), isobutyl-methylxanthine (0.5 mM) and indomethacin (200 μM)). Two groups of myoblasts received MMP1 at concentrations of 10 and 100 ng/mL for the duration of differentiation. Cell cultures were

maintained for 14 days, with media changed every 2 days. After 2 weeks, cell cultures were fixed with 10% formalin for 10 minutes and stained with Oil Red O (Sigma), which is an indication of intracellular lipid accumulation. After being fixed with formalin solution, cells were rinsed with 60% isopropanol, then incubated in filtered Oil Red O working solution at room temperature and rinse with double-distilled water after 15 minutes. Images were captured on a Leica DMIRB microscope (Deerfield, IL) with a Retiga 1300 digital camera and acquired using Northern Eclipse software (version 6.0; Empix Imagining, Mississauga, ON, Canada). Once images were acquired, water was removed from the wells and they were allowed to dry. The remaining Oil Red O was eluted by adding 100% isopropanol for 10 minutes and then transferred to a 96 multiwell plate, where the optical density (OD) was measured at 500 nm for 0.5 seconds.

2.2.8 *In Vivo* MMP1 Administration via the GM Muscle

The use of animals and the procedures performed were approved by the Institutional Animal Care and Use Committee of the University of Pittsburgh. Five week old C57BL/6J mice (Jackson Laboratory) were subjected to MMP1 injection. A microsyringe was used to inject 200 ng of MMP1 in PBS into the GM muscle of the left leg, while the right leg was injected with only sterile saline and served as a control. Mice were sacrificed 3 and 5 days after the MMP1 injection and the GM muscle were harvested to obtain cryo-sections for immunohistochemical analysis.

2.2.9 Immunohistochemistry

Cross-sectional tissue sections of the GM muscle were fixed in 4% formalin. Afterward, tissue slides were rinsed with PBS and 10% HS was used to block unspecific binding for 1 hour. Primary antibodies, dystrophin [1:200, Abcam] and Pax7 [1:100, DHSB]) were applied. For the Pax7 (produced in mice), the Vector Mouse on Mouse (MOM) kits (Vector Labs) were used to improve antibody specificity. Species specific secondary antibodies, Alexa Fluor 488 and 594 (1:400, Invitrogen), were used and the cell nuclei were counterstained with DAPI.

2.2.10 Measurement of Results and Statistical Analysis

Comparisons of groups were completed using a one-way ANOVA, where significance levels were determined using Tukey HSD pairwise comparison. The differences between the means of samples were considered statistical significance if $P < 0.05$.

2.3 RESULTS

2.3.1 Stem Cell Marker Promotion in C2C12 Myoblasts

Previous research has shown the ability of MMP1, administered to C2C12 myoblasts from ATCC, to increase cell migration distances (Wang, Pan et al. 2009). In an effort to further observe the effect of MMP1 on cell migration, a retroviral vector was created to transfect C2C12

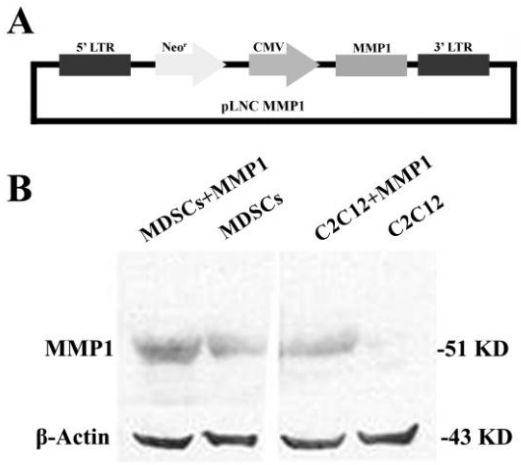

Figure 2.1: MMP1 Protein Expression
The function of MMP1 was extended in the construction of a retrovirus containing both a 5' and 3' long terminal repeats (LTR), a neomycin resistant gene (Neo^r) and a cytomeyalovirus (CMV) promoter (A). The MMP1 retrovirus was transfected into mouse C2C12 myoblasts and MDSCs, where an increased MMP1 expression was observed when compared to non-transfected cells by western blot (B). β-actin was used as a loading control.

myoblasts so they consistently expressed the MMP1 gene. The retrovirus consisted of both a 5' and 3' long terminal repeats (LTR), a neomycin resistant gene (Neo^r), a cytomeyalovirus (CMV) promoter and the MMP1 gene (Figure 2.1, A). Through western blot analysis, transfection of the MMP1 gene in to C2C12 cells and production of the MMP1 enzyme was confirmed (Figure 2.1, B). MDSCS were also transfected with the MMP1 gene retrovirus. Non-transfected MDSCs did express the MMP1 enzyme; however, the transfected MDSCs expressed an elevated level of MMP1. When comparing the expression of MMP1 between both cell types, transfected C2C12 myoblasts and non-transfected MDSCs had relatively similar levels of MMP1 expression. With similar levels of MMP1 expression, this prompted further interest as to whether MMP1 had any effect on the C2C12 myoblasts to contribute to other attributes related to the naturally isolated MDSCs.

To elucidate this finding, MMP1 transfected C2C12 myoblasts (Figure 2.2, A) and non-transfected C2C12 myoblasts (Figure 2.2, B) were subjected to ICC for the expression of Sca1

(green) and desmin (red). A qualitative inspection of the staining indicated a greater percentage of the MMP1 transfected C2C12 myoblasts expressed Sca1 with only specs of desmin at the perimeter compared to the non-transfected C2C12 myoblasts, which largely expressed desmin with some expressing Sca1. This observation was then assessed by treating non-transfected C2C12 myoblasts with MMP1 at 10 fold increases in concentration (0-100 ng/mL) for 6 hours (Figure 2.2, C). RT-PCR analysis revealed that increases in the administration of MMP1 to the C2C12 cells, also increase their gene expression of Sca1 to comparable levels of MDSCs (lane M) where gene expression of GAPDH served as a loading control.

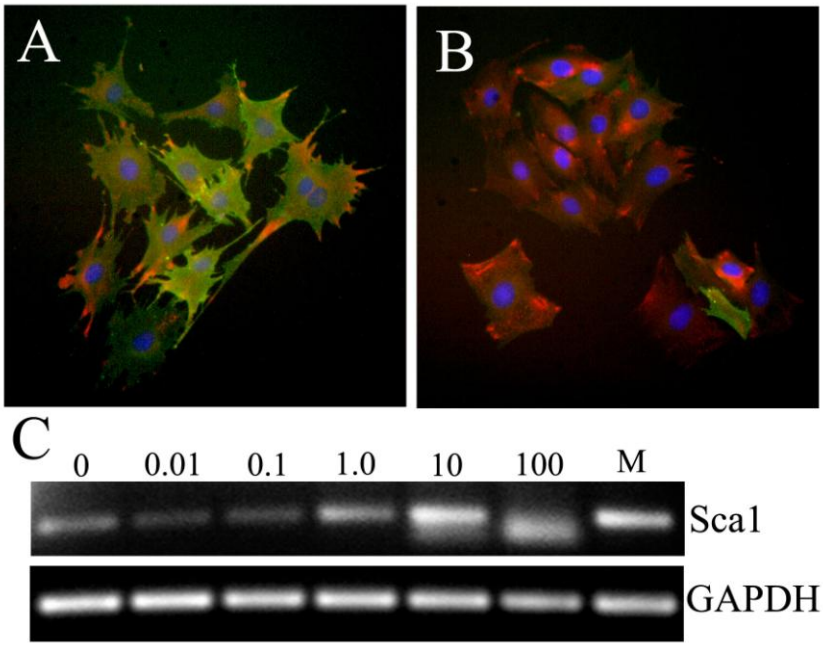

Figure 2.2: Stem Cell Marker Expression of C2C12 Myoblasts
MMP1 transfected C2C12 cells (A) and non-transfected C2C12 cells (B) were stained for Sca1 (green) and desmin (red). C2C12 myoblasts treated at 10 fold increases in concentration of MMP1 (ng/mL) for 6 hours were assessed by RT-PCR analysis for the gene expression of Sca1, where lane M represents a positive control for MDSCs and GAPDH served as a loading control (C).

Like the previous experiment, the expression of octamer-binding transcription factor 4 (Oct4), which is typically associated with maintaining the pluripotency of embryonic stem cells, was observed. C2C12 myoblasts were treated with 100 ng/mL of MMP1 for 6 hours (Figure 2.3,

A) and compared to untreated C2C12 myoblasts (Figure 2.3, B). Plated at the same cell density, the C2C12 myoblasts that received MMP1 indicated a greater protein expression of Oct 4 (green). Using RT-PCR analysis, MMP1 was administered to the C2C12 myoblasts at 10 fold increases in concentration (0-100 ng/mL) for 6 hours (Figure 2.3, C). These results indicated that there was a dose dependent stimulation in the gene expression of Oct4 using higher concentration of MMP1. Again, the Oct4 expression was observed in MDSCs, where the gene expression of Oct4 appeared lower than the highest concentration of MMP1 (100 ng/mL) administered to the C2C12 myoblasts.

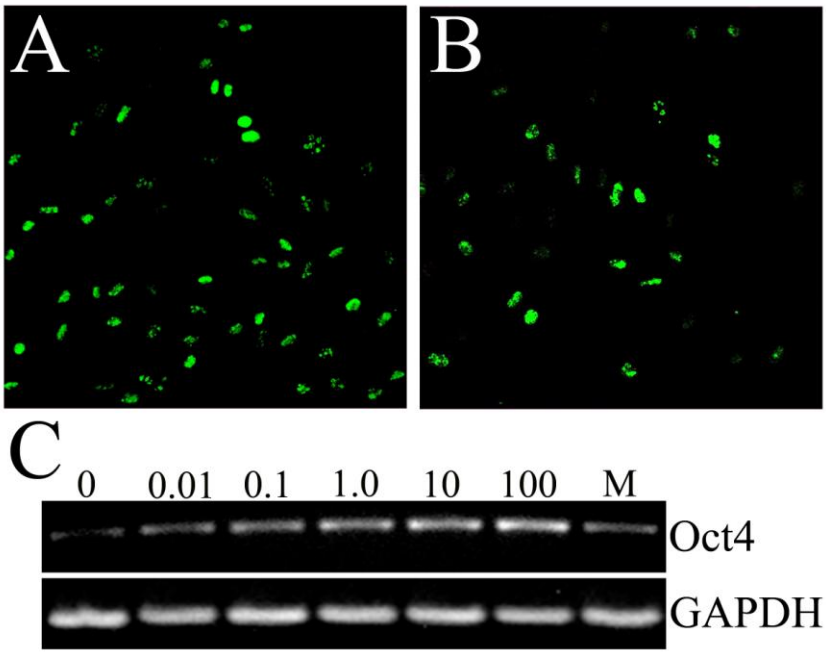

Figure 2.3: Oct4 Expression of C2C12 Myoblasts
Administering MMP1 stimulates Oct4 expression in C2C12 myoblasts in vitro. A greater number of C2C12 myoblasts expressed Oct4 (green) after 6 hours of treatment (A) compared to no treatment (B). Similarly, a 10-fold concentration dose increase in MMP1 administration to C2C12 myoblasts for 6 hours shows a gradual increase in the gene expression of Sca1, where lane M represents the gene expression for MDSCs (C).

2.3.2 Stem Cell Characteristics of Primary Mouse Myoblasts Treated With MMP1

A number of research publications suggest that C2C12 myoblasts feature traits that are similar to adult stem cells including stem cell marker and a capacity for multiple differentiation (Epting, Lopez et al. 2004; Decraene, Benchaouir et al. 2005; Li, Peng et al. 2005; Fujita, Endo et al. 2010). Instead of using the cell line, C2C12 cells, a more preferable group of cells would be the use of terminally differentiated primary mouse myoblasts treated with MMP1. For this study, primary mouse myoblasts isolated from the GM muscle of mice by the preplate technique were used to assess the effects of MMP1 stimulation (Li, Pan et al. 2010).

To conciliate any concerns that the effects of MMP1 administration to C2C12 myoblasts was the result of influencing cell proliferation, this aspect of cell behavior was examined. In these experiments, primary mouse myoblast proliferation was evaluated using several treatments of MMP1. Two groups of primary mouse myoblasts were pretreated with conditioned media of 100ng/mL of MMP1 for 6 and 24 hours and then cultured in proliferation for the duration of the cell proliferation assay. Another two groups of cells were treated with either 10 or 100 ng/mL of MMP1 in proliferation media at the beginning of the proliferation assay. Using a live cell imager, images of cell proliferation were captured at 20 minute intervals over a period of 3 days. The number of cells per field of view was plotted as a function of time and an exponential regression line was fitted to the data using the equation, $N_i = N_o e^{kt_i}$, and the PDT was calculated. The administration of MMP1 based on pretreatment times (Figure 2.4, A) or the use of different concentrations (Figure 2.4, B) was observed to have no effect on the PDT. The PDT consistently was maintained at approximately 17.5 hours. An alternative evaluation of cell

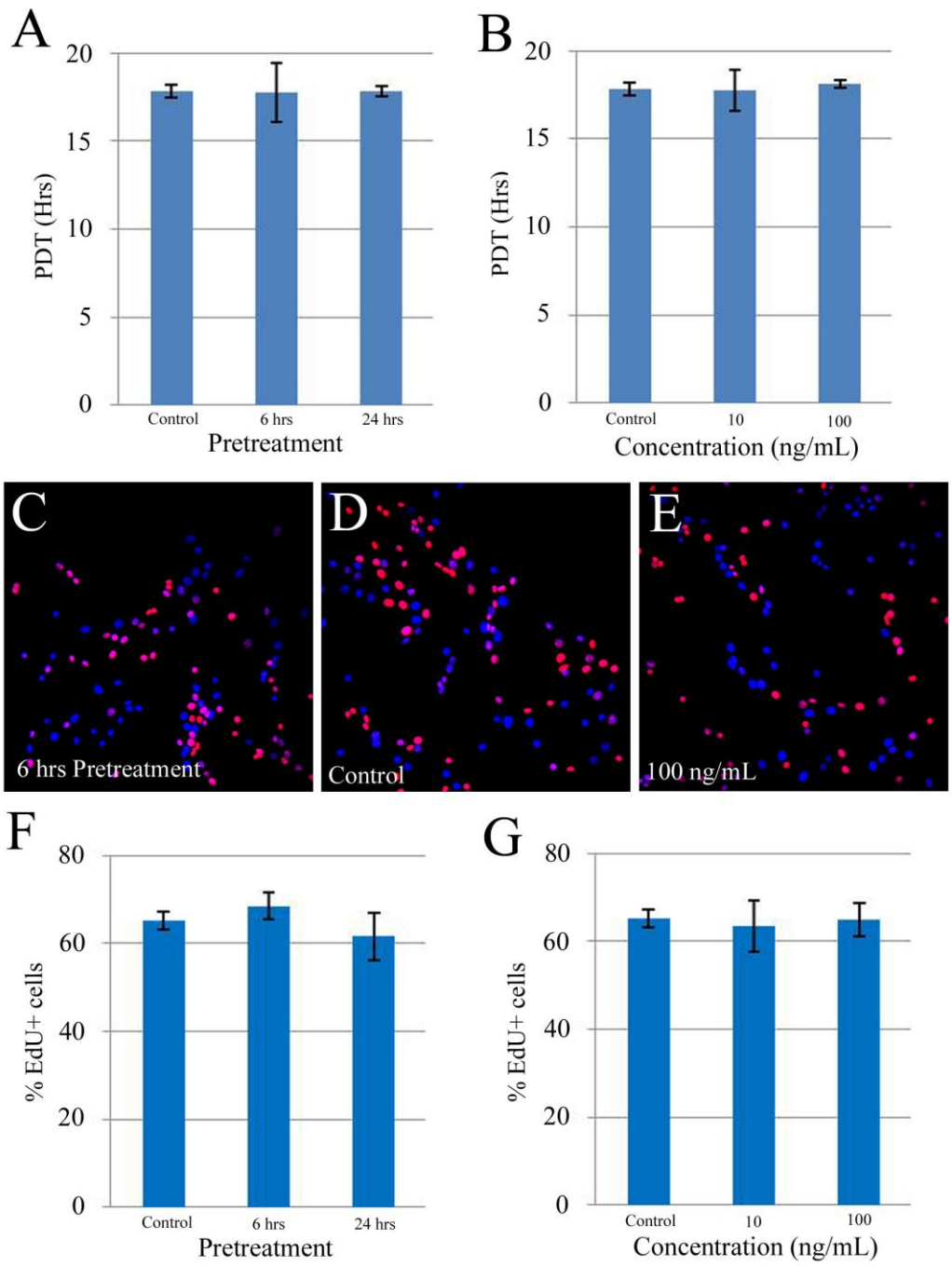

Figure 2.4: Primary Mouse Myoblast Proliferation
The population doubling time of primary mouse myoblasts was unaffected based on pretreatment time (A) and different concentrations (B) of MMP1 administered to the cells based on analysis using live cell imaging. A cell proliferation assay using the incorporation of EdU (red) into the cell nuclei shows no difference between 6 (C) and 24 hours of pretreatment (F), and different MMP1 concentrations of 10 and 100 (E) ng/mL with EdU during culture (G), compared with the control group (D). All cells were stained with Hoechst 33342 (blue).

proliferation was performed in succession to validate the PDT results. In an EdU assay, EdU, a nucleoside analog of thymidine, is incorporated into DNA during active DNA synthesis and detected at a later time point using the azide and alkyne by a copper-catalyzed covalent reaction. This assay was used to investigate the percentage of primary mouse myoblasts that incorporated the EdU based on 6 (Figure 2.4, C) and 24 hour pretreatments or the use of 10 and 100ng/mL (Figure 2.4, E) of MMP1 in comparison to the control (Figure 2.4, D). Approximately 60% of the primary mouse myoblasts in culture incorporated EdU into their DNA regardless of pretreatment (Figure 2.4, F) or the use of different concentrations (Figure 2.4, G) of MMP1.

With evidence that MMP1 does not influence cell proliferation, two markers associated with MDSCs expression, CD34 and Sca1, were analyzed (Lee, Qu-Petersen et al. 2000; Jankowski, Haluszczak et al. 2001; Jankowski, Deasy et al. 2002). Primary mouse myoblasts were administered 100ng/mL of MMP1for 0, 3, 6, 12, 18, and 24 hours and their gene expression of CD34 and Sca1 were assessed (Figure 2.5). Minimal expression of CD34 and Sca1 were observed in the control (0 hours) samples, however by 6 hours of stimulation, an increase in the gene expression of CD34 and Sca1 was observed. This upregulated gene expression continued for up to 18 hours, but by 24 hours, it had begun to diminish. The Notch signaling pathway is often associated with the activation of resident MDSCs and their proliferation (Brack, Conboy et al. 2008). In this experiment, the gene expression of Notch1 was examined and no differences were observed based on the length of MMP1 stimulation.

Further MMP1 administration to primary mouse myoblasts was conducted in an effort to assess the optimal dosage of MMP1 to upregulate CD34 and Sca1. Based on the previous analysis, it appeared that MMP1 instigated an increase in CD34 and Sca1 primarily between 6 and 18 hours. Therefore, the gene expression of these genes was assessed at 6 (Figure 2.6, A)

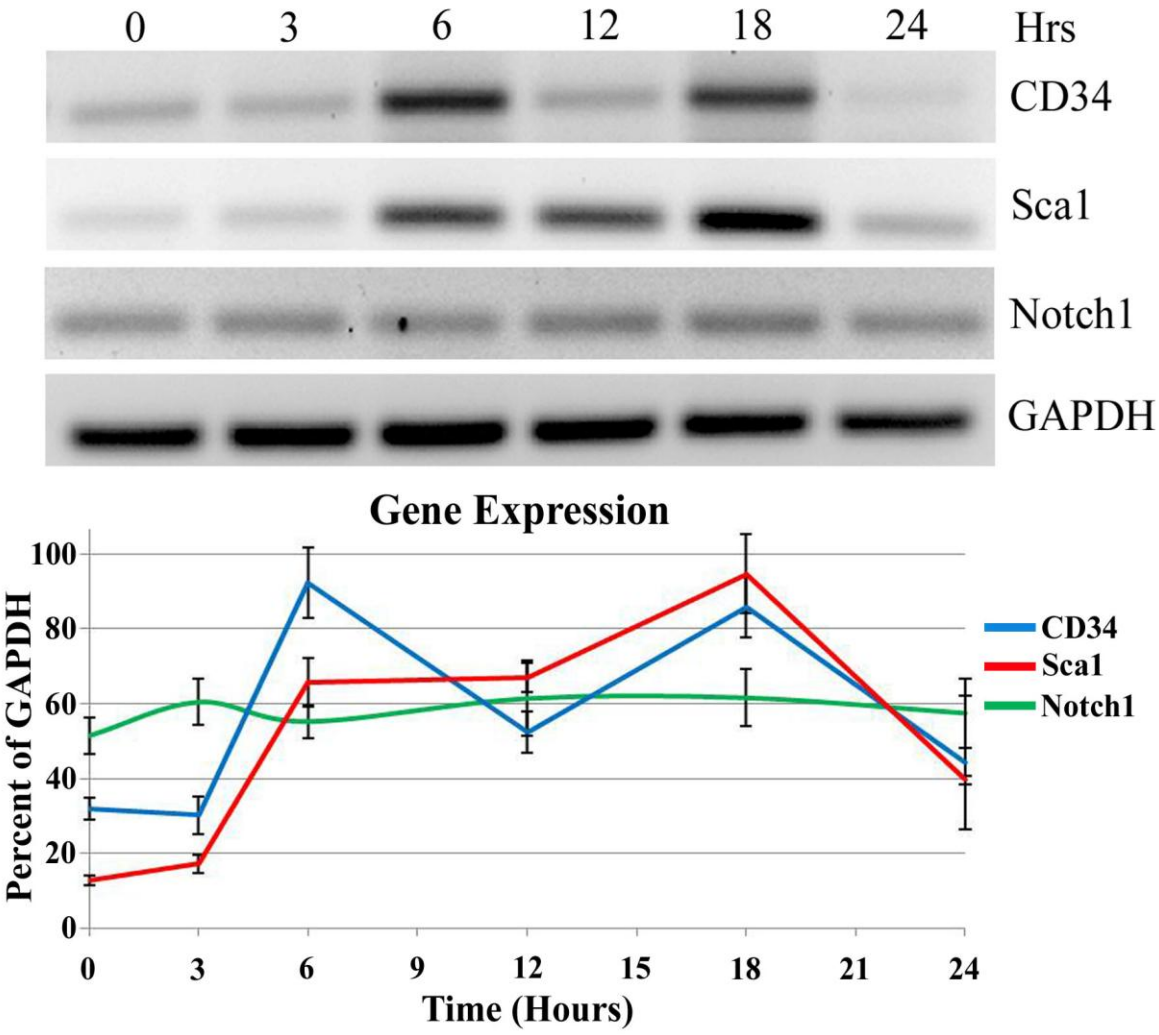

Figure 2.5: Gene Expression of Primary Mouse Myoblasts at Different Time Points
Changes in the gene expression of stem cell markers, CD34 and Sca1, are observed with primary mouse myoblasts treated with 100 ng/mL of MMP1 for different lengths of time. A signaling pathway gene, Notch1, was observed to have no effect from MMP1 as well as the loading control gene, GAPDH.

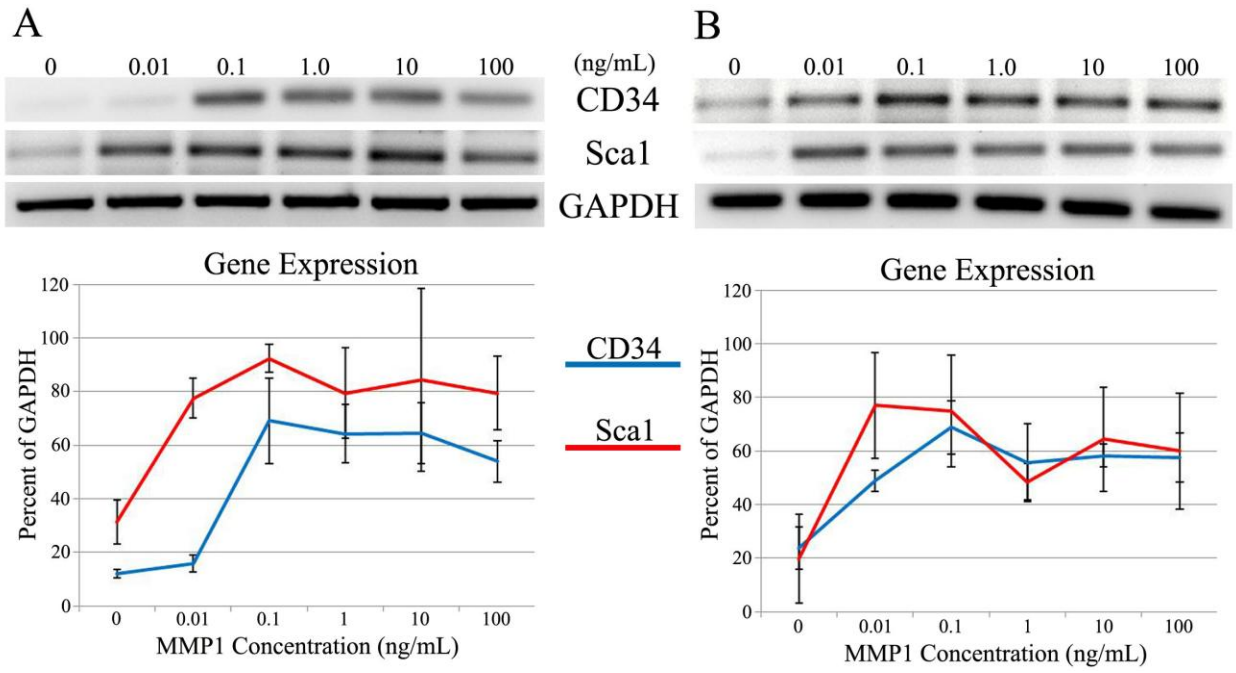

Figure 2.6: Stem Cell Gene Expression of Primary Mouse Myoblasts
Changes in the gene expression of stem cell markers, CD34 and Sca1, are observed with primary mouse myoblasts treated with 10 fold concentration increases from 0-100 ng/mL of MMP1 for the treatment times of 6 (A) and 18 (B) hours. GAPDH was used as a loading control gene.

and 18 (Figure 2.6, B) hours after MMP1 stimulation by 10 fold increase in concentration from 0 – 100 ng/mL. For the control samples, a minimal amount of gene expression was observed for CD34 and Sca1 at either 6 or 18 hours. For the 6 hours treated samples, an increase in the gene expression of CD34 was observed starting with a dosage of 0.1ng/mL to 100ng/mL whereas the an increase in the gene expression was observed at a MMP1 dosage of 0.01ng/mL and remained elevated up until 100ng/mL. For the primary mouse myoblasts treated with MMP1 for 18 hours, the increase in gene expression for CD34 and Sca1 was seen with the lowest concentration of 0.01ng/mL, which remained elevated above the control for dosages up to 100ng/mL. GAPDH was used as a loading control in these experiments for gene expression.

The gene expression results of the primary mouse myoblasts were further analyzed by their protein expression after MMP1 stimulation. These cells were administered 100ng/mL of

MMP1 for 24 hours of MMP1 (Figure 2.7, E-H) and compared to controls (Figure 2.7, A-D) using ICC. Primary mouse myoblasts that did not receive MMP1 stimulation did not express

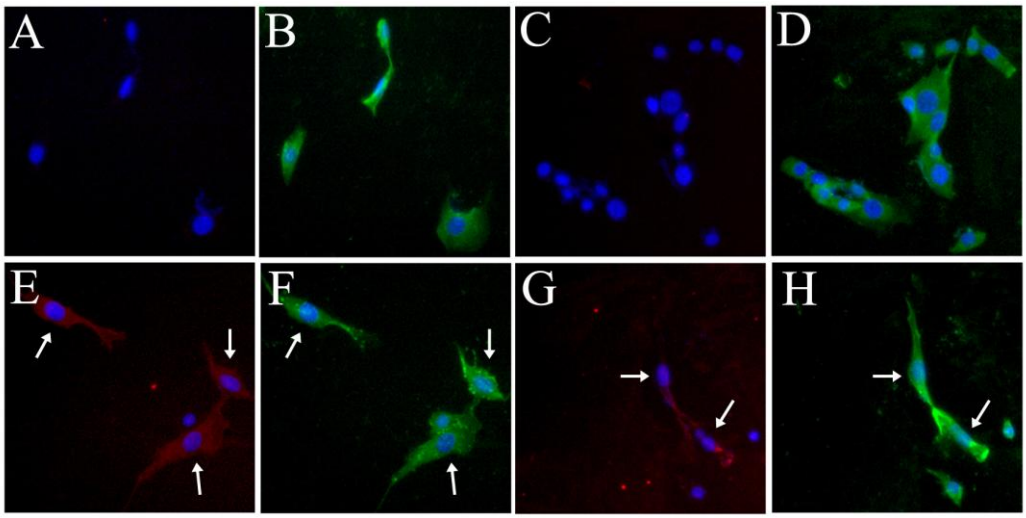

Figure 2.7: Stem Cell Marker Expression of Primary Mouse Myoblasts
Primary mouse myoblasts treated with 100 ng/mL of MMP1 for 24 hours (E-H) compared to non-treated primary mouse myoblasts (A-D). After 24 hours of stimulation, these cells began expressing Sca1 (E) and CD34 (G) compared to untreated cells (A,C), while the expression of desmin (B, D, F, H) remained relatively unaffected as denoted by the arrows.

Sca1 (Figure 2.7, A) nor CD34 (Figure 2.7, C), however after 24 hours with 100ng/mL of MMP1 in culture, Sca1 (Figure 2.7, E) and CD34 (Figure 2.7, G) expression was observed, although not all cells expressed these proteins. The protein expression of desmin was also evaluated, but no differences were found without (Figure 2.7, B, D) or with (Figure 2.7, F, H) MMP1 treatment.

To validate the results of gene expression and ICC, western blotting was used to assess the protein expression of these stem cell markers. The total protein from primary mouse myoblasts was isolated after cultured with MMP1 from 0 – 100ng/mL with ten-fold increases in concentration for 18 hours and observed for expression of Sca1 and Pax7 (Figure 2.8). Primary mouse myoblasts that did not receive any form of MMP1 treatment did not express Sca1 or Pax7, however increases in the expression of these proteins were observed with increasing

concentrations of MMP1 stimulation. The highest level of expression for both proteins was observed with the administration of 0.01ng/mL of MMP1.

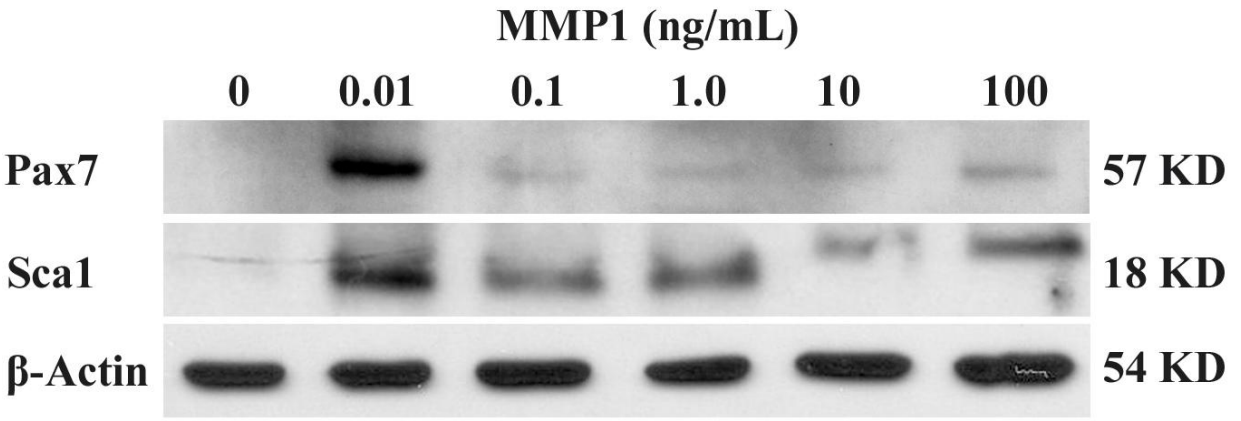

Figure 2.8: Primary Mouse Myoblast Western Blot Analysis
Changes in the protein expression of Pax7 and Sca1, are observed with primary mouse myoblasts treated with 10 fold concentration increases from 0-100 ng/mL of MMP1 for 18 hours of treatment. β-actin was used as a loading control.

In order to explore the influence of MMP1 to promote stem characteristics in primary mouse myoblasts, multiple differentiation assays are necessary. These cells are of the myogenic lineage and previous results have demonstrated the ability of MMP1 to actively aid in a greater amount of myotube formation (Wang, Pan et al. 2009). The multipotency of these primary mouse myoblasts to undergo osteogenic differentiation after the administration of MMP1 was examined. Primary mouse myoblasts we plated and cultured in osteogenic differentiation media supplemented with 50ng/mL of BMP4, a minimal amount such that osteogenesis was not driven solely my BMP4 without any influence of MMP1. After 5 and 7 days of osteogenic induction, the myoblasts were fixed and stained for ALP expression to signify osteogenic differentiation. Several forms of MMP1 treatment: 6 (Figure 2.9, B) and 24 (Figure 2.9, C) hours of pretreatment with 100ng/mL, and continuous treatment of 100ng/mL of MMP1 (Figure 2.9, D) for the duration of osteogenesis were observed in comparison to the control (Figure 2.9, A). For

primary mouse myoblasts that received any form of MMP1 treatment, a greater percentage of ALP positive cell were observed in comparison to the control at 5 days and at 7 days the percent of ALP positive cells increased even more. Continuous treatment of MMP1 for the 7 days of osteoinduction resulted in approximately 18% of the cells positive for ALP expression, whereas the MMP1 pretreated groups were observed to have roughly 16% of their cells expressing ALP in comparison to, at most, 8% of the cells not treated with MMP1 expressed ALP.

The osteogenic differentiation potential of the primary mouse myoblasts after exposure to MMP1 treatment was further investigated using two additional stains to examine osteogenesis, Von Kossa (Figure 2.10, A-D) and alizarin red (Figure 2.10, E-H). Identical treatment groups: control (Figure 2.10, A, E), 6 (Figure 2.10, B, F), and 24 (Figure 2.10, C, G) hours of treatment with 100ng/mL of MMP1 prior to osteogenic differentiation, and 100ng/mL for the entirety of osteogenic differentiation (Figure 2.10, D, H) were tested. The Von Kossa stain was used to assess mineralization of the primary mouse myoblasts after 7 days in osteogenic differentiation media. Mineralization was observed only in the test groups that received MMP1 treatment, however, it appeared more frequent with the cells cultured with osteogenic differentiation media supplemented with MMP1 and the cells pretreated for 24 hours. No mineralization was observed in the non-treated MMP1 groups. Von Kossa staining, by itself, is sometimes considered not sufficient enough to detect mineralization *in vitro* since the silver ions of the staining solution are reacting with the phosphate in culture. In addition, an alizarin red stain was applied to identify the presence of any calcium-rich deposits among the primary mouse myoblasts. Similar to the outcome of the Von Kossa staining, no alizarin red was observed in non-treated samples; however, primary mouse myoblasts that did receive some form of MMP1 stimulation did exhibit alizarin in sparsely distributed clumps after 7 days during osteogenesis.

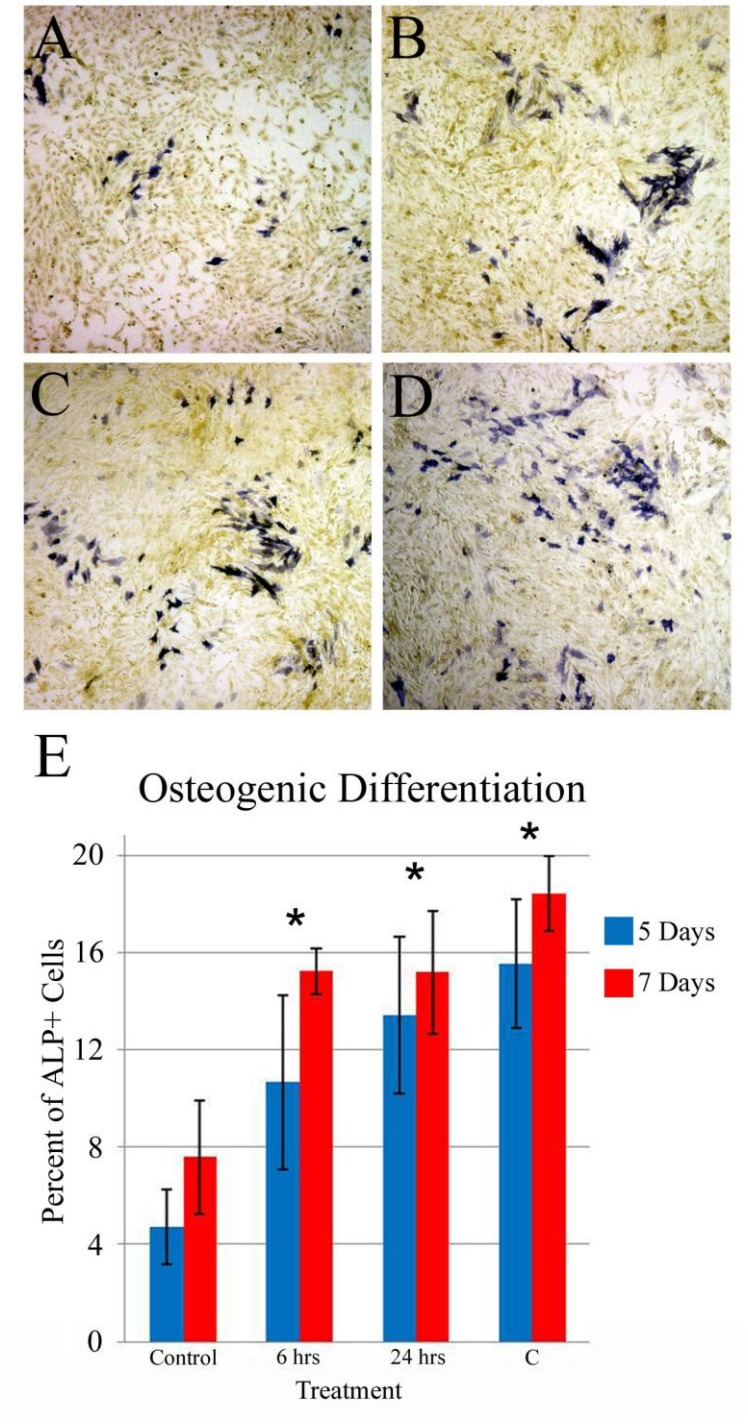

Figure 2.9: Primary Mouse Myoblast ALP Expression
Primary mouse myoblasts treated with MMP1 exhibited a greater potential to undergo osteogenic differentiation. Four groups were investigated: no treatment (A), 6 (B) and 24 (C) hours pretreatment with 100 ng/mL MMP1 before initiating osteogenesis; and MMP1 treatment for the duration of the osteogenic differentiation (D, denoted as C in (E)). ALP positive cells are dark blue under bright field microscopy. The percentage of ALP positive cells after 5 and 7 days of osteogenic differentiation is shown in (E). There is a significant difference (*$P<0.05$) between the control and other groups.

osteogenic differentiation (Figure 2.10, D, H) were tested. The Von Kossa stain was used to assess mineralization of the primary mouse myoblasts after 7 days in osteogenic differentiation media. Mineralization was observed only in the test groups that received MMP1 treatment, however, it appeared more frequent with the cells cultured with osteogenic differentiation media supplemented with MMP1 and the cells pretreated for 24 hours. No mineralization was observed in the non-treated MMP1 groups. Von Kossa staining, by itself, is sometimes considered not sufficient enough to detect mineralization *in vitro* since the silver ions of the staining solution are reacting with the phosphate in culture. In addition, an alizarin red stain was applied to identify the presence of any calcium-rich deposits among the primary mouse myoblasts. Similar to the outcome of the Von Kossa staining, no alizarin red was observed in non-treated samples; however, primary mouse myoblasts that did receive some form of MMP1 stimulation did exhibit alizarin in sparsely distributed clumps after 7 days during osteogenesis.

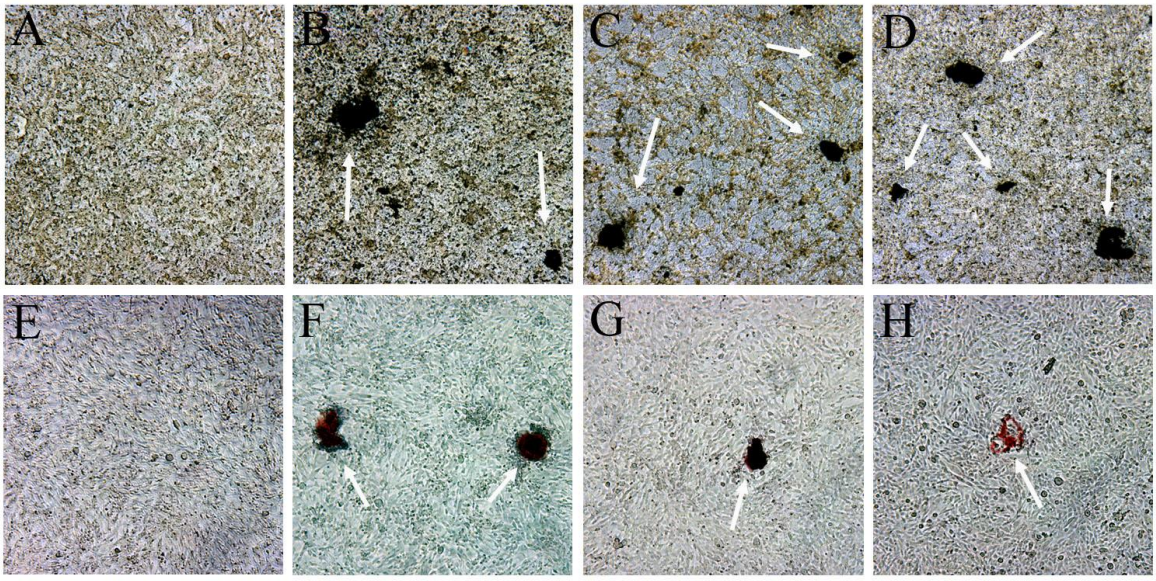

Figure 2.10: Von Kossa and Alizarin Red Stains of Primary Mouse Myoblasts
Primary mouse myoblasts treated with MMP1 exhibited positive expression for calcium deposition by Von Kossa (A-D) and Alizarin red (E-H) stain after osteogenic differentiation for 7 days. Four groups were investigated: no treatment (A & E), 6 (B & F) and 24 (C & G) hours pretreatment with 100 ng/mL MMP1 before initiating osteogenesis; and MMP1 treatment for the duration of the osteogenic differentiation (D & H). All images were taken at 10x magnification using phase contrast microscopy with white arrows denoting calcium deposition.

To establish that the increased osteogenic differentiation potential of the primary mouse myoblasts was not the result of an interaction between MMP1 and BMP4 influencing cell proliferation, and EdU assay was performed. Using the same treatment groups, primary mouse myoblasts were cultured in osteogenic media for 5 days, with the EdU solution incubated during the final 12 hours of osteoinduction. There was no significant difference found in the percent of cells that incorporated EdU between any of the groups tested (Figure 2.11). Approximately 30% of the primary mouse myoblasts in each group were undergoing cell proliferation during osteogenic differentiation, which is about half the percentage of these same cells that were proliferating in their normal growth media as measured during a 12 hours period.

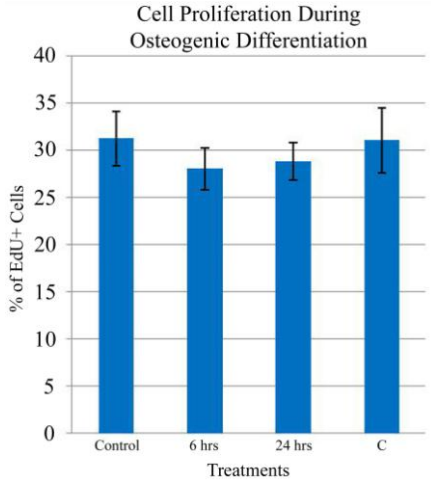

Figure 2.11: Cell Proliferation during Osteogenic Differentiation
The percentages of primary mouse myoblasts that are positive for EdU expression. No difference (*P<0.05) is observed between the control, 6 and 24 hours of pretreatment with 100ng/mL of MMP1, and continuous treatment with 100ng/mL (denoted as "C" above) during the osteogenesis for 5 days.

Another assay used to test cell multipotency after MMP1 stimulation was an adipogenic differentiation assay. In this experiment, 1 group of myoblasts treated with 100ng/mL of MMP1 for 6 hours (Figure 2.12, B) prior to adipogenic differentiation and 2 groups of myoblasts treated with either 10 (Figure 2.12, C) or 100ng/mL (Figure 2.12, D) of MMP1 for the duration of the study were observed in combination with a non-treated group (Figure 2.12, A). After 2 weeks, all

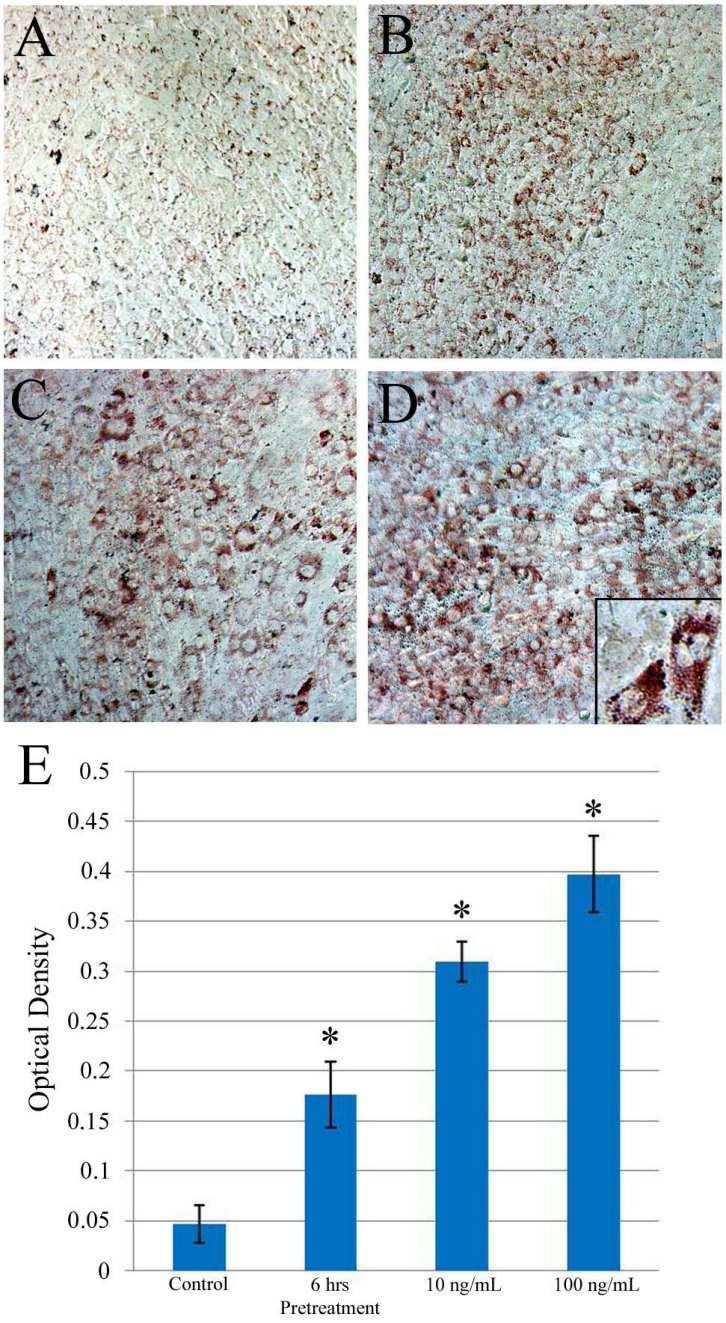

Figure 2.12: Adipogenic Differentiation of Primary Mouse Myoblasts
Primary mouse myoblasts treated with MMP1 exhibited accumulation of lipids (red) within the cytoplasm after 2 weeks as shown with oil red O staining. Four groups were investigated: no treatment (A), 6 hours pretreatment with 100ng/mL MMP1 (B) before adipogenesis induction; and MMP1 treatment of 10 (C) and 100ng/mL (D) for the duration of the adipogenic differentiation (a magnified image is also included). The optical density was used to quantify adipogenesis. There is a significant difference (*P<0.05) between the control and other groups.

cells were fixed and an Oil Redo O stain was performed to assess intracellular lipid accumulation, which is indicative of the adipogenic phenotype. Cytoplasmic lipid droplets were quantified by removing the total amount of Oil Red O within the cells using 100% isopropanol alcohol and measuring the OD at 500nm (Figure 2.12, E). Primary mouse myoblasts that received any form of MMP1 treatment had a significantly higher amount of intracellular lipid accumulation. The greatest amount of lipid accumulation was observed with 100ng/mL of MMP1 supplemented in the adipogenic differentiation, followed by 10ng/mL of MMP1 and then 6 hours of MMP1 pretreatment. True adipocytes typically exhibit large lipid droplets within the cell membrane, while the intracellular lipids of the primary mouse myoblasts after 2 weeks for adipogenesis were small and abundant.

2.3.3 *In Vivo* Administration of MMP1

To further elucidate the potential of MMP1 to influence stem cell behavior, *in vivo* experiments were performed. Using C57BL/6J mice, 200ng of MMP1 was injected into the GM muscle of one limb, where the contralateral limb served as a control and was injected with sterile saline. No injury was inflicted upon the mice at, before or after the MMP1 injection. After 3 (Figure 2.13, A, B) and 5 (Figure 2.13, C, D) days after injections, the selected regions of skeletal muscle were harvested and the MMP1 injection muscle tissue (Figure 2.13, B, D) was compared to the control (Figure 2.13, A, C). Comparison between the sample groups was examined by the number of Pax7 positive cells, where Pax7 is known as a marker of satellite cells in adult muscle (Peault, Rudnicki et al. 2007). The percentage of Pax7 positive cells (Figure 2.13, E) observed in the GM muscle treated with MMP1 at 3 and 5 days was approximately 11% and 8%, respectively, significantly higher in comparison to the 3% of Pax7 positive cells present in GM muscle treated

only with saline. Likewise, the number of Pax7 positive cells observed for MMP1 treated muscle tissue was roughly 115 and 80 per mm^2, at 3 and 5 days respectively. This was significantly greater than the number of Pax7 positive cells observed for the non-treated skeletal muscle tissue, where 35 Pax7 positive cells were observed per mm^2. These results suggest that the administration of MMP1 has an impact *in vivo* such that a greater increase in the muscle satellite population is found.

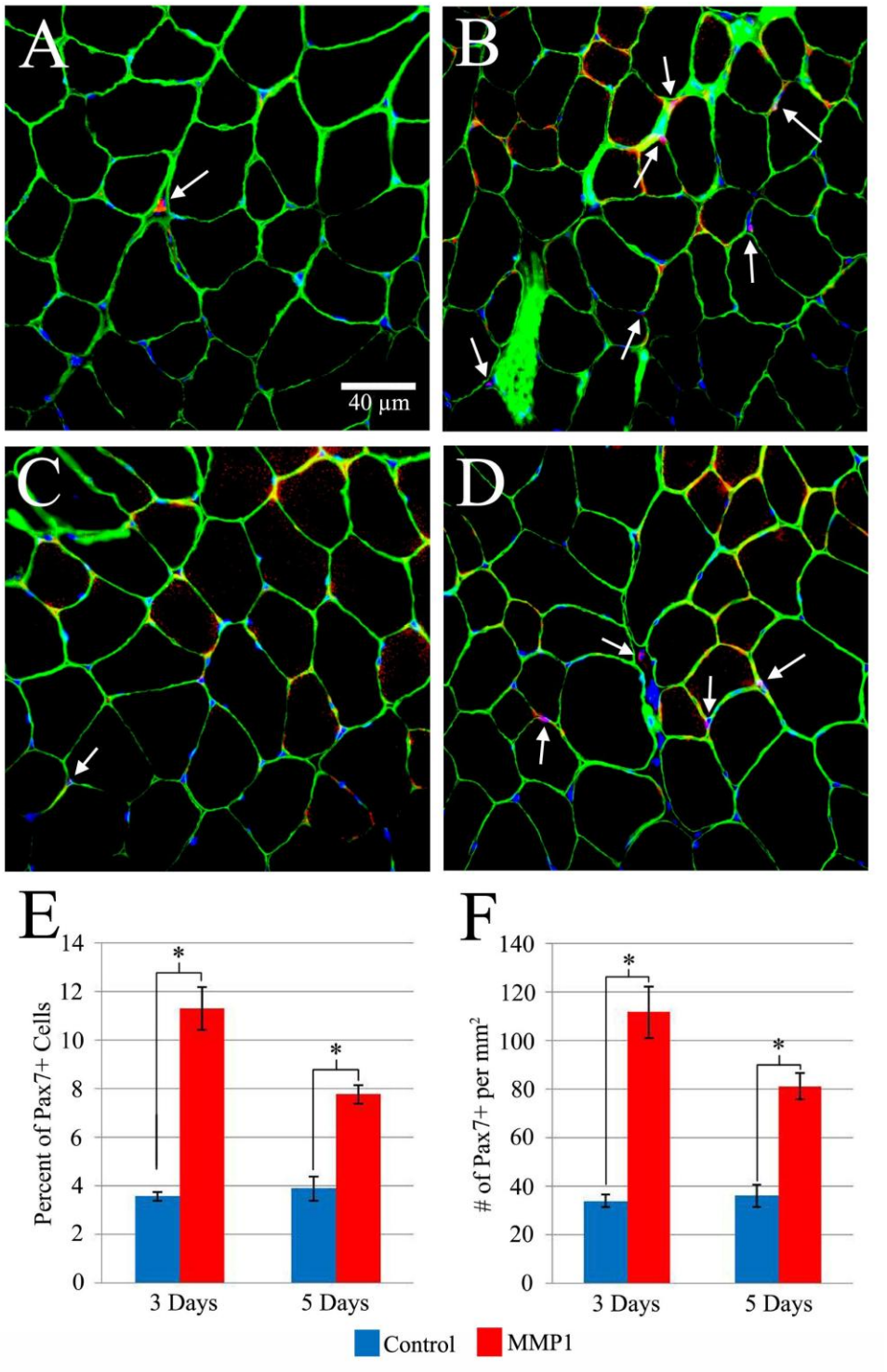

Figure 2.13: In Vivo Pax7 Expression with MMP1
Pax7 expression (red, indicated by arrows) was increased 3 (B) and 5 (D) days after MMP1 administration to the GM muscles of mice in comparison to GM muscles 3 (A) and 5 (C) days after receiving saline. Dystrophin (green) and cell nuclei (blue) were also counterstained. The percentage of Pax7 positive cells (E) and the number of Pax7 positive cells per mm^2 was quantified. There is a significant difference (*$P<0.05$) between the control and MMP1 treatment.

2.4 DISCUSSION AND CONCLUSION

With the increasing popularity of using cell therapies in tissue regeneration, a large number of tissue sources are under investigation for isolating multipotent adult stem cells (Curran, Pu et al. 2011; Guo, Draheim et al. 2011; Nath, Offers et al. 2011; Seeberger, Eshpeter et al. 2011; Sharifiaghdas, Taheri et al. 2011). While many scientists have published successful stem cell isolation methods, adult stem cells still remain difficult to isolate, purify and expand in culture. These limitations with adult stem cells provided the motivation for research involving the therapeutic use of iPS cells which involves reprogramming a patient's own terminally differentiated cells into a stem cell for transplantation (Takahashi and Yamanaka 2006; Takahashi, Tanabe et al. 2007; Mauritz, Martens et al. 2011; Yazawa, Hsueh et al. 2011). Being such a new area of stem cell research, iPS cells are also met by limitations including potentially harmful effects from the genome integrating viruses, low efficiency of reprogramming and the uncertainty of which cell type works best for transfection. In these studies, a more naturally occurring enzyme, MMP1, shows promise in influencing stem cell behavior during tissue remodeling.

There is no doubt that literature has demonstrated the importance of MMPs in the regeneration of skeletal muscle tissue (Guerin and Holland 1995; Allen, Teitelbaum et al. 2003; Ohtake, Tojo et al. 2006; Yamada, Tatsumi et al. 2006; Bani, Lagrota-Candido et al. 2008; Hnia, Gayraud et al. 2008). For MMP1 alone, research has detailed the benefit of MMP1 administration in laceration injuries to improve skeletal muscle healing by degrading fibrotic scar

tissue (Bedair, Liu et al. 2007; Kaar, Li et al. 2008). Scar tissue, which impedes the proper wound healing at later stages of muscle recovery, is degraded by MMP1 to further facilitate the myoblast migration and myogenic differentiation for *in vitro* and *in vivo* conditions (Wang, Pan et al. 2009). The results of this study suggest that MMP1 includes the potential to stimulate the expression of markers, Sca1 and CD34, which are closely associated with MDSCs and this expression varies by the MMP1 dosage and timing (Deasy, Li et al. 2004; Deasy, Gharaibeh et al. 2005). Some studies have indicated a possible link between MMP activity and stem cell behavior. One investigation found the elevated MMP9 activity mutually increased with the number of Sca1 positive cells in order to stimulate cell migration and activation of muscle precursor cells (Bani, Lagrota-Candido et al. 2008). Other studies have found that in addition to MMP activity, mechanical stimulation may also play role in influencing stem cell behavior (Guerin and Holland 1995; Yamada, Tatsumi et al. 2006; Kasper, Glaeser et al. 2007).

MMPs are known their impressive behavior of triggering tissue remodeling through the degradation of ECM components, which further allow cell proliferation, migration, differentiation, apoptosis and angiogenesis (McCawley and Matrisian 2001; Creemers, Davis et al. 2003; Visse and Nagase 2003; Menon, Singh et al. 2005; Pereira, Strasberg-Rieber et al. 2005; Shan, Morris et al. 2007; McCawley, Wright et al. 2008; Yang, Liu et al. 2009; Zeng, Yao et al. 2009). In these results, MMP1 is observed to promote cell differentiation of primary mouse myoblast to the osteogenic lineage as evinced by the expression of ALP, an early osteogenic marker, and adipogenic lineage by uptake of Oil Red O in small lipid droplets within the cell cytoplasm. While MMP1 can be credited with a number of tasks aiding tissue regeneration, ultimately is has no influence over myoblast proliferation as assessed by analysis of PDT and incorporation of EdU during DNA synthesis. Gene expression data demonstrates that MMP1

administration has no effect on the Notch1 receptor, where Notch signaling is closely associated with proliferation of muscle satellite cells and its inhibition can have detrimental effects on muscle regeneration (Luo, Renault et al. 2005; Brack, Conboy et al. 2008). This provides evidence that MMP1 is not simply stimulating proliferation of MDSCs or muscle satellite cells that may be present in the primary mouse myoblast population, therefore expression of the Notch1 receptor is most likely serving an alternative function. Instead, MMP1 is actively promoting MDSCs markers and a capacity for increased cell differentiation comparable to processes such as cell dedifferentiation or transdifferentiation. The expression of MMPs during the dedifferentiation and blastema formation in injured newts has been well documented (Miyazaki, Uchiyama et al. 1996; Kato, Miyazaki et al. 2003; Vinarsky, Atkinson et al. 2005; Stevenson, Vinarsky et al. 2006).

MMP1 stimulation was also observed to increase the protein expression of Pax7 in *in vitro* and *in vivo* conditions. Pax7 positive cells often referred to as muscle satellite cells or muscle progenitor cells (Zammit, Relaix et al. 2006; Peault, Rudnicki et al. 2007; Pawlikowski, Lee et al. 2009). In comparison to another study, relaxin was administered to mice subjected to a laceration injury and observed to increase the expression of Pax7 positive cells (Mu, Urso et al. 2010). The positive effects of relaxin therapy were attributed to an elevated expression of MMP2 and MMP9, which contributed to repressing fibrosis development at later phases of skeletal muscle healing.

Collectively, MMPs appear to play a valuable role in the regeneration of injured and diseased skeletal muscle tissue. While their expression in healthy tissue is infinitesimal, they are greatly upregulated when necessary. These results in conjunction with prior work illustrate the benefits of MMPs, particular MMP1, in muscle regeneration. Future studies are necessary to

determine the applicability of administering MMP1, or MMPs, in a clinical setting to improve skeletal muscle healing or function of other injured tissues.

3.0 MMP INHIBITION IMPAIRS MDSC BEHAVIOR

3.1 INTRODUCTION

Skeletal muscle is a dynamic tissue system that is essential for respiration, structural support, and movement, and is therefore highly vascularized and innervated to achieve these functions (Charge and Rudnicki 2004; Grefte, Kuijpers-Jagtman et al. 2007). As a consequence of its large size, it is susceptible to many types of injuries that include contusion, blunt force trauma, ischemia, lacerations and burns (Charge and Rudnicki 2004; Nozaki, Li et al. 2008; Ritenour, Christy et al. 2010; Wu, Wolf et al. 2010). In response to these injuries, understanding the complexity of the cellular and molecular events during the healing process is vital to improve the quality of life for individuals suffering from skeletal muscle injuries.

The three phases that occur during skeletal muscle injury and repair are inflammation and degeneration, regeneration and fibrosis formation (Huard, Li et al. 2002). Inflammation is initiated first when disrupted blood vessels encompassing the damaged area stimulate migration of inflammatory cells as well as the calcium dependent proteolysis of the myofibers, thus causing degeneration. MMPs and other chemokines are released by macrophages to amplify the immune response and recruit additional cells (Chazaud, Sonnet et al. 2003; Chazaud, Brigitte et al. 2009). During the second phase of regeneration, MDSCs become activate and migrate toward the bordering areas of the damaged myofibers where MyoD and Myf5 are upregulated to induce

differentiation into myoblasts (Ehrhardt and Morgan 2005; Ten Broek, Grefte et al. 2010). Eventually, the down regulation of Pax3 and Pax7 will lead to an increased expression of myogenin to facilitate myogenesis and form new myofibers (Grefte, Kuijpers-Jagtman et al. 2007; Boonen and Post 2008; Ten Broek, Grefte et al. 2010). The processes of the second stage are often undermined by the formation of fibrosis during the final phase. Myofibroblasts, at the site of injury, will secrete ECM components such as collagen types I and III as well as fibronectin to aid in tissue repair, but unfortunately an excessive secretion and inefficient turnover of the collagen during remodeling causes an unwanted accumulation of these constituents, thus forming scar tissue (Huard, Li et al. 2002; Serrano and Munoz-Canoves 2010).

In the present chapter, the inhibition of MMPs on stem cells derived from skeletal muscle tissue and C2C12 myoblasts was investigated. A broad spectrum MMP inhibitor, GM6001, which is known to inhibit MMP1, MMP2, MMP3, MMP8 and MMP9, was administered to both cell types. MMP inhibition had a negative impact on MDSCs characteristics by impairing stem cell marker expression. In turn, this affected MDSC migration and their ability to properly aid in the repair by causing erroneous skeletal muscle healing when GM6001 was injected into a laceration injury model of mice. These findings suggest that MMPs play an important role in tissue remodeling and their inhibition can have a tumultuous impact on wound healing.

3.2 METHODS

3.2.1 Isolation and Culture of MDSCs and C2C12 Myoblasts

MDSCs were isolated from the GM muscle of 3-week-old C57BL/10J mice using a modified preplate technique (Gharaibeh, Lu et al. 2008; Li, Pan et al. 2010) and C2C12 myoblasts were purchased from ATCC (American Type Culture Collection). Both cell types were cultured in proliferation media containing phenol red DMEM supplemented with 10% FBS, 10% HS, 1 % P/S, and 0.5% CEE at 5% CO_2 and 37^{o}C.

3.2.2 Wound Migration Assay

MDSCs and C2C12 myoblasts were grown to near confluency in a non-coated multiwell plate. Prior to creating an artificial wound, several wells were treated with 25 µM of GM6001 for 3 and 6 hours. After the given amount of GM6001 pretreatment, an artificial wound was created by disrupting the cell monolayer with a sterile plastic pipette tip. Cellular debris was aspirated and proliferation media was added to the GM6001 pretreated cell groups. Another 2 groups of C2C12 myoblasts and MDSCs were treated with 2.5 and 25 µM GM6001 after creating an artificial wound. A live automated cell imager consisting of an inverted Nikon Eclipse TE 2000U microscope and Photometrics ES Cool Snap CCD camera was used to take images of cell migration into the artificial wound at 10 minute intervals for 6 hours. Cell migration was measured in microns (µm) by the distance traveled from the original wound site at 1, 3 and 6 hours.

3.2.3 Single Cell Migration

A live automated cell imager consisting of an inverted Nikon Eclipse TE 2000U microscope and Photometrics ES Cool Snap CCD camera was used to take images of single cell migration for 2 hours at 3 minute intervals. Proper environmental conditions were maintained in a microincubator at 37^{o}C and at 5% CO_2. Similar treatment groups were used as the wound migration assay, but only for MDSCs. All data analysis was assessed as previously described (Nishita, Tomizawa et al. 2005; Bae, Ding et al. 2009). A series of images were analyzed using NIH ImageJ analysis software to track the centroid positions (x,y) of cell nuclei (which were assumed to be the representations of cell-bodies). Net translocation distance was measured as the distance between the starting point and the end point of cells after 2 hours. Migration speed was calculated as total length of the migration path during the 2 hour period. The directional persistency index was calculated as the ratio of the net translocation distance to the cumulative length of the migration path. The change in the direction of cellular centroid movement between consecutive images (i-1, i, i+1) was calculated as $\Delta\theta = \theta_{i,i+1} - \theta_{i,i-1}$, where

$$\theta_{i,i+1} = \cos^{-1}\left(\frac{x_{i+1} - x_i}{\sqrt{(x_{i+1} - x_i)^2 + (y_{i+1} - y_i)^2}}\right),$$

and from these values, the standard deviation of $\Delta\theta$ was determined.

3.2.4 Proliferation Kinetics

A live cell automated imager captured images of the number of MDSCs and C2C12 cells per field of view at 20 minute intervals for 3 days. The population doubling time (PDT) as represented in the exponential equation $N_i = N_o 2^{\frac{t_i}{PDT}}$, was calculated by fitting an exponential

trendline to several measurements of N over the 3 day period. The exponential regression method provides a fitted curve in the form of $N_i = N_o e^{kt_i}$, where $k = \frac{\ln(2)}{PDT}$ and $PDT = \frac{\ln(2)}{k}$ (Deasy, Gharaibeh et al. 2005). The Click-iT EdU imaging kit (Invitrogen) was used to evaluate the cell proliferation as per the manufacturer's instructions. Briefly, MDSCs and C2C12 myoblasts were seeded on a 12 multiwell collagen coated plate at 2.5 x 10^3 cells and grown in proliferation media containing 0.1% EdU for 12 hours. Later, the cells were fixed and a specific secondary antibody, Alexa Fluor 594 (Invitrogen, 1:400), was used for EdU detection. Hoechst 33342 (Invitrogen) was used as a counter stain to visualize the cell nuclei at a 1:2000 dilution.

3.2.5 RT-PCR

MDSCs were subjected to a 25 µM treatment of GM6001 for 3 and 6 hours. Total RNA was extracted from the cells using the RNeasy plus mini kit (Qiagen) and cDNA was generated using the iScript cDNA Synthesis kit (Bio-Rad). For RT-PCR analysis after myogenic differentiation, the total RNA was also extracted from MDSCs after treatment with 25 µM of GM6001 for 3 and 6 hours and then cultured in myogenic differentiation media for 1 day. The sense and anti-sense primers for RT-PCR and their product size are found in Appendix B. The cycling parameter used for all primers were as follows: 94^{o}C for 5 minutes; PCR for 30 cycles of: denature for 45 seconds at 95^{o}C, anneal for 30 seconds (53^{o}C – 56^{o}C) and extend for 45 seconds at 72^{o}C. RT-PCR was performed using a Bio-Rad MyiQ thermal cycler.

3.2.6 Myogenic Differentiation

MDSCs were cultured in proliferation media until they nearly reached confluency. MDSCs were pretreated with 25 μM of GM6001 (Millipore) in DMEM for 3 and 6 hours prior to myogenic differentiation media (DMEM supplemented with 2% HS and 1% P/S). An additional group of cells did not receive a pretreatment, but instead received 25 μM of GM6001 for the duration of myogenic differentiation. At 5 and 7 days, MDSCs were fixed with formalin and evaluated for the presence of skeletal fast myosin heavy chain (MHC) positive myotubes (1:300, Sigma) and counterstained with DAPI (1000 ng/mL, Sigma). Fluorescent images captured on a Leica DMIRB microscope (Deerfield, IL) with a Retiga 1300 digital camera and acquired using Northern Eclipse software (version 6.0; Empix Imagining, Mississauga, ON, Canada). The fusion index was quantified by the ratio of the total number of nuclei in myotube fused cells with the total number of nuclei of the entire cell population (Urish, Vella et al. 2009).

3.2.7 Osteogenic Differentiation

Osteogenic differentiation was performed as previously described (Zheng, Cao et al. 2006). MDSCs were plated in a multiwell dish (3.0×10^3 cells per cm^2) and allowed to attach to the dish for 24 hours. Prior to osteogenic induction, MDSCs were treated with 25 μM of GM6001 (Millipore) in DMEM for 3 and 6 hours. After treatment, cells were cultured in osteogenic differentiation media (DMEM supplemented with β-glycerolephosphate (10mM, Sigma), dexamethasone (0.1 μM, Sigma), ascorbate-2-phosphate (50 μM, Sigma), BMP4 (25 ng/mL, R&D Systems), 10% FBS and 1% P/S). One group of MDSCs was treated continuously with 25 μM of GM6001 for the duration of osteogenic induction. Osteogenesis was assessed by

observing ALP activity 3 days after initial osteogenic induction using an alkaline phosphatase kit from Sigma (86C-1KT). Calcium deposition was also observed after osteogenic differentiation using Von Kossa and Alizarin red stains.

3.2.8 Adipogenic Differentiation

Adipogenic differentiation was performed as previously described (Zheng, Cao et al. 2006). MDSCs were plated in a multiwall dish (2.0×10^3 cells per well) and allowed to attach to the dish for 24 hours. Two groups of MDSCs received GM6001 at concentrations of 2.5 and 25 μM for the duration of adipogenic differentiation. Adipogenic differentiation media was DMEM supplemented with insulin (10 μM), dexamethasone (1 μM), isobutyl-methylxanthine (0.5 mM) and indomethacin (200 μM). Cell cultures were maintained for 14 days, with media changed every 2 days. After 2 weeks, cell cultures were fixed with 10% formalin for 10 minutes and stained with Oil Red O (Sigma), which is an indication of intracellular lipid accumulation. After being fixed with formalin solution, cells were rinsed with 60% isopropanol, and then incubated in filtered Oil Red O working solution at room temperature and rinse with double-distilled water after 15 minutes. Images were captured on a Leica DMIRB microscope (Deerfield, IL) with a Retiga 1300 digital camera and acquired using Northern Eclipse software (version 6.0; Empix Imagining, Mississauga, ON, Canada). Once images were acquired, water was removed from the wells and they were allowed to dry. The remaining Oil Red O was eluted by adding 100% isopropanol for 10 minutes and then transferred to a 96 multiwell plate, where the OD was measured at 500 nm for 0.5 seconds.

3.2.9 Laceration Injury Model

The laceration injury model was performed as previously described (Bedair, Liu et al. 2007). Four week old C57BL/10J mice (Jackson Laboratory) were anesthetized by isofluorane for the duration of the procedure. A posterior longitudinal skin incision was performed to permit exposure of the entire GM muscle. The GM muscle was cut at the largest diameter with a surgical blade, through the lateral 50% of their widths and 100% thickness. After controlling the bleeding by simple compression the skin was sutured with 4.0 silk thread. Both of the legs were similarly injured. After the injuries, animals were returned to their cages for recovery with commercial pellets and water ad libitum. The right leg GM muscle received 25 mg/kg body weight of GM6001 (Millipore), where the opposing left leg receive an injection of a sodium solution as a control at 1 and 4 days following the laceration injury. Three mice each were sacrificed at 7 and 12 days after laceration for analysis of fibrosis development and 2 mice were sacrificed at 5 days following laceration injury for examination stem cell marker histology. At the time sacrifice, the GM muscles were isolated, mounted, and snap frozen in liquid-nitrogen cooled 2-methylbutane. Samples were then serially sectioned at 10 μm widths at -28^{o}C with a cryostat for histological analysis.

3.2.10 Histology

The sections of GM muscle from each mouse were washed in PBS and stained with Masson's modified trichrome staining kit (IMEB) according to the manufacturer's specifications. This technique stains the muscle tissue red, collagen (or fibrous tissue) blue and the cell nuclei black. Five randomly selected high powered image fields of three sectioned slices of the injured area

were obtained using a Nikon Eclipse 800 fitted with a Spot camera (Diagnostic Instruments). Images were analyzed using CellProfiler image analysis software to measure the percent area of the collagen of the tissue section (Carpenter, Jones et al. 2006). Red and blue colors of each image were separated using the software program, where the area of the blue region was calculated and expressed as a percentage of the entire cross-sectional area of the muscle.

For immunohistochemistry, cross-sectional tissue sections of the GM muscle were fixed in 4% formalin. Afterward, the tissue slides were rinsed with PBS and 10% HS was used to block unspecific binding for 1 hour. Primary antibodies, dystrophin [1:200, Abcam] and Pax7 [1:100, DHSB]) were applied. For the Pax7 (produced in mice), the Vector Mouse on Mouse (MOM) kits (Vector Labs) were used to improve antibody specificity. Species specific secondary antibodies, Alexa Fluor 488 and 594 (1:400, Invitrogen), were used and the cell nuclei were counterstained with DAPI.

3.2.11 Measurement of Results and Statistical Analysis

RT-PCR analysis was performed using ImageJ software (version 1.32j, National Institutes of Health, Bethesda, MD) where the integrated density (product of the area and the mean gray value) of bands was calculated. All molecular bands were represented as a percentage of a standard gene, GAPDH. All data are expressed as a mean ± SD. Comparisons of groups were completed using a one-way ANOVA, where significance levels were determined using Tukey HSD pairwise comparison. Statistical significance was determined if $p < 0.05$.

3.3 RESULTS

3.3.1 Cell Migration

Cell migration was investigated based on pretreatment time (3 or 6 hours) with 25 µM of GM6001 prior to creating an artificial wound and administering GM6001 at two different concentrations (2.5 or 25 µM) after an artificial wound. Both pretreatment time and MMP inhibitor concentration reduced migration distance into the artificial wound for both cell types. Non-treated MDSCs (Figure 3.1, D-F) migrated further at 1, 3 and 6 hours after the artificial wound area was created in comparison to MDSCs that received 25µM of GM6001 as a pretreatment for 3 (Figure 3.1, A-C) and 6 hours as well as MDSCs that were administered GM6001 at concentrations 2.5 and 25 µM (Figure 3.1, G-I) during the cell migration period. A difference in the migration distances of MDSCs was observed between the control and the GM6001 pretreatment groups (Figure 3.1, J), as well as the MDSCS that received different concentrations of GM6001 (Figure 3.1, K). MDSCs treated with 25 µM of GM6001 migrated a shorter distance compared to the MDSCs treated with 2.5 µM of GM6001. A similar pattern of cell migration is observed for C2C12 myoblasts, despite their shorter migration distances in comparison to the MDSCs. Pretreatment times with GM6001 did reduce C2C12 migration 1 and 3 hours after the artificial wound was created, but at 6 hours, migration distances of C2C12 cells pretreated for 3 hours were comparable to the control (Figure 3.1, L). C2C12 myoblasts pretreated with GM6001 for 6 hours traveled significantly shorter distances than the untreated MDSCS, even at 6 hours after creating the artificial wound. C2C12 myoblast migration distances in response to different dosages of GM6001 were not nearly as significant compared to the MDSC migration results (Figure 3.1, M). Those cells that were treated with 2.5 µM of GM6001

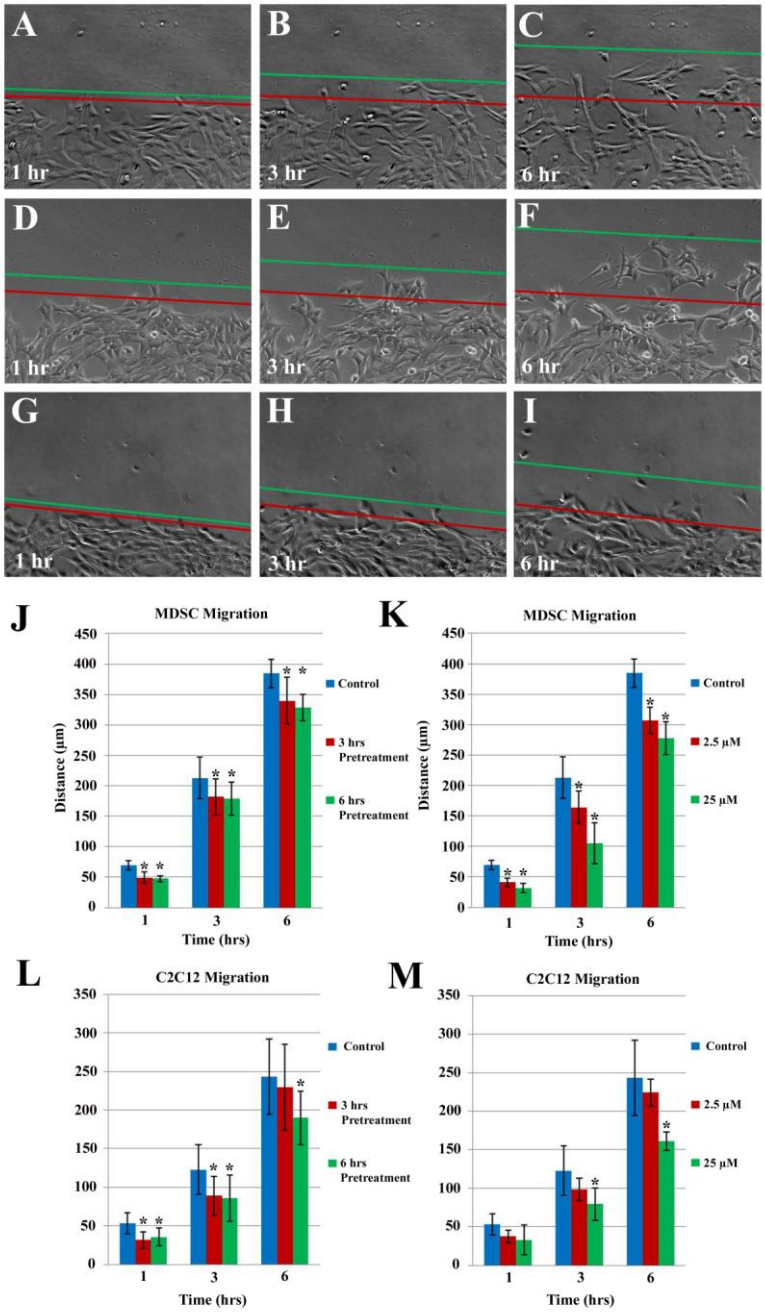

Figure 3.1: MDSC and C2C12 Cell Migration

Cell migration is reduced with the administration of GM6001. A-I: phase contrast images taken of MDSCs using a live automated cell imager at 1 (A, D, G), 3 (B, E, H) and 6 (C, F, H) hours of MDSCs pretreated for 3 hours with 25µM GM6001 prior to an artificial wound (A, B, C), MDSCs with no treatment (D, E, F), and 25µM GM6001 added to cell culture after artificial wound (G, H, I). The red line indicates the initial edge of the wound and the green line indicates the position of the cells after 1, 3 or 6 hours of migration into the wound area. Statistical analysis of MDSC (J, K) and C2C12 myoblast (L, M) migration based on pretreatment time with 25µM GM6001 and concentration (0, 2.5, 25µM) after the creation of an artificial wound. There is a significant difference (*P<0.05) from the non-treated group (control) at each time point.

had reduced migration distances, yet the results were not significant compared with the control, suggesting that their cell migration is not dominated by MMP activity. At a ten-fold increase, 25 μM GM6001 did significantly reduce the migration at 3 and 6 hours after beginning the wound assay.

For gene expression analysis, MDSCs grown to near confluency received 25μM GM6001 for 3 and 6 hours prior to examination for cell adhesion genes. The RNA content of the MDSCs was isolated and cell adhesion genes, β-catenin, N-cadherin and NCAM were evaluated (Figure 3.2). For the cell adhesion markers, there appears to be some gene expression in the MDSCs that did not receive GM6001 treatment. By three hours of treatment with GM6001, the gene expression of β-catenin and N-cadherin increased and continued at 6 hours of treatment. The gene expression of NCAM, however, remained unaffected by the GM6001 treatment at 3 hours, but by 6 hours, there was an increase in its expression. TIMP1, which is recognized for its inhibitory role of MMPs and anti-apoptotic affects on cells, exhibited the opposite relation to GM6001 treatment. The gene expression of TIMP1 is relatively high in untreated MDSCs and is not influenced by GM6001 treatment after 3 hours, but by 6 hours of treatment with GM6001, its gene expression has become very minimal.

To further investigate the affect of GM6001 on cell migration, time-lapse video microscopy was used to examine the migration pathways of MDSCs under different treatments. This experiment is representative of the *in vivo* conditions of MDSCs, whereby single MDSCs would migrate in response to an injury, instead of a clustered group. Similar treatment groups of GM6001 were observed as before, where several plates of MDSCs treated with 25μM for 3 and 6 hours prior to time-lapse video microscopy. Two other groups were administered 2.5 μM and 25 μM of GM6001, and then immediately subjected to video imaging. All of the actual cell

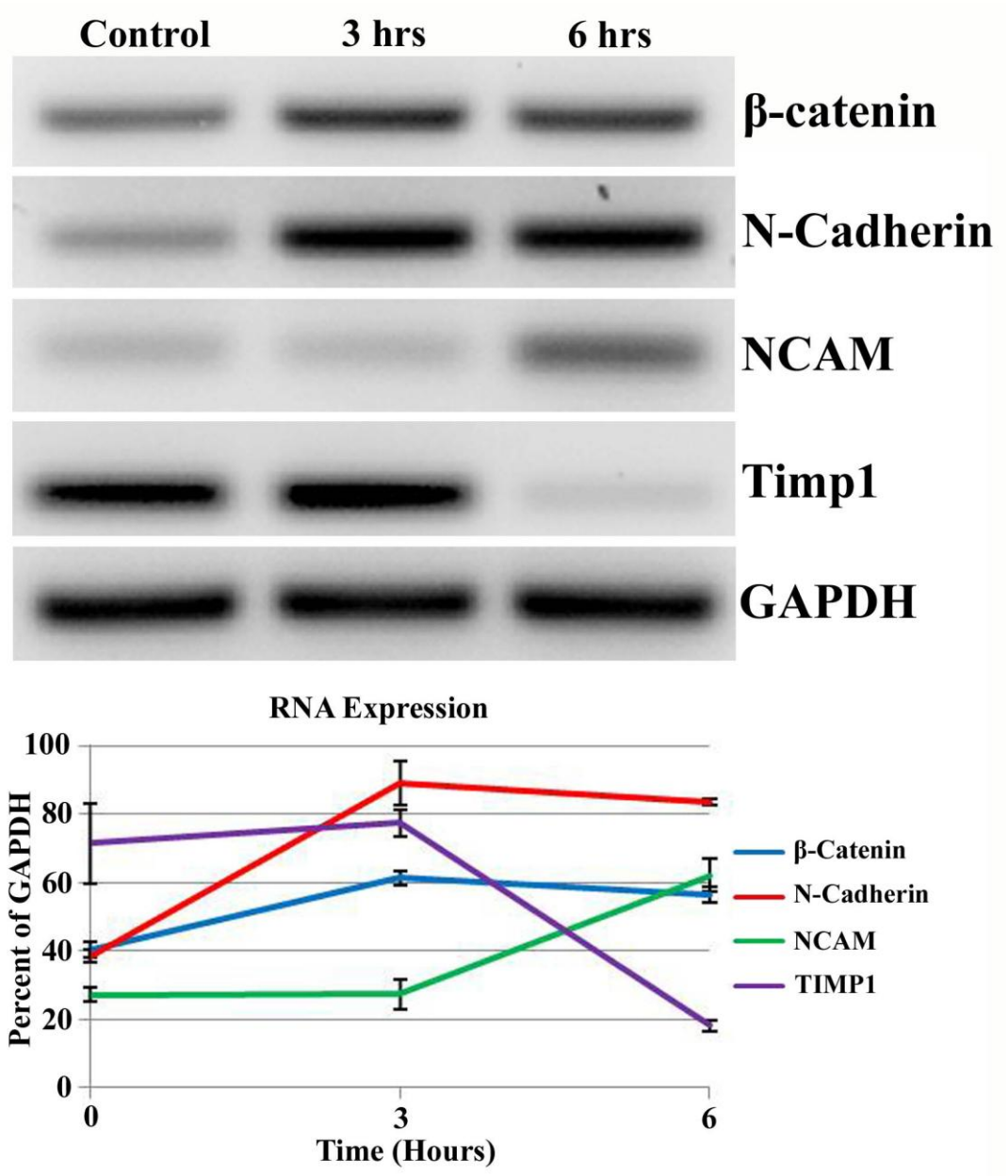

Figure 3.2: MDSC Adhesion Gene Expression
Gene expression of MDSCs is altered by GM6001 administration, Cell adhesion genes, β-catenin, N-cadherin and NCAM, in addition to TIMP1 are evaluated 3 and 6 hours after treatment with 25 μM of GM6001. GAPDH was used as a loading control.

trajectories from each of the different groups were obtained from a 2 hour period where the data was pooled from 3 experiments (Figure 3.3). The trajectories of MDSCs not treated with GM6001, migrated much further than the MDSCs pretreated with GM6001 or MDSCs administered different concentrations of GM6001.

Quantitative analysis of the single cell migration path revealed a significantly decreased net translocation distance (straight distance from the cell's origin to the end point) (Figure 3.4, A, B) and decreased migration speed (total length of the migration path per hour) (Figure 3.4, C, D) for MDSCs that received any form of GM6001 treatment. Interestingly, there was no difference in the net translocation distance and migration speed between the different concentrations of GM6001. However since these cells were administered GM6001 at the initiation of the cell trajectory recording, these MDSCs were not exposed to GM6001 nearly as long as the pretreatment groups, thus their net translocation distance and migration speed were higher than the pretreatment groups, but still lower compared to the control. When the time-lapse video recording was started with the groups pretreated with GM6001, the media was replaced and then substituted with only DMEM. This data indicates that the effect of GM6001 exposure occurs quite quickly and when removed, it continues to have a residual impact on cell migration.

As a result, differences in the directional persistency index (ratio of the net translocation distance to the cumulative length of the migration path) (Figure 3.5, A, B) and the centroid directional movement (a measure of the change in the direction of the centroid movement of a single cell) (Figure 3.5, C, D) of MDSCs were observed. MDSCs not treated with GM6001 tended to migrate further from their starting location by maintaining the same direction of their pathway as demonstrated with a higher directional persistency index in comparison to MDSCs treated with any form of GM6001. These results corresponded moderately with the results of

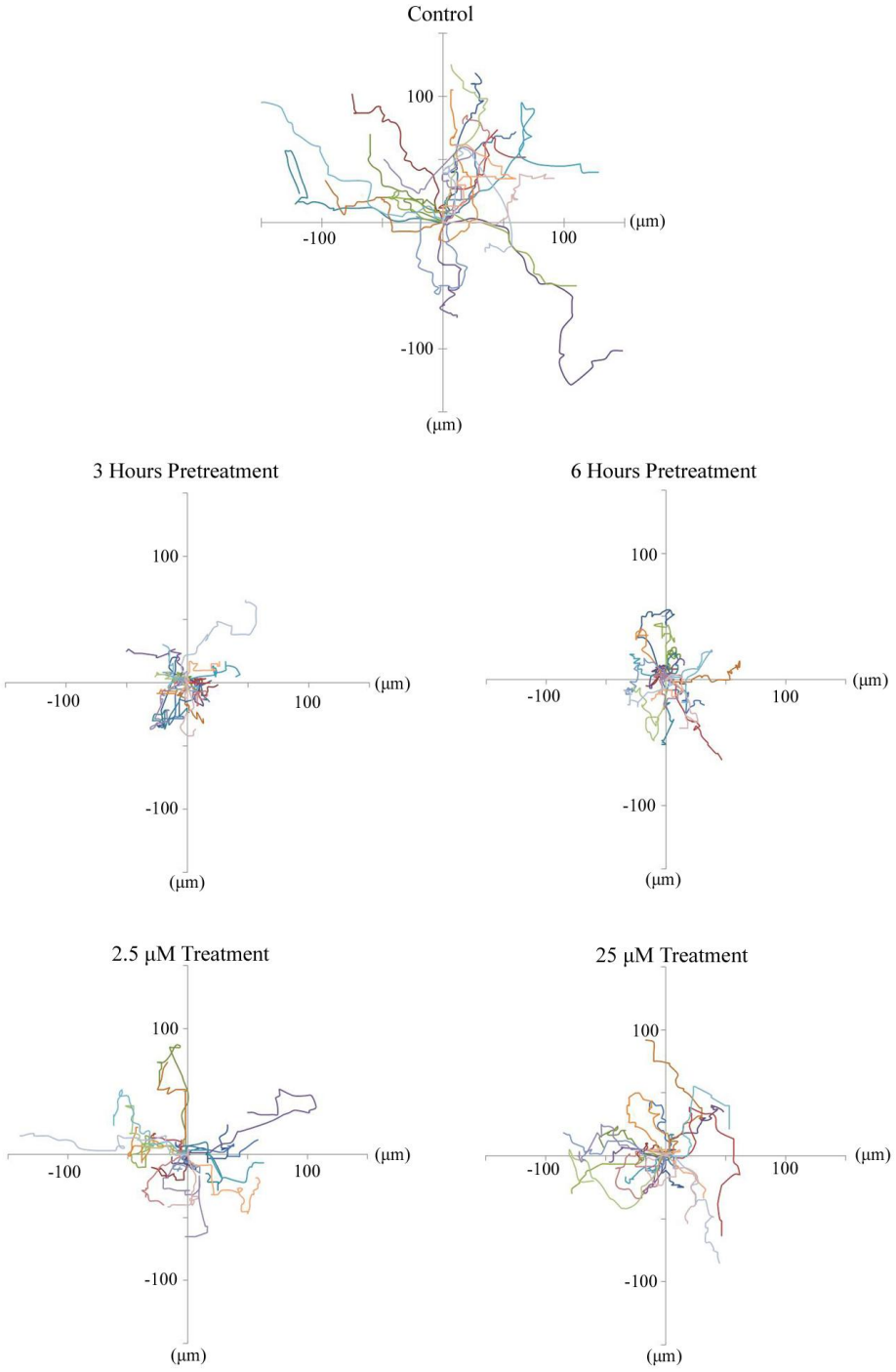

Figure 3.3: Single Cell Migration Pathways of MDSCs
The migration paths of 20 individual MDSCs of different experimental groups captured in a time-lapse motility assay (data was pooled from three independent experiments.)

centroid directional movement. The change centroid directional movement (Δθ) was calculated as a function of time, from which the standard deviation of Δθ was determined where a higher value indicates a larger fluctuation in the directionality of the cell movement. A lower directional persistency index value for the MDSCs that received any form of GM6001 treatment typically corresponded with a higher value of the standard deviation of Δθ, however only the MDSCs pretreated with 25 µM of GM6001 for 3 hours was significantly different from the control. Non-treated MDSCs exhibited a higher directional persistency index with a lower standard deviation of Δθ.

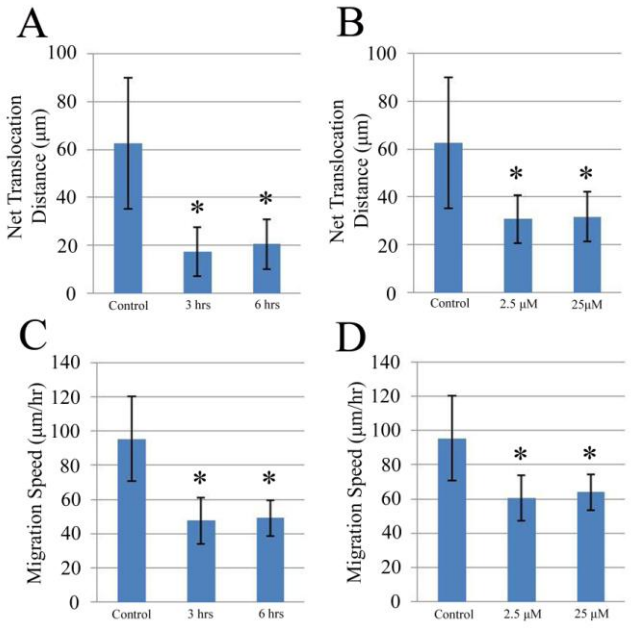

Figure 3.4: Net Translocation Distance and Migration Speed of Single MDSCs
The net translocation distance (straight distance from the start to the end point) of each MDSC over a 2 hour period is represented as the mean ± standard deviation of the paths of 20 randomly selected cells that were either pretreatment with 25 µM of GM6001 (A) prior to image capture or treated with different concentrations (B) at the start of image capture. The migration speed (total length of the migration path per hour) of each cell is shown as the mean ± standard deviation of 20 randomly selected cells that were either pretreated with 25 µM of GM6001 (C) prior to image capture or treated with different concentrations (D) at the start of image capture. There is a significant difference (*P<0.05) from the non-treated group (control) and each treatment.

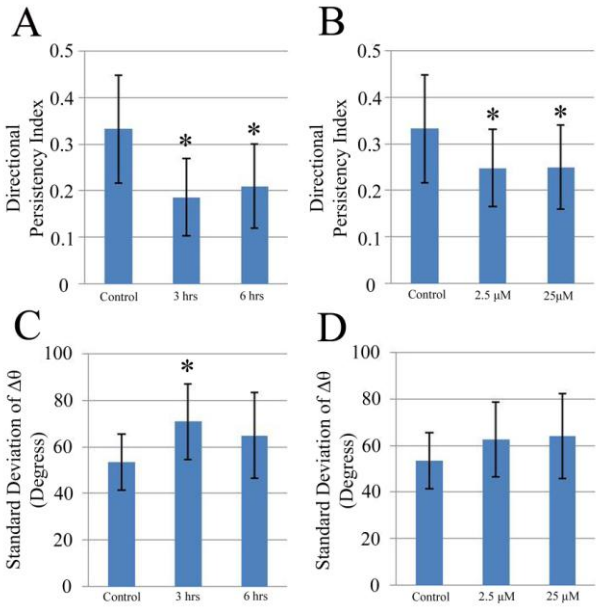

Figure 3.5: Directional Persistency Index and Centroid Directional Movement
The directional persistency index (ratio of the net translocation distance to the cumulative length of the migration path) of each MDSC over a 2 hour period is represented as the mean ± standard deviation of the paths of 20 randomly selected cells that were either pretreated with 25 µM of GM6001 (A) prior to image capture or treated with different concentrations (B) at the start of image capture. The centroid directional movement (a measure of the change in the direction of the centroid movement of a single cell) is shown as the mean ± standard deviation of 20 randomly selected cells that were either pretreated with 25 µM of GM6001 (C) prior to image capture or treated with different concentrations (D) at the start of image capture. There is a significant difference (*P<0.05) from the non-treated group (control) and each treatment.

3.3.2 Cell Proliferation

The expression or secretion of MMPs is associated with cell proliferation depending on cell type. In these experiments, MDSC proliferation was evaluated with a variety of GM6001 treatments and in comparison with GM6001 treated C2C12 myoblasts. MDSCs and C2C12 myoblasts were treated with 25µM of GM6001 for 3 and 6 hours. After the allotted time of treatment, the supplemented GM6001 culture media was replaced with normal muscle cell proliferation media and live cell imaging was used to capture images at fixed locations. Similarly, two groups of cells received cell proliferation media supplemented with either 2.5 µM or 25 µM and then imaged using a live cell imager. Once the data was collected over a period of 3 days, the number

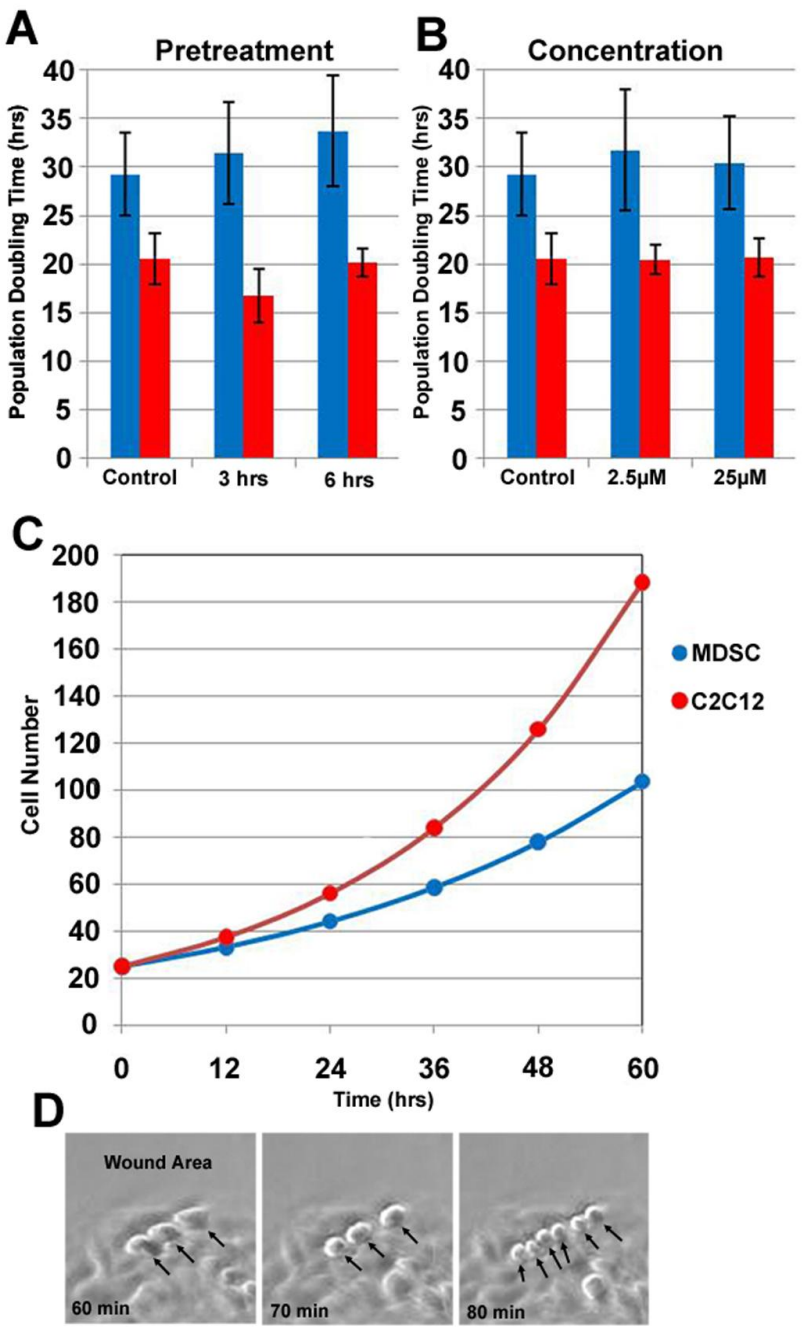

Figure 3.6: MDSC and C2C12 Myoblast Population Doubling Time
The population doubling time of MDSCs and C2C12 myoblasts were unaffected based on pretreatment time (A) and different concentrations (B) of GM6001 administered to the cells. A representative graph (C) showing the cell number of each cell type using the average PDT in the equation, $N_i = N_o 2^{(ti/PDT)}$, with N_o = 25 cells. Three C2C12 myoblasts are shown undergoing cell division 60, 70 and 80 minutes at the edge of an artificially created wound, in vitro (D), as denoted by the black arrows.

of cells per field of view was plotted as a function of time. The exponential regression line was fitted to the data using the equation, $N_i = N_o e^{kt_i}$, and the PDT was calculated.

The results of this study indicated that there was no difference in the PDT of MDSCs nor C2C12 myoblasts treated with GM6001 for different time periods (Figure 3.6, A) or that received different concentrations of GM6001 (Figure 3.6, B). There was, however, a difference in the cell proliferation between both groups. MDSCs had a PDT of approximately 30 hours, while the C2C12 myoblasts had a PDT of around 20 hours. The difference in PDT would typically result in double the number of C2C12 myoblasts over MDSCs after 60 hours. During the artificial wound assay, the migration distances of the control group of C2C12 myoblasts were significantly less than the control group of the MDSCs. Specifically, more cell proliferation of the C2C12 myoblasts was observed at the edges of the artificially created wound assay during the 6 hour time period (Figure 3.6, D).

Cell proliferation of MDSCs and C2C12 myoblasts was confirmed using an EdU assay. The EdU is a nucleoside analog of thymidine that is incorporated into DNA during active DNA synthesis and is detected by the copper-catalyzed covalent reaction between the azide and the alkyne. The percentage of MDSCs that incorporated EdU (Figure 3.7, A) with or without GM6001 treatment was roughly 40%, much lower than the percentage of C2C12 myoblasts that incorporated EdU at around 80% (Figure 3.7, B) over a 12 hour incubation period. Similarly, there was no difference in EdU incorporation for MDSCs or C2C12 myoblasts that were pretreated (Figure 3.7, C) or received varying concentrations (Figure 3.7, D) of GM6001 treatment compared to the control.

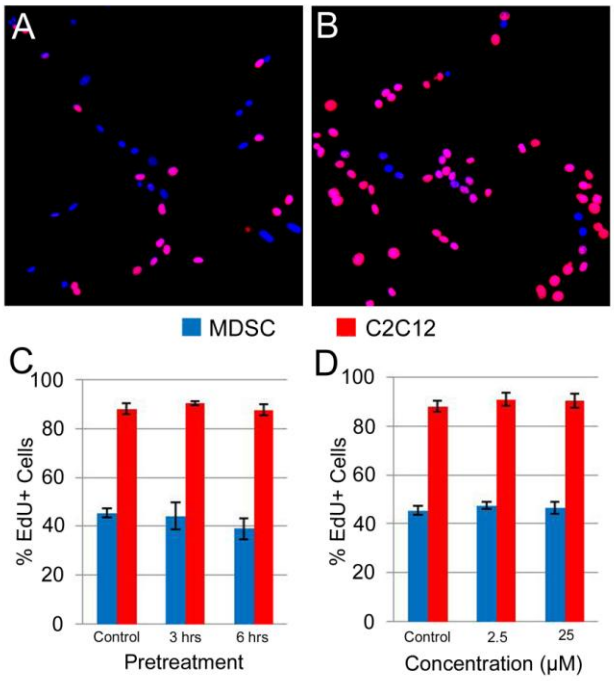

Figure 3.7: MDSC and C2C12 EdU Assay
C2C12 cells (B) exhibit a greater expression of EdU (red) compared to MDSCs (A) regardless of MMP inhibition pretreatment (C) or different concentrations (D). All cells were stained with Hoechst 33342 (blue).

3.3.3 Stem Cell Characteristics and Multiple Differentiation

Since MMP1 stimulation influenced primary mouse myoblasts to exhibit stem cell characteristics, this prompted further investigation whether MMP inhibition had any detrimental effects on MDSC behavior besides impairing cell migration. As previously published, MDSCs characteristically express Sca1 and CD34 (Lee, Qu-Petersen et al. 2000; Jankowski, Haluszczak et al. 2001; Jankowski, Deasy et al. 2002). At the gene expression level, normal MDSCs express a high level of CD34 and Sca1 (Figure 3.8). When these cells are treated with 25 μM of GM6001 for 3 and 6 hours, their gene expression of Sca1 and CD34 is markedly reduced. The decrease in gene expression of Sca1 appears dependent on time, whereas, the gene expression of CD34 initially decreases at 3 hours, and then increases at 6 hours, but not to its original level.

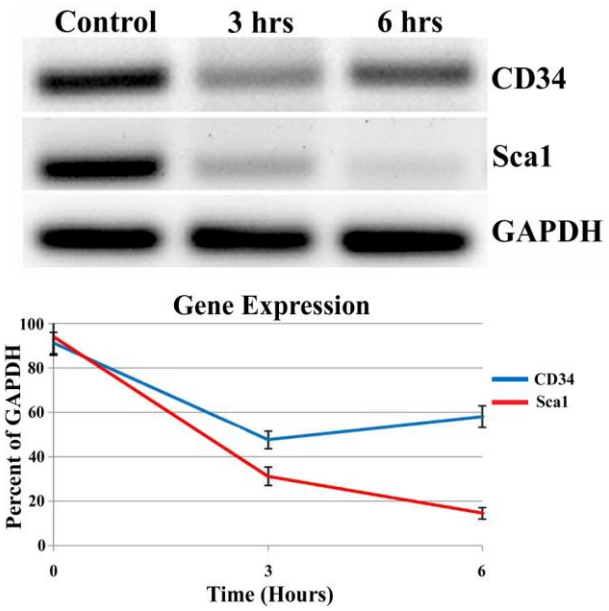

Figure 3.8: MDSC Gene Expression of Stem Cell Markers
The gene expression of MDSCs treated with 25μM of GM6001 for 3 and 6 hours. These results indicate that MDSCs treated with an MMP inhibitor had reduced expression of stem cell markers, CD34 and Sca1. GAPDH was used as a loading control.

With apparent differences in the gene expression of markers associated with MDSCs, their attribute of multipotency was explored. MDSCs normally proliferate when cultured in growth media with serum, however, in serum free conditions; they exhibit a tendency to differentiate in multinucleated myotubes. MMP inhibition was investigated to determine whether it would reduce myotube formation *in vitro* using a myogenic differentiation assay. Four groups were assessed including: no treatment (Figure 3.9, A), 3 (Figure 3.9, B) and 6 (Figure 3.9, C) hours pretreatment with GM6001, and GM6001 treatment for the duration of the myogenic differentiation assay (Figure 3.9, D). After 5 and 7 days in myogenic differentiation media, the fusion index was quantified using fluorescent microscopy by the ratio of the number of cell nuclei within the myotube fused cells stained positive for MHC to the total number of nuclei of the entire cell population (Figure 3.9, E). When comparing the different GM6001 treatment groups, there were no differences in the fusion index, however, all forms of GM6001 treatment

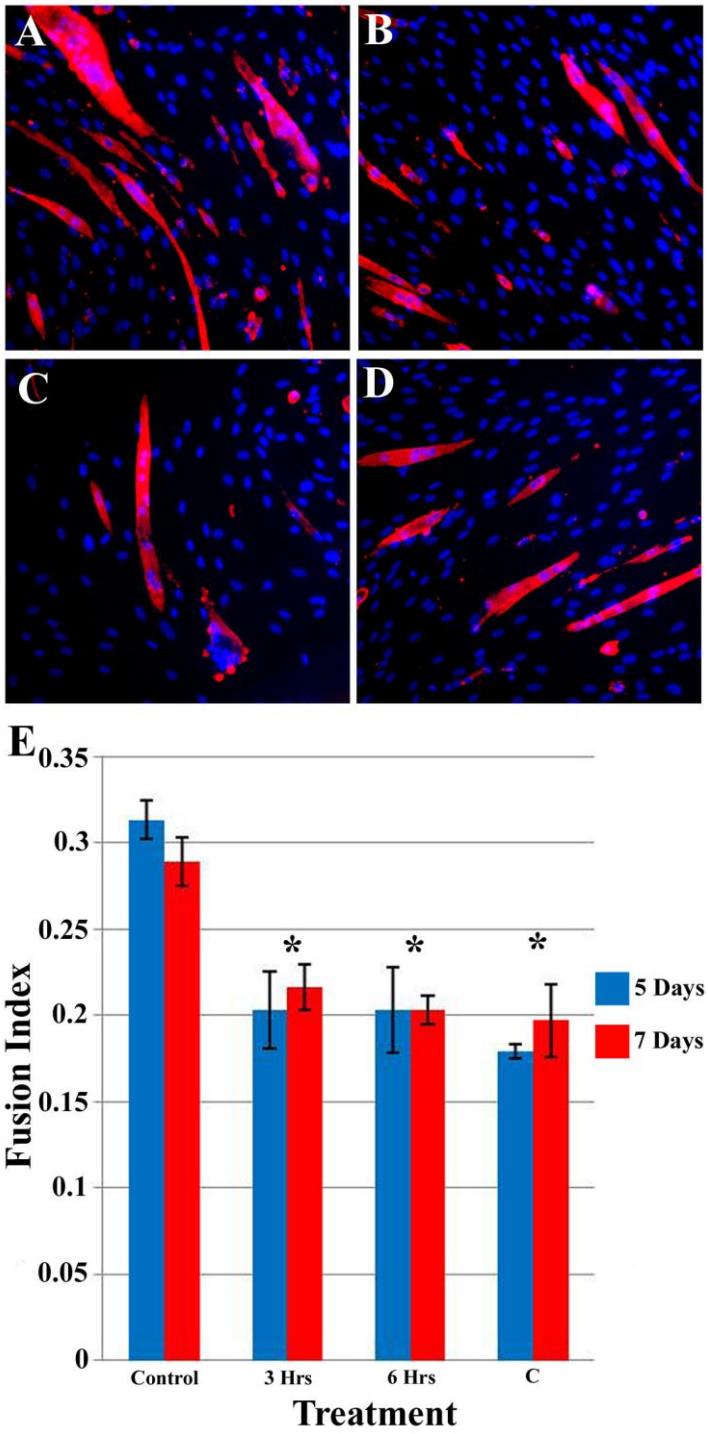

Figure 3.9: MDSC Myogenic Differentiation
MMP inhibitor, GM6001, reduces muscle cell myotube formation. Immunostaining of MHC (red) in MDSC (A-D). Control, no GM6001 treatment (A); 3 (B) and 6 (C) hours pretreatment with GM6001 before myogenic differentiation; and myogenic differentiation media with GM6001 and no pretreatment (D, H). E: Statistical analysis of the fusion index of MDSCs after 5 and 7 days. There is a significant difference (*P<0.05) between treated groups and the non-treated group (control) at each time point.

negatively affected the myogenic differentiation potential of the MDSCs by producing a lower fusion index. There was no difference seen between groups subjected to 5 or 7 days of myogenic differentiation.

For gene expression analysis, MDSCs received GM6001 pretreatment for 3 and 6 hours prior to the addition myogenic differentiation media, and 1 day later, the mRNA was isolated for RT-PCR. Genes in the myogenic regulatory factor family, MyoD, Myf5 and Myf6 were observed (Figure 3.10). The gene expression of MyoD was very strong in the initiation of myogenic differentiation of MDSCs, but the expression was severely affected with the administration of GM6001 for 3 and 6 hours. Myf5 and Myf6 exhibited similar influence, with more of a decrease in expression occurring at 6 hours for Myf5 and 3 hours for Myf6. M-cadherin, known as an adhesion molecule associated with terminal muscle cell differentiation in myotubes, showed a decrease in gene expression by 6 hours of GM6001 treatment, resembling an expression pattern of Myf5. One gene related to cell signaling and myogenesis of muscle cells, Notch1, were examined. Notch1 exhibited similar behavior as the gene expression as M-cadherin gene, where its gene expression was significantly reduced after 6 hours with GM6001 treatment. These data suggest that the use of GM6001 has a negative impact on myotube formation by altering the expression of genes related to myogenesis.

The multipotency of MDSCs has been observed by its capacity to undergo osteogenic differentiation in addition to myogenic differentiation (Corsi, Pollett et al. 2007; Kim, Lee et al. 2008; Payne, Meszaros et al. 2010). MDSCs were plated at a moderate density and cultured in osteogenic differentiation media supplemented with a minimal amount of BMP4 (25 ng/mL) such that osteogenesis was driven by the MDSCs multipotency, not BMP4. After 3 days of osteogenic induction, MDSCs were assessed for ALP expression to mark cell differentiation

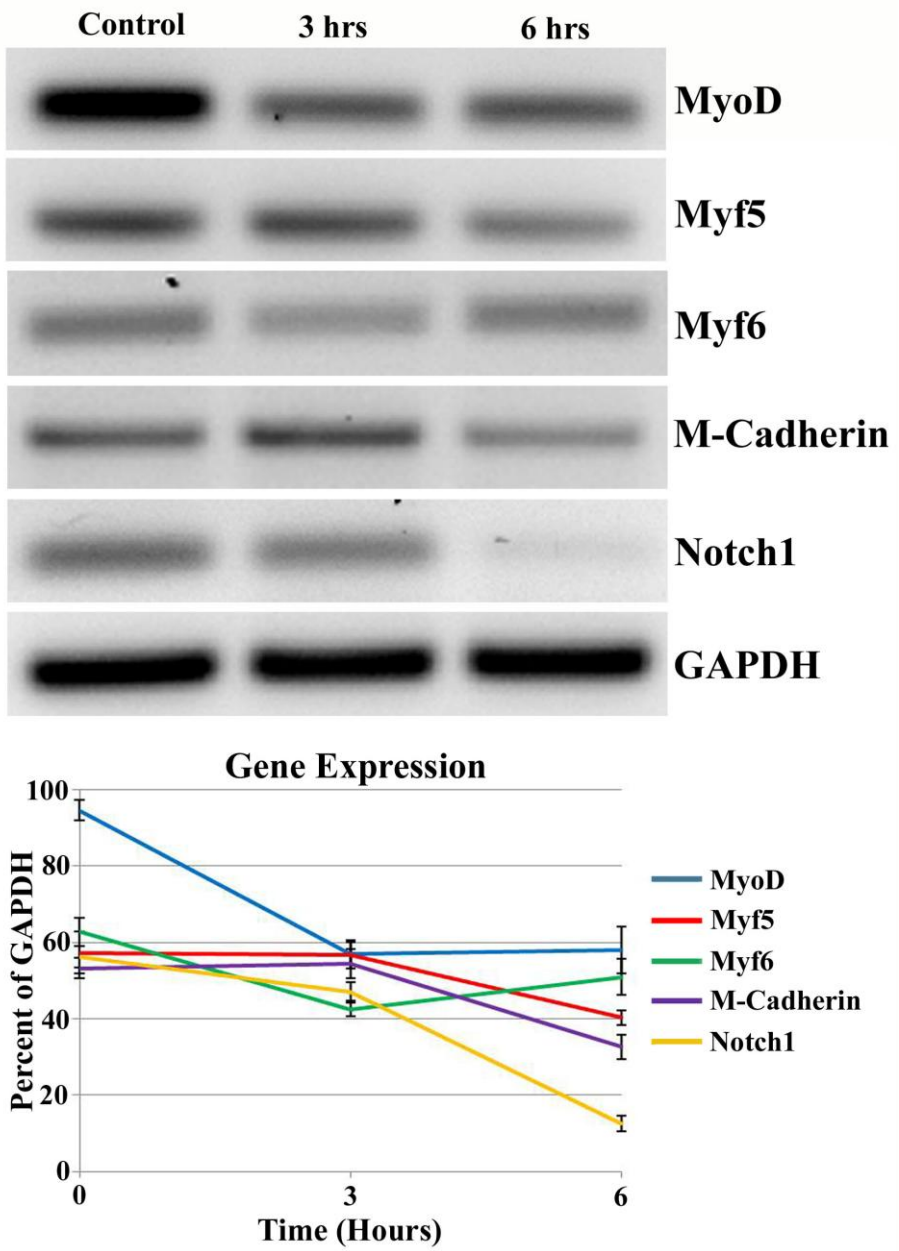

Figure 3.10: MDSC Myogenic Gene Expression
MMP inhibitor, GM6001, negatively impacts genes associated with myotube formation in MDSCs. Gene expression was examined for 4 genes related to myogenic differentiation (MyoD, Myf5, Myf6 and M-cadherin) and 1 signaling genes (Notch1) after 3 and 6 hours pretreatment with GM6001 and 1 day cultured with myogenic differentiation media. GAPDH was used as loading control.

All forms of GM6001 treatment: 3 (Figure 3.11, B) and 6 (Figure 3.11, C) hours of pretreatment with 25µM of GM6001, and continuous treatment of 25µM of GM6001 (Figure 3.11, D) negatively impacted their osteogenic differentiation potential compared to non-treated cells (Figure 3.11, A). Approximately 60% of the MDSCs that received some form of GM6001 treatment expressed ALP in comparison to 85% of the cells in the control (Figure 3.11, E).

The osteogenic differentiation potential of MDSCs was further examined using to alternative stains to test osteogenesis, Von Kossa (Figure 3.12, A-D) and alizarin red (Figure, 3.12, E-H). The same treatment groups: control (Figure 3.12, A, E), 3 (Figure 3.12, B, F), and 6 (Figure 3.12, C, G) hours treatment with 25µM with GM6001 prior to osteogenic induction, and 25µM of GM6001 for the entire duration of osteogenic differentiation (Figure 3.12, D, H) were tested. The Von Kossa stain was used to assess mineralization of the MDSCs after 7 days in

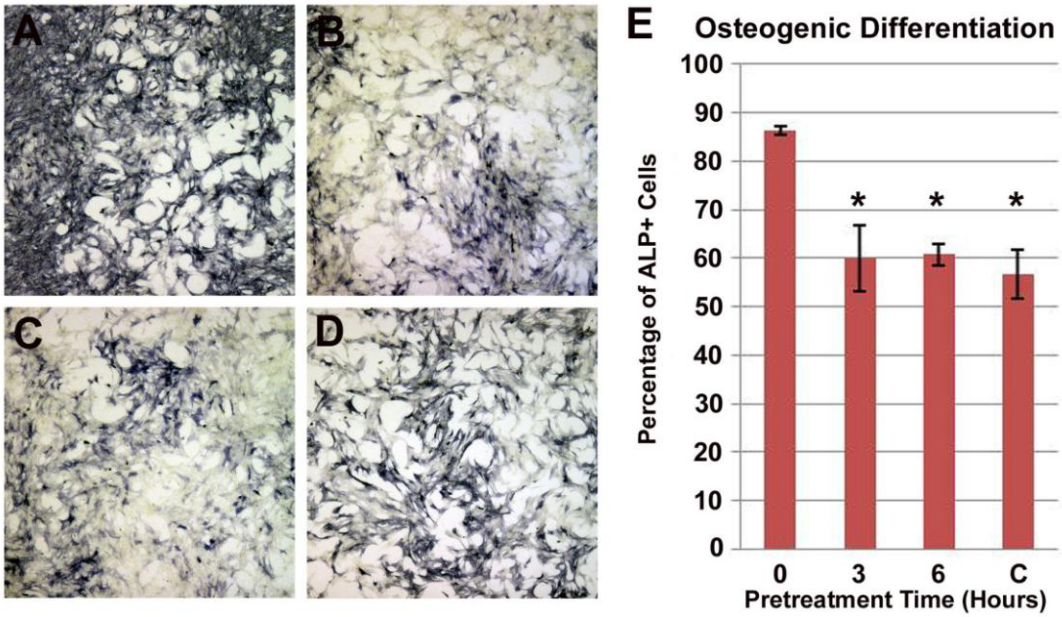

Figure 3.11: MDSC ALP Expression
MDSC treated with GM6001 exhibited a reduced osteogenic differentiation potential. Four groups were investigated: no treatment (A), 3 (B) and 6 (C) hours pretreatment with 25 µM of GM6001 before osteogenic differentiation; and GM6001 treatment for the duration of the osteogenic differentiation (denoted as C in (E)). ALP positive cells are dark blue under bright field microscopy. The percentage of ALP positive cells after 3 days of osteogenic differentiation is shown in (E). There is a significant difference (*P<0.05) between the control and other groups.

osteogenic differentiation media by the presence of a black color. Mineralization was observed in all of the test groups of MDSCs, however, the mineralization that occurred in the control groups appeared more frequently and larger. Since the Von Kossa stain alone is often not considered sufficient enough to detect *in vitro* mineralization because the silver ions in the staining solution are reacting on the phosphate in the cell culture, an alizarin red stain was also employed (Bonewald, Harris et al. 2003). Alizarin red identifies the calcium-rich deposits in the MDSCs and the results of the staining yielded a similar outcome as the Von Kossa staining.

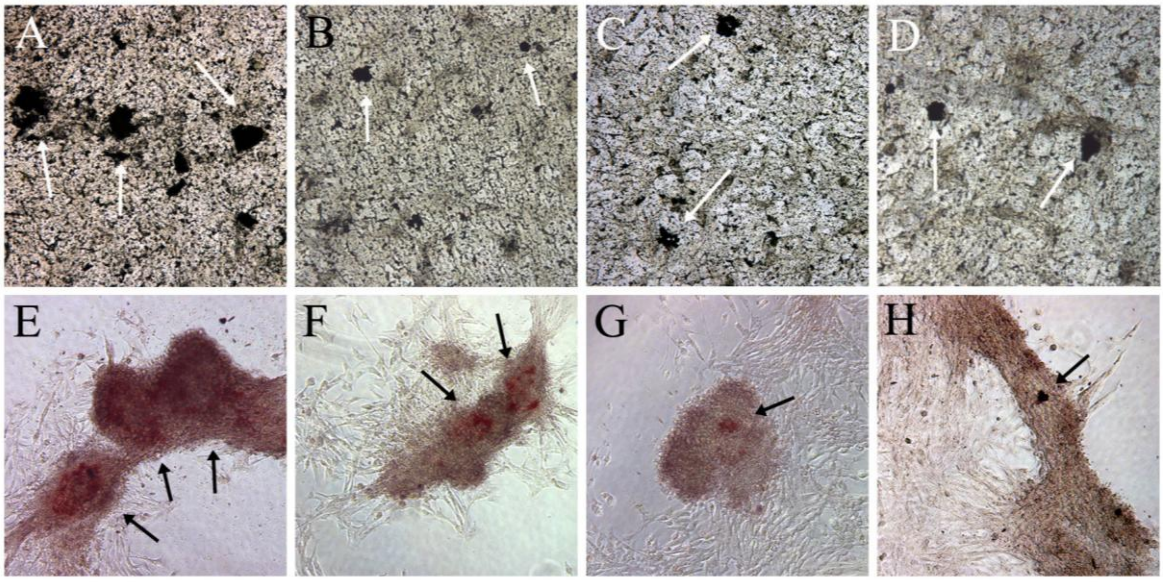

Figure 3.12: Von Kossa and Alizarin Red Stains of MDSCs
MDSCs treated with GM6001 exhibited a reduced expression for calcium deposition by Von Kossa (A-D) and Alizarin red (E-H) stain after 7 days of osteogenic differentiation. Four groups were investigated: no treatment (A & E), 3 (B & F) and 6 (C & G) hours pretreatment with 25 µM of GM6001 before initiating osteogenesis; and 25 µM of GM6001 treatment for the duration of the osteogenic differentiation (D & H). All images were taken at 10x magnification using phase contrast microscopy with white arrows denoting calcium deposition for the Von Kossa stain and black arrows denoting the red from the Alizarin red stain.

MDSCs only began to exhibit alizarin red when they grew in noticeably clustered manner. Within these clustering of cells, more alizarin red was found for the control group of MDSCs compared to MDSCs that were administered any form of GM6001. Only one spec of alizarin red

was detect on a cluster of MDSCs within the treatment group that received GM6001 for the duration of osteogenesis.

To verify that the reduced osteogenic differentiation potential of the MDSCs was not the effect of GM6001 interacting with BMP4 to decrease cell proliferation, an EdU assay was employed. Using the identical treatment groups as before, MDSCs were cultured in osteogenic differentiation media for 5 days, with the EdU solution incubated during the final 12 hours of osteogenic induction. The results of the assay yielded no difference between any of the groups during osteogenic differentiation in the percentage of cells that incorporated EdU into their DNA (Figure 3.13). Approximately 15% of the MDSCs across all groups were actively proliferating during osteogenic differentiation, which was considerably less than the 40% of MDSCs that were proliferating during a 12 hour period while in normal proliferation media.

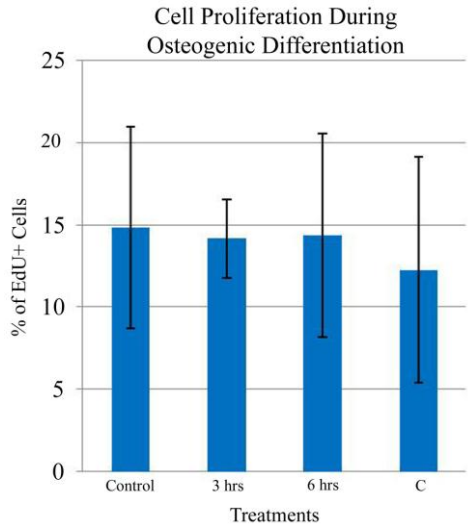

Figure 3.13: Cell Proliferation During Osteogenic Differentiation with MDSCs
The percentage of MDSCs that incorporated EdU during cell division is shown. No difference (*P<0.05) is observed between the control, 3 and 6 hours of pretreatment with 25 µM of GM6001, and continuous treatment with 25 µM GM6001 during the osteogenic differentiation assay for 5 days.

Finally, the ability of MDSCs to undergo adipogenesis in the presence of an MMP inhibitor was investigated. In this experiment, 2 groups of MDSCs were cultured in adipogenic differentiation media supplemented with either 2.5 µM (Figure 3.14, B) or 25 µM (Figure 3.14,

C) of GM6001 and compared to control groups of MDSCs (Figure 3.14, A). An Oil Red O staining was performed after 2 weeks, revealing the cytoplasmic lipid droplets, which are an indication of the adipogenic phenotype. The degree of lipid droplet accumulation was quantified by removing the total amount of Oil Red O within the MDSCs and measuring its OD at 500nm (Figure 3.14, D). While there was no difference between the groups treated with GM6001, there was a significantly higher accumulation of lipids within the non-treated MDSCs. Unlike adipocytes where lipid droplets have a large appearance within the cell, the intracellular lipids in the MDSCs after 2 weeks of adipogenesis were small and in abundance within the cytoplasm.

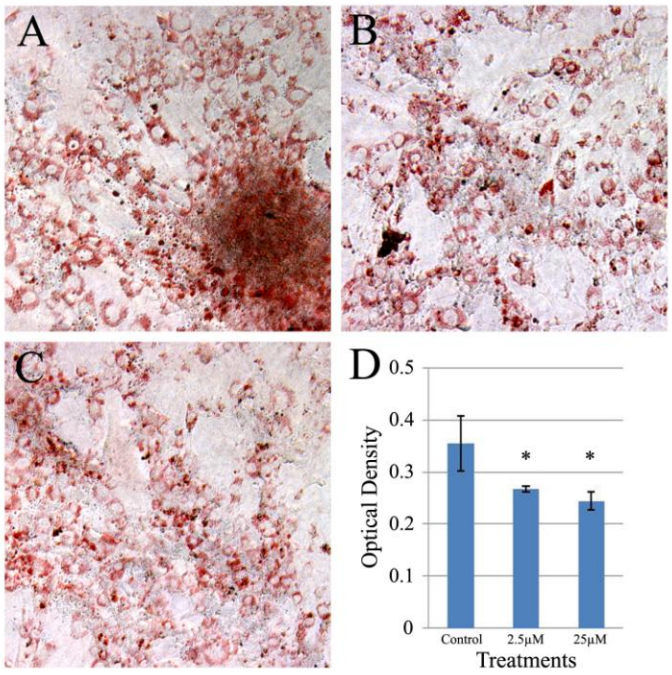

Figure 3.14: Adipogenic Differentiation of MDSCs
Primary mouse myoblasts treated with GM6001 exhibited reduced accumulation of lipids (red) within the cytoplasm after 2 weeks as shown with oil red O staining. Three groups were investigated: no treatment (A), 2.5 µM (B) and 25 µM (C) of GM6001 for the duration of the adipogenic differentiation. The optical density was used to quantify adipogenesis (D). There is a significant difference (*P<0.05) between the control and other groups.

3.3.4 *In Vivo* Effects of MMP Inhibition

As demonstrated, the use of a broad spectrum MMP inhibitor, GM6001, has a number of negative effects on MDSCs as well as C2C12 myoblasts *in vitro*, which play important roles in the healing of skeletal muscle tissue. During skeletal muscle injury, MDSCs or muscle progenitor cells are activated from their residing location between the basal lamina and myofibers (Peault, Rudnicki et al. 2007). These cells can be detected by their expression of Pax7, which regulates the maintenance of these MDSCs by regulating other myogenic genes such as MyoD and Myf5 (Pawlikowski, Lee et al. 2009). For *in vivo* experimentation, laceration injuries were performed on the GM muscle of several mice with injections of 25mg/kg GM6001 at 1 and 4 days following the injury. On day 5, the GM was harvested and histologically observed for Pax7 and dystrophin expression. A qualitative assessment revealed that mice which did not receive GM6001 treatment after a laceration injury (Figure 3.15, A) expressed more Pax7

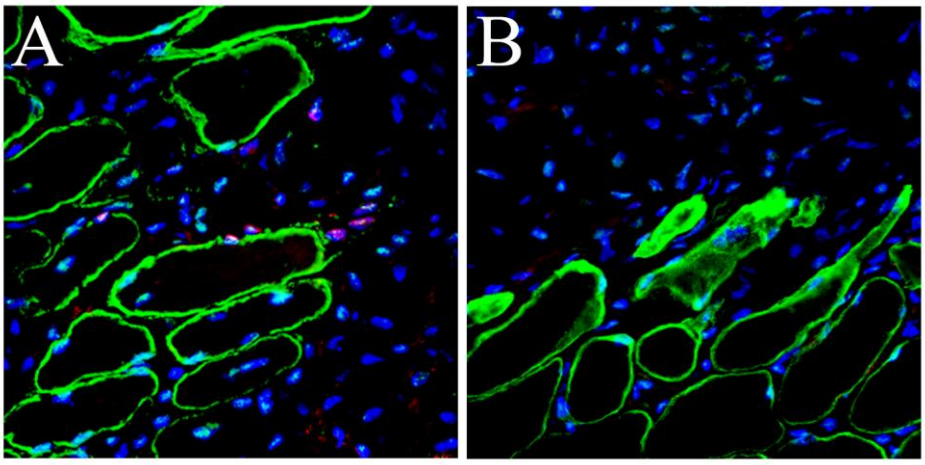

Figure 3.15: Pax7 Expression after GM6001 Administration
Pax7 expression (red) was reduced 5 days after laceration injury with GM6001 administration (B) in comparison to non-treated laceration injuries (A). Dystrophin (green) and cell nuclei (blue) were also counterstained.

positive cells in comparison to mice who received GM6001 treatment (Figure 3.15, B). The expression of dystrophin in either case appeared to be relatively unaffected by GM6001 administration.

At later time points, the GM muscle was isolated and analyzed for collagen deposition during muscle recovery. The GM muscle that received GM6001 treatment at 7 days (Figure 3.16, B) had an elevated level of collagen deposition compared to GM muscle that did not receive treatment (Figure, 3.16, A). Similar results were also observed at 12 days after the laceration injury, where the percentage of collagen deposition with GM6001 treatment was greater than the GM muscle that did not receive any form of treatment (Figure 3.16, C). The percentage of collagen deposition decreased with more recovery time, however, there was no significant difference between muscle tissue that did or did not receive GM6001 treatment.

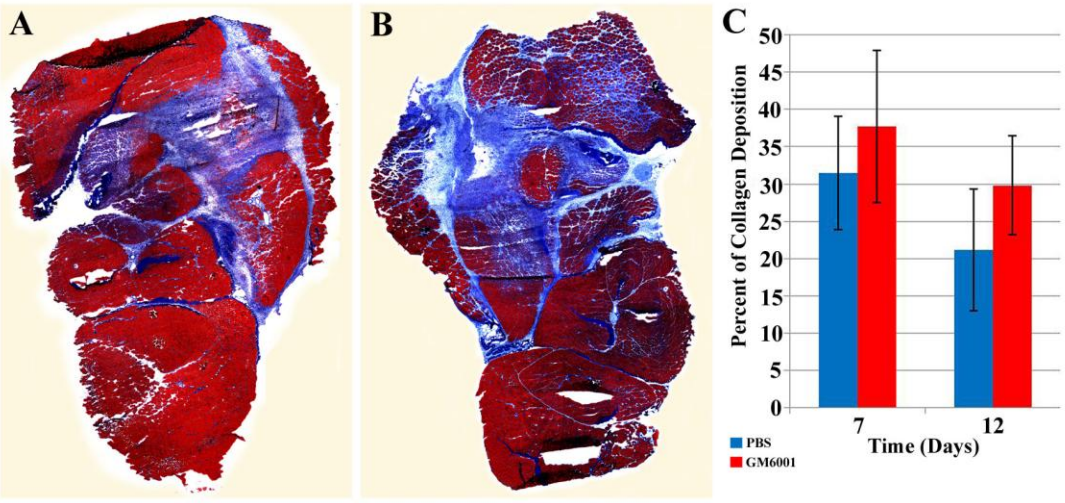

Figure 3.16: Collagen Deposition after Laceration Injury
GM6001 treatment of injured mouse skeletal muscle tissue exhibits elevated levels of collagen deposition (B) 7 days post laceration injury than the non-treated skeletal muscle tissue (A). Masson's modified trichrome staining was used to identify normal healthy skeletal muscle tissue (red) and collagen (blue). While an elevated level of collagen deposition was observed 7 and 12 after laceration injury, there was no significant difference (C).

3.4 DISCUSSION AND CONCLUSIONS

The wound healing process of skeletal muscle is a complex series of events that aim to reestablish the original architecture of the afflicted tissue (Hurme, Kalimo et al. 1991; Grefte, Kuijpers-Jagtman et al. 2007). This regenerative process is aided by MMPs that initially degrade components of the ECM, allowing greater cell motility to the injury site for proliferation and repair of the damaged tissue structure (Page-McCaw, Ewald et al. 2007). While inflammatory cells such as macrophages and neutrophils are some of the first responders to the damaged tissue, ultimately MDSCs are the forerunner leading the recovery. Unfortunately, all efforts to repair the skeletal muscle tissue are impeded by the development of fibrous scar tissue injury, two weeks after the initial injury(Huard, Gharaibeh et al. 2010).

As observed using an artificial wound assay, the use of a MMP inhibitor, GM6001, severely reduced the migration distance of MDSCs based on pretreatment time and dosage. The migration of C2C12 myoblasts was also impaired; however at a lower concentration (2.5 μM), cell migration was not affected. In a similar study, a 10 μM dose of GM6001 did not produce a lower migration distance in comparison to the control, suggesting that migration of the myoblasts is not solely guided by the MMPs (Mu, Urso et al. 2010). While the results of the wound migration assay demonstrated a significant reduction in the migration distance of MDSCs using GM6001, it may not be the most appropriate model. In the *in vivo* setting, MDSCs are not located in large clusters; therefore a more ideal model is observing single cell migration. Likewise, using the same treatment groups, MMP inhibition was found to reduce both cell migration, speed and its directional persistency index over a 2 hours period. These results were comparable to those conducted in another study where two different types of MMP inhibitors were found to decrease the migration speed of C2C12 myoblasts over a 24 hour period, yet

increase the directional persistency index (Nishimura, Nakamura et al. 2008). Moreover, a number of publications provide evidence in suggested the importance of MMPs in skeletal muscle healing by actively promoting myoblast migration and demonstrated the opposite outcome when they are inhibited (El Fahime, Torrente et al. 2000; Allen, Teitelbaum et al. 2003; Barnes, Szelenyi et al. 2009; Wang, Pan et al. 2009).

MDSCs exhibit some gene expression of cell adhesion markers, β-catenin, N-cadherin and NCAM, but when treated with an MMP inhibitor, these genes are significantly increased. Several studies verify this conclusion stating that the expression of these genes, particularly N-cadherin, results in an increase in cell adhesion causing reduced migration and invasion (Wilby, Muir et al. 1999; Prag, Lepekhin et al. 2002; Blindt, Bosserhoff et al. 2004). Other studies have produced contradicting results suggesting that N-cadherin expression plays an important role in cell migration; however, its role may truly vary depending on the cell type and environment (Brand-Saberi, Gamel et al. 1996; Hazan, Phillips et al. 2000; Derycke and Bracke 2004; Lyon, Koutsouki et al. 2010). For results presented, N-cadherin may contribute to cell migration for normal MDSCs, however when clustered together in culture and treated with a MMP inhibitor, the adhesion proteins are elevated above natural conditions, thus cell migration is impaired.

MMP inhibition does not influence the rate of cell proliferation for either MDSCs or the C2C12 myoblasts. These results were confirmed using both a population doubling assay by live cell imaging and an EdU assay. As observed, the cell proliferation occurred much faster for the C2C12 myoblasts than the MDSCs, while MDSCs tended to migrate further even when comparing either control groups or GM6001 treatments. Similar to *in vivo* studies, MDSCs are one of the early responders, in addition to inflammatory cells, that actively participate in myoblasts' proliferation and differentiation to facilitate skeletal muscle healing (Huard, Li et al.

2002; Charge and Rudnicki 2004; Ehrhardt and Morgan 2005; Grefte, Kuijpers-Jagtman et al. 2007; Boonen and Post 2008; Ten Broek, Grefte et al. 2010). This data suggests that cell proliferation may have an inverse relationship with distance migrating cells travel. Qualitatively, cell division appeared quite frequently at the edges of the artificial wound created for the wound assay for C2C12 myoblasts, which corresponds with their lower population doubling time and reduced cell migration distance. Because of their behavior in response to injuries, MDSCs are better suited to aid in the wound healing process.

The most unique characteristic of MDSCs during skeletal muscle healing is their ability to undergo multiple differentiations into various cell lineages. Their multipotency has been demonstrated in a plethora of investigations through differentiating along cells types as osteogenic, myogenic, chondrogenic, adipogenic, neuro-like cells, urinary bladder cells and hepatocyte-like cells (Lee, Qu-Petersen et al. 2000; Romero-Ramos, Vourc'h et al. 2002; Cao, Zheng et al. 2003; Deasy, Gharaibeh et al. 2005; Lavasani, Lu et al. 2006; Matsumoto, Kubo et al. 2008; Nozaki, Li et al. 2008; Smaldone and Chancellor 2008; Kubo, Cooper et al. 2009; Li, Corsi-Payne et al. 2009; Bellayr, Gharaibeh et al. 2010; Payne, Meszaros et al. 2010). When a broad spectrum MMP1 inhibitor is administered to MDSCs, it is observed that their multiple differentiation capacity into myogenic, osteogenic and adipogenic cells are reduced. Similar findings were made in other investigations where the myogenic and adipogenic differentiation capacity of C2C12 myoblasts and adipocytes, respectively, were significantly impaired through the use of the MMP inhibitor, batimastat (Bouloumie, Sengenes et al. 2001; Chavey, Mari et al. 2003; Ohtake, Tojo et al. 2006). This decrease in cell differentiation can be attributed to the decrease in the stem cell markers, Sca1 and CD34, of MDSCs as evaluated through gene

expression analysis. While MMP inhibition significantly represses the multipotency of MDSCs, it is discernable that MMPs are not the sole regulators of cell differentiation.

During the repair phase of skeletal muscle healing, myogenic factors, MyoD, Myf5, and Myf6, as well as M-cadherin becoming highly upregulated during injury (Grefte, Kuijpers-Jagtman et al. 2007; Ten Broek, Grefte et al. 2010). The characteristic response was observed for MDSCs after 1 day in myogenic differentiation media, however, their gene expression of MyoD and Myf5 were noticeably reduced with GM6001 treatment. The gene expression of Myf6 was downregulated with 3 hours of GM6001 treatment, but almost returned to its original level after 6 hours of treatment, suggesting that MMP inhibition is ineffectual in adversely impacting all myogenic differentiation genes. Perhaps the most perplexing outcome of the genes associated with early MDSC myogenic differentiation is the decrease in Notch1 expression. Notch signaling is commonly identified for its involvement with proliferation of satellite muscle cell progeny, where inhibition of Notch signaling prevents the expansion of these cell and therefore inhibits effective muscle regeneration (Luo, Renault et al. 2005; Brack, Conboy et al. 2008). For MDSCs, the gene expression of Notch1 was observed to decrease with a 6 hour pretreatment of GM6001 before initiating myogenic differentiation, where a 3 hour pretreatment with GM6001 exhibited comparable levels to the control. While a decrease in the gene expression of the Notch1 receptor may suggest reduced MDSC cell proliferation, thus inhibiting myogenic differentiation, ultimately there are a total of four Notch receptors interacting with 3 delta-like (DLL) and 2 Jagged (JAG) ligands to influence a downstream transcription factors of the CBF1/Su(H)/LAG1 (CSL) family (Lai 2004). Further experimentation would be necessary to elucidate how or if MMP inhibition has any effect on the actual Notch signaling pathway, other than decreasing the gene expression of Notch1. Instead, the Notch1 receptor may be more

closely linked to Notch signaling influencing cell differentiation by potential adhesion forces between DLL ligands and itself as its gene expression parallels that of the adhesion marker, M-cadherin.

In vivo experiments using mice were performed to examine the effect of GM6001 administration during skeletal muscle healing. Pax7 is commonly used to identify MDSCs or muscle satellite cells that help orchestrate the wound healing process (Peault, Rudnicki et al. 2007; Pawlikowski, Lee et al. 2009). Through qualitative inspection, the presence of Pax7 cells were observed 5 days post laceration injury in comparison to GM6001 treated laceration injuries, where Pax7 positive cells were undetectable. At later time points when fibrosis develops and impedes muscle regeneration, lacerated muscles at 7 and 12 days post injury exhibited an increase in the amount of collagen content compared to the control (Huard, Li et al. 2002; Li, Foster et al. 2004). While the result in collagen deposition between both groups at the two time points was not significantly different, this outcome can potentially be attributed to the administering 25mg/kg body weight of GM6001, which was half the amount of the recommended dosage (50-100mg/kg body weight).

Generally, the results of this study demonstrate the importance of MMPs in skeletal muscle healing. Not only do they aid in the myogenic differentiation and maturation, they influence MDSCs in their task to aid in tissue recovery. Because MMPs are sometimes regarded with a negative connotation in literature, these studies provide meaningful results that they may benefit individuals affected by skeletal muscle injuries or diseases.

4.0 CONCLUSION AND FUTURE DIRECTIONS

MMPs are unique because of their multiple influences on cell behavior that contribute to the remodeling process of tissue. In both of my research objectives, MMPs have demonstrated their impact on MDSCs and myoblasts when it comes to influencing stem cell behavior in skeletal muscle tissue. In particular, MMP1 orchestrates skeletal muscle healing through degradation of ECM constituents, actively promotes myoblast migration and myogenic differentiation; and promotes stem cell characteristics with myoblasts, which enrich the healing process. Furthermore, when MMPs are inhibited, the wound healing process in impaired by the detrimental effect on the stem cell characteristics of MDSCs. This inhibition can have negative consequences when it comes to using MDSCs to pursue alternative cell therapies. While the results of these studies provide a greater understanding of MMPs in their role during skeletal muscle regeneration, future investigations must build on this work in order to culminate an optimal strategy to treat skeletal muscle injuries.

4.1 MMP STUDIES

MMP1 treatment as explored in this research exhibited the potential to promote stem cell behavior in terminally differentiated cells. Additional studies would be necessary to determine whether this characteristic behavior is observed in alternative cell types. With approximately 23

known MMPs, continued research is integral to revealing their entire role in tissue remodeling. MMPs play a prominent role in the scarless regeneration of amputated newt digits, which mammals do not possess. A greater exploration between the similarities and differences of newt wound healing and mammalian healing can ultimately contribute to new discoveries with medicine and technology. This includes understanding the mechanisms that induce blastema formation.

This knowledge would greatly improve mammalian muscle regeneration by suppressing the development of fibrosis at later stages of healing as well as having applications in reducing scar formation in other organs. The two areas that should be the focus of regenerative medicine are the preventative methods of scarring and treatments for fibrosis once the healing process is terminated. Perhaps one approach to augment wound repair is fostering a greater expression of certain factors, such as MMPs, while minimizing negative ones (i.e. TGF-β). However, caution must be used to ensure that this unbalanced nature of protein expression does not consequently lead to an overexpression or underexpression of therapeutic components. These situations can subsequently lead to erroneous healing disorders such as promotion tumor metastasis and invasion or degenerative disorders that are sometimes associated with an over expression of MMPs.

Currently, work performed between Dr. Thomas Walters at the United States Army Institute of Surgical Research and Dr. Yong Li's Laboratory of Molecular Pathology is investigating how MMP1 might be useful in reducing the formation of scar tissue and promote skeletal muscle regeneration in an IR injury model (Appendix C). Pursuing research opportunities as these will help advance them toward a clinical application.

4.2 SIRNA MMP1

In regards to the second objective of this dissertation, preliminary work has been pursued to better understand the specific role of MMP1 with muscle stem cells. As observed in aim 1, MMP1 stimulation of primary mouse myoblasts promoted stem cell characteristics. In an effort to provide greater support for this finding, an alternative investigation was performed to knockdown MMP1 expression in MDSCs. Three groups of MDSCs were evaluated: MDSCs culture in the siRNA transfection media, MDSCs in normal media (control) and MDSCs treated with siRNA-MMP1 (Figure 4.1). Unfortunately, administering a siRNA to MDSCs targeting MMP1 proved unsuccessful. Future efforts are necessary to successfully knock down the expression of MMP1 within MDSCs to determine if MMP1 has a crucial role in the stem cell behavior of MDSCs.

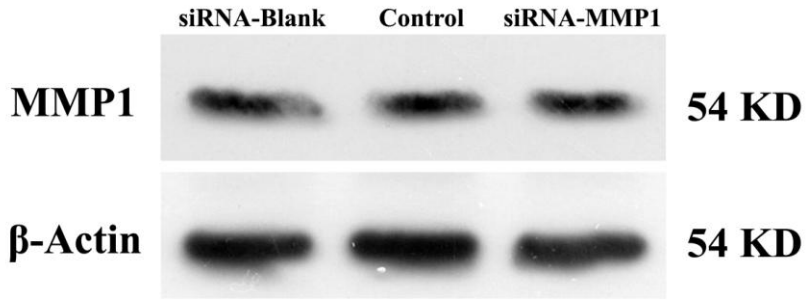

Figure 4.1: siRNA MMP1 Results
A siRNA vector of MMP1 was administered to MDSCs for 24 hours. It was unsuccessful in knocking down the expression of MMP1.

APPENDIX A

ISOLATION OF MDSCS BY THE PREPLATE TECHNIQUE

Primary myoblasts and MDSCs used throughout these studies were isolated from mouse skeletal muscle tissue using a modified preplate technique developed in the Stem Cell Research Center at the University of Pittsburgh (Qu-Petersen, Deasy et al. 2002; Gharaibeh, Lu et al. 2008; Li, Pan et al. 2010). The GM muscles were isolated from the three-week old C57BL/10J male mice. The remnants of any tendon or fat are removed and the muscle tissue is minced into a course slurry using micro-scissors. The slurry is then subjected to enzymatic dissociation in 0.2% collagenase-type XI for 60 minutes at 37^{o}C. Afterward, the slurry was centrifuged and re-suspended in dispase (2.4 units/mL in HBSS) for 45 minutes at 37^{o}C. The cell suspension was then centrifuged, transferred to 0.2% trypsin in HBSS for 30 minutes, and centrifuged again. Finally, the mixture was added to proliferation media and passed through a series of needles and through a 70μm cell strainer. The cells were re-suspended in proliferation media and plated into a collagen-coated T25 flask, marked PP1, and incubated at 37^{o}C at 5% CO_2. The PP1 population is mostly fibroblast cells. After 2 hours, non-adhering cells in the supernatant are directly transferred to a new flask labeled PP2. At every 24 hours, the supernatant is transferred to a new

flask and labeled PP3-PP6. PP3 are mostly myoblasts and the slow adhering cells of PP6 are MDSCs, which appear small, round and are sparse in number.

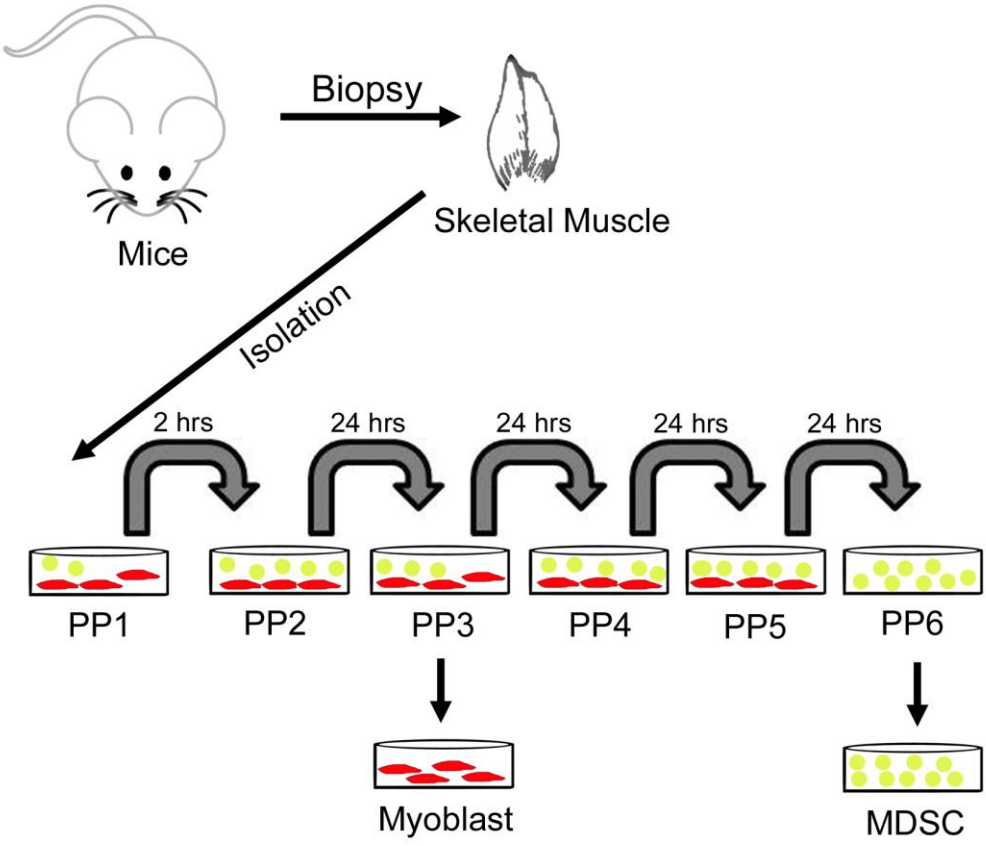

Figure A.1: Illustration of MDSC isolation of muscle tissue using the preplate technique

APPENDIX B

INFORMATION FOR RT-PCR ANALYSIS

Below is the information containing the sense and anti-sense primers used to perform gene analysis.

Table B.1 Sequences for Primers used in RT-PCR

Gene	Primer Sequences	Product Size
MyoD	Sense: 5' - GGCTACGACACCGCCTACTA - 3'	204
	Anti-Sense: 5' - GTTCTGTGTCGCTTAGGGAT - 3'	
Notch1	Sense: 5' - GCCGCAAGAGGCTTGAGAT - 3'	129
	Anti-Sense: 5' - GGAGTCCTGGCATCGTTGG - 3'	
Timp1	Sense: 5' - CTTGGTTCCCTGGCGTACTC - 3'	153
	Anti-Sense: 5' - ACCTGATCCGTCCACAAACAG - 3'	
GAPDH	Sense: 5' - CCTCTGGAAAGCTGTGGCGT - 3'	190
	Anti-Sense: 5' - TTGGCAGGTTTCTCCAGGCG - 3'	
Myf5	Sense: 5' - CCTGTCTGGTCCCGAAAGAAC - 3'	132
	Anti-Sense: 5' - TAGACGTGATCCGATCCACAAT - 3'	
Myf6	Sense: 5' - GCACCGGCTGGATCAGCAAGAG - 3'	191
	Anti-Sense: 5' - CTGAGGCATCCACGTTTGCTCC - 3'	
M-Cad	Sense: 5' - TCGGGCTGCTTGCCCAGAG - 3'	222
	Anti-Sense: 5' - CCCTGGATGCTGTAGATGACACTGC - 3'	
N-Cad	Sense: 5' - CTGGGACGTATGTGATGACG - 3'	150
	Anti-Sense: 5' - TGATGATGTCCCCAGTCTCA - 3'	
NCAM	Sense: 5' - GTACTCGGTACGACTGGCG - 3'	97
	Anti-Sense: 5' - TGGAGGAGGGCTATGGACTG - 3'	
β-Catenin	Sense: 5' - CCCTGAGACGCTAGATGAGG - 3'	172
	Anti-Sense: 5' - TGTCAGCTCAGGAATTGCAC - 3'	
Sca1	Sense: 5' - CCTACTGTGTGCAGAAAGAGC - 3'	242
	Anti-Sense: 5' - CAGGAAGTCTTCACGTTGACC - 3'	
CD34	Sense: 5' - TCTCTGCCTGATGAGTCTGCTGC - 3'	193
	Anti-Sense: 5' - TCTCTGAGATGGCTGGTGTGGTC - 3'	
Oct4	Sense: 5' - GGCTTCAGACTTCGCCTCC - 3'	213
	Anti-Sense: 5' - AACCTGAGGTCCACAGTATGC - 3'	

APPENDIX C

ISCHEMIA REPERFUSION INDUCES FIBROSIS FORMATION IN THE SKELETAL MUSCLE OF MICE

C.1 INTRODUCTION

Extremity trauma constitutes the majority of war wounds, and is a significant problem in civilian medicine (Owens, Kragh et al. 2007). A large portion of these involve muscle trauma in the form of ischemia reperfusion injury (IR) caused by vascular trauma, tourniquet use and/or compartment syndrome. IR results in inflammation, edema, and oxidative stress, which impairs the skeletal muscle healing process (Kauvar, Baer et al. 2007).

When muscle injuries are left untreated they can develop fibrosis, an excessive accumulation of connective tissue that causes scars to form in tissue after several weeks (Li, Fu et al. 2005). This scar tissue has a negative impact on the ability of muscle to regenerate and regain its original function. The goal of this study was to investigate tissue damage and fibrosis development in a tourniquet induced IR mouse model. Previous research has explored the use of antifibrosis agents to improve muscle healing by preventing fibrotic tissue development. In this investigation, a timeline of fibrotic development from IR injury was established to determine the timing at which potential therapies may be administered to reverse scar tissue formation.

C.2 METHODS

C.2.1 Ischemia Reperfusion Injury

Mice were anesthetized with 2% isofluorane gas prior to and for the duration of tourniquet application modeling ischemia reperfusion (IR). A single, randomly selected hind limb was elevated and a pneumatic tourniquet (D.E. Hokanson, Inc.), modified to fit the hind limb of a mouse, was wrapped snuggly against the proximal portion of the limb and inflated to 250 mmHg by a portable tourniquet system (delfi Medical Innovation, Inc.) to ensure complete occlusion of blood flow to the limb for a duration of 2 hours. Body temperature was maintained at 37^{o}C with the use of a water heated surgical bed during this procedure. After 2 hours, the pneumatic tourniquet was removed. Animals were returned to their home cages once they recovered from anesthesia and allowed to regain consciousness. At 3, 5, 7, 10, 14, 21, and 28 days following the initial tourniquet application, five mice from each of the time points were sacrificed and their TA and GM muscles were harvested. The muscles of the uninjured contralateral limb served as controls.

C.2.2 Histology

The sections of GM and TA muscles from every mouse were washed in PBS and stained with Masson's modified trichrome staining kit (IMEB) according to the manufacturer's specifications.

This technique stains the muscle tissue red, collagen (or fibrous tissue) blue and the cell nuclei black. Five randomly selected high powered image fields of three sectioned slices of the injured area were obtained using a Nikon Eclipse 800 fitted with a Spot camera (Diagnostic Instruments). Images were analyzed using CellProfiler image analysis software to measure the percent area of the collagen of the tissue section (Carpenter, Jones et al. 2006). Red and blue colors of each image were separated using the software program, where the area of the blue region was calculated and expressed as a percentage of the entire cross-sectional area of the muscle. The muscles of the contralateral limb were also evaluated for the percentage of native collagen, which yielded the equation: $C_D = T_B - N_B$, where C_D is the percentage of the afflicted area [0 – 7 days] or collagen deposition [10 - 28 days], T_B is the total percentage of the blue area in the IR injured muscle and N_B is the total percentage of the blue area from the contralateral uninjured limb. Muscle sections were also stained with hematoxylin and eosin to qualitatively assess myofiber regeneration at 0, 3, 5, 7, 10, 14, 21, and 28 days after IR injury. Myofiber regeneration can be examined for centrally located nuclei (blue) with in the myofibers (pink).

C.3 PRELIMINARY RESULTS

The objective of this study was to establish an IR model in mice by evaluated the progression of fibrotic development in skeletal muscle tissue over time. To accomplish this, mice were subjected to a modified tourniquet application for 2 hours and then allowed to recover 3, 5, 7, 10, 14, 21, or 28 days before being euthanized and their GM and TA muscles isolated for analysis. Masson's modified trichrome stain was used to assess the damage that occurred early after IR injury. The color blue from this stain indicates interstitial collagen, however, since the onset of

fibrosis typically occurs between 10 and 14 days, the blue color at earlier time points is the result of migrating inflammatory cells, cellular debris and some degraded ECM components (Li, Fu et al. 2005). This afflicted area was examined in the TA (Figure C.1, A-D) and GM (Figure C.1, E-H) muscles at 0 (Figure C.1, A, E), 3 (Figure C.1, B, F), 5 (Figure C.1, C, G), and 7 (Figure C.1, D, H) days after the IR injury was applied. The percentage of skeletal muscle tissue afflicted by the IR injury was quantified (Figure C.1, I), where the amount of damage increased to its greatest observed value at 5 days with 50% for the TA muscle and 65% for the GM muscle, after the application of the tourniquet. At 7 days, after the initial application of the IR injury, the amount of afflicted tissue in both the TA and GM decreased to approximately 35% of the area for both muscle types. No significant difference was observed between the two muscle groups.

Collagen deposition was assessed separately in both the TA (Figure C.2, A-D) and GM (Figure C.2, E-H) muscles for days 10 (Figure C.2, A, E), 14 (Figure C.2, B, F), 21 (Figure C.2, C, G), and 28 (Figure C.2, D, H) after IR injury. The damage area characterized as collagen deposition was a much deeper blue than trichrome stains at earlier time points after IR injury. Damage in these tissues at later time points indicates that fibrotic tissue development initially accumulated around dead blood vessels and then throughout the myofibers. When quantified, the amount of collagen deposition in the GM muscles between 10 and 28 days was observed to be slightly greater than the collagen deposition in the TA muscle (Figure C.2, I). The percentage of collagen deposition for the GM muscle was 35% at day 10 and decreased to 22.5% by day 28, where the amount of collagen deposition observed in the TA muscle was approximately 25% at day 10 and decreased to 15% by day 28. The reason for the differences in the amount of collagen deposition between each muscle tissue is unknown.

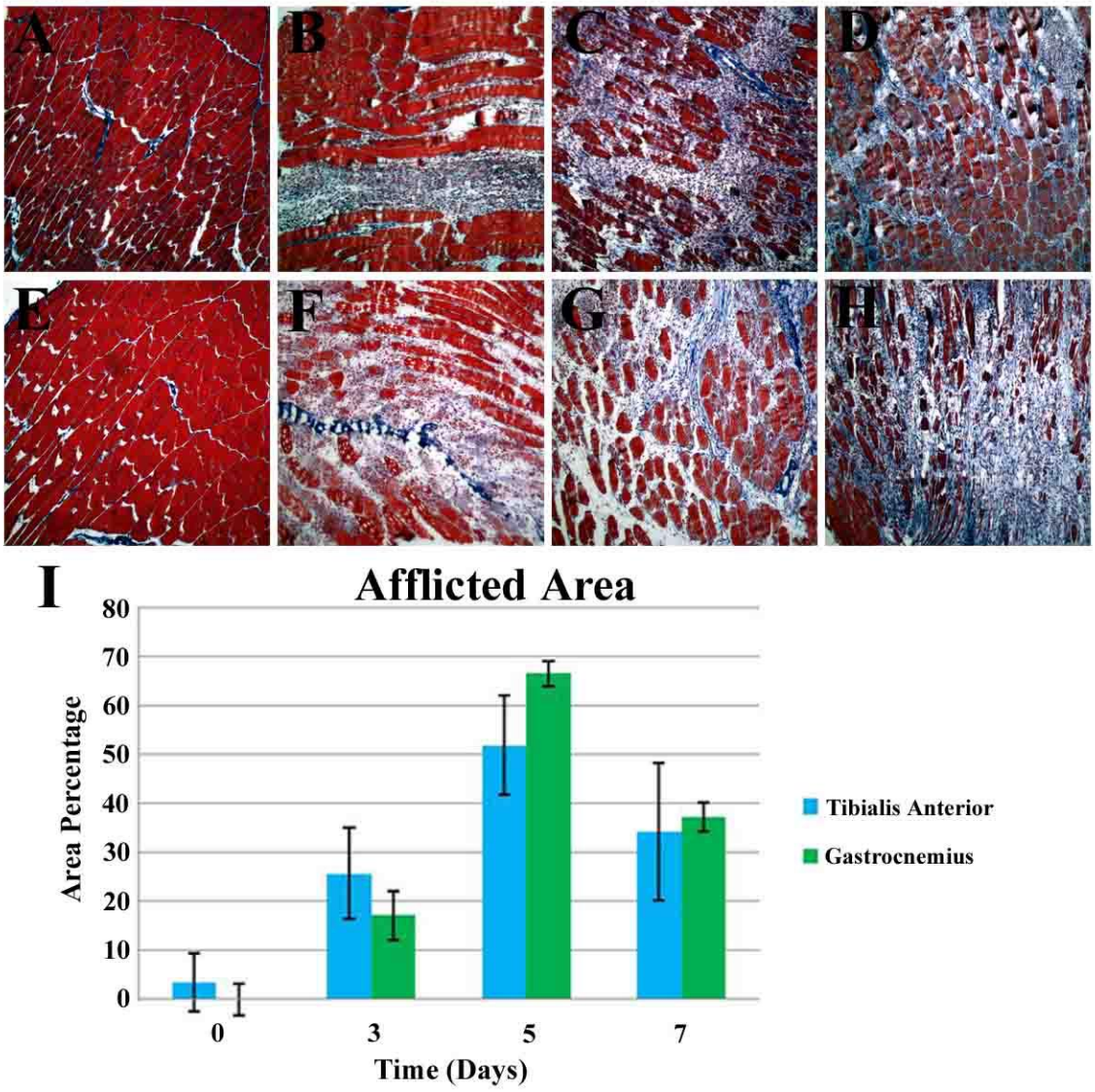

Figure C.1: Initial Damage from IR Injury
The progression of tissue damage from IR injury is illustrated in the TA (A-D) and the GM (E-H) muscles. Non-injured samples show only native collagen present (A, E), whereas 3 (B, F), 5 (C, G) and 7 (D, H) days after administering IR injury, the extent of tissue damage has dramatically increased. Images were taken at 10x magnification.

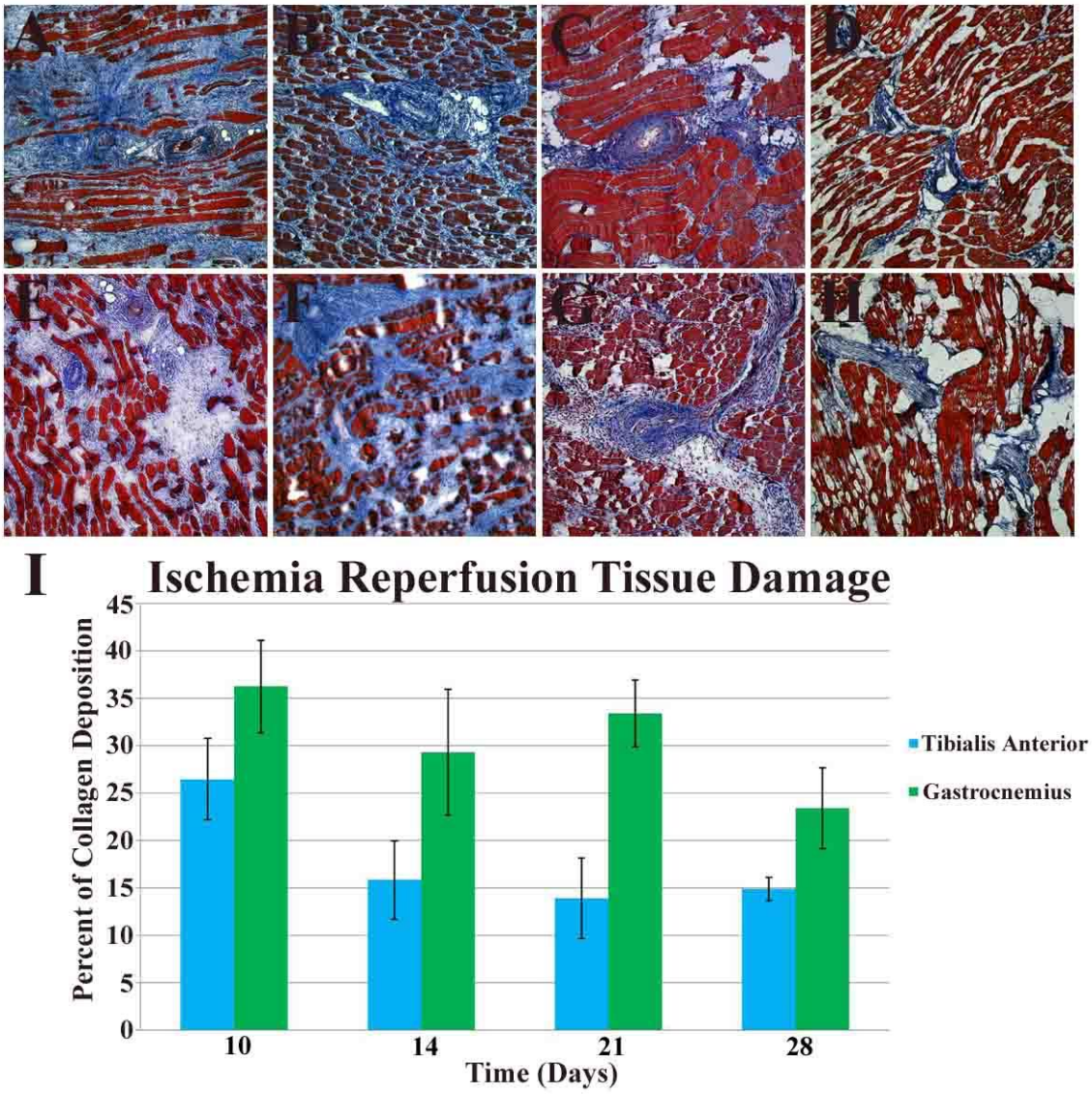

Figure C.2: Collagen Deposition from IR Injury
The progression of collagen deposition at later time points after initial IR injury is illustrated in the TA (A-D) and the GM (E-H) muscles. Fibrotic development is shown at 10 (A, E), 14 (B, F), 21 (C, G) and 28 (D, H) days. The percent of collagen deposition between 10 and 28 days after injury was quantified (I). Images were taken at 10x magnification.

Using a hematoxylin and eosin stain, the pathology of the IR injury model was qualitatively examined for myofiber regeneration. For normal healthy skeletal muscle tissue, the cell nuclei are located at the edges of the myofibers, however, in an injured scenario, the cell nuclei become centrally located in an effort to repair the damaged myofiber. At day 3 after the IR injury, the damage area in the skeletal muscle tissue is apparent, but the myofiber regeneration does not begin until the fifth day after injury and continues until day 28 (Figure C.3). Both the trichrome as well as hematoxylin and eosin staining reveal that the damage occurring from IR is centrally located within the muscle tissue, where myofibers at the perimeter of the muscle appeared relatively unharmed. By day 28, the ability of the skeletal muscle tissue to properly restore its original structure and function is impaired by fibrosis formation

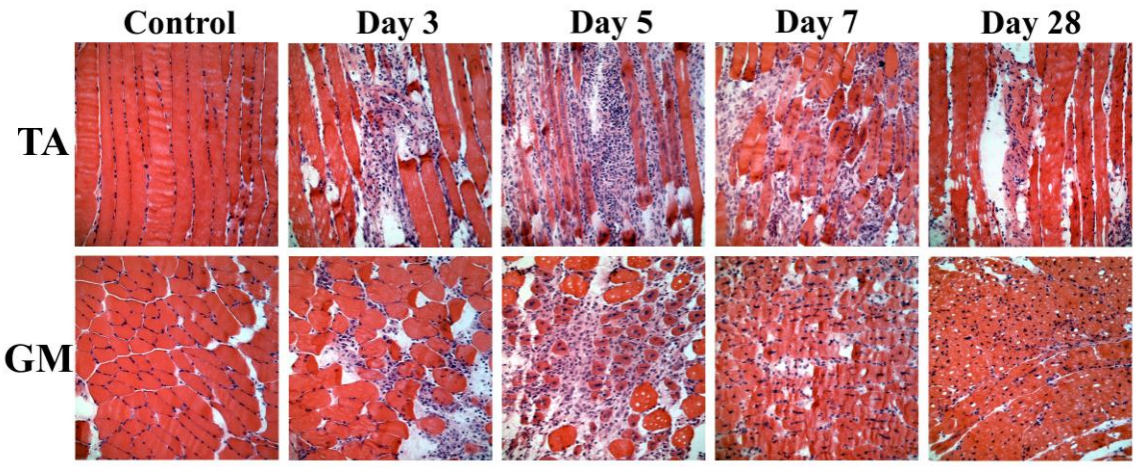

Figure C.3: Myofiber Regeneration after IR Injury
The progression of myofiber regeneration from day 0 to day 28 after IR injury is illustrated in the TA (imaged longitudinally) and the GM (imaged cross-sectionally) muscles.

C.4 FUTURE WORK

For future investigations of anti-fibrosis agents, an IR injury modeling compartment syndrome in mice has been established. Based on this data, fibrosis formation was observed to typically start 10 days after the application of the tourniquet and does not significantly diminish. Two dosages of MMP1 (10ng and 100ng), which is reported to degrade collagens I and III, will be administered in combination with green fluorescent beads at 10 days after the initial IR with 6 mice per test group (Table C.1). At days 7, 14, and 21 after administering MMP1 to the IR injury, both the TA and GM muscles will be isolated for evaluation of the treatment. The local site of injection will be visualized by the presence of the green fluorescent beads. Both harvested muscle tissues will be subjected to similar techniques measuring collagen deposition and myofiber regeneration.

Table C.1 Proposed number of mice to test MMP1 as an anti-fibrosis agent

	Days		
	7	14	21
Control	6	6	6
10 ng	6	6	6
100 ng	6	6	6
TOTAL	18	18	18

This work was made possible by a grant from the Department of Defense (W81XWH-09-2-0099). Animal studies were performed in Dr. Thomas Walters' laboratory at the United States Army Institute of Surgical Research in Fort Sam Houston with the help of Melissa Sanchez.

BIBLIOGRAPHY

Akhavani, M. A., L. Madden, et al. (2009). "Hypoxia upregulates angiogenesis and synovial cell migration in rheumatoid arthritis." Arthritis Res Ther **11**(3): R64.

Alagoz, M. S., C. A. Uysal, et al. (2006). "Reverse homodigital artery flap coverage for bone and nailbed grafts in fingertip amputations." Ann Plast Surg **56**(3): 279-283.

Alexakis, C., T. Partridge, et al. (2007). "Implication of the satellite cell in dystrophic muscle fibrosis: a self-perpetuating mechanism of collagen overproduction." Am J Physiol Cell Physiol **293**(2): C661-669.

Allen, D. L., D. H. Teitelbaum, et al. (2003). "Growth factor stimulation of matrix metalloproteinase expression and myoblast migration and invasion in vitro." Am J Physiol Cell Physiol **284**(4): C805-815.

Bae, Y. H., Z. Ding, et al. (2009). "Loss of profilin-1 expression enhances breast cancer cell motility by Ena/VASP proteins." J Cell Physiol **219**(2): 354-364.

Bai, S., R. Thummel, et al. (2005). "Matrix metalloproteinase expression and function during fin regeneration in zebrafish: analysis of MT1-MMP, MMP2 and TIMP2." Matrix Biol **24**(4): 247-260.

Baker, A. H., D. R. Edwards, et al. (2002). "Metalloproteinase inhibitors: biological actions and therapeutic opportunities." J Cell Sci **115**(Pt 19): 3719-3727.

Bani, C., J. Lagrota-Candido, et al. (2008). "Pattern of metalloprotease activity and myofiber regeneration in skeletal muscles of mdx mice." Muscle Nerve **37**(5): 583-592.

Barnes, B. R., E. R. Szelenyi, et al. (2009). "Alterations in mRNA and protein levels of metalloproteinases-2, -9, and -14 and tissue inhibitor of metalloproteinase-2 responses to traumatic skeletal muscle injury." Am J Physiol Cell Physiol **297**(6): C1501-1508.

Bedair, H., T. T. Liu, et al. (2007). "Matrix metalloproteinase-1 therapy improves muscle healing." J Appl Physiol **102**(6): 2338-2345.

Bedair, H. S., T. Karthikeyan, et al. (2008). "Angiotensin II receptor blockade administered after injury improves muscle regeneration and decreases fibrosis in normal skeletal muscle." Am J Sports Med **36**(8): 1548-1554.

Bellayr, I. H., B. Gharaibeh, et al. (2010). "Skeletal muscle-derived stem cells differentiate into hepatocyte-like cells and aid in liver regeneration." Int J Clin Exp Pathol **3**(7): 681-690.

Blindt, R., A. K. Bosserhoff, et al. (2004). "Downregulation of N-cadherin in the neointima stimulates migration of smooth muscle cells by RhoA deactivation." Cardiovasc Res **62**(1): 212-222.

Bonewald, L. F., S. E. Harris, et al. (2003). "von Kossa staining alone is not sufficient to confirm that mineralization in vitro represents bone formation." Calcif Tissue Int **72**(5): 537-547.

Boonen, K. J. and M. J. Post (2008). "The muscle stem cell niche: regulation of satellite cells during regeneration." Tissue Eng Part B Rev **14**(4): 419-431.

Bouloumie, A., C. Sengenes, et al. (2001). "Adipocyte produces matrix metalloproteinases 2 and 9: involvement in adipose differentiation." Diabetes **50**(9): 2080-2086.

Brack, A. S., I. M. Conboy, et al. (2008). "A temporal switch from notch to Wnt signaling in muscle stem cells is necessary for normal adult myogenesis." Cell Stem Cell **2**(1): 50-59.

Brand-Saberi, B., A. J. Gamel, et al. (1996). "N-cadherin is involved in myoblast migration and muscle differentiation in the avian limb bud." Dev Biol **178**(1): 160-173.

Brockes, J. P. (1997). "Amphibian limb regeneration: rebuilding a complex structure." Science **276**(5309): 81-87.

Campbell, L. J. and C. M. Crews (2008). "Wound epidermis formation and function in urodele amphibian limb regeneration." Cell Mol Life Sci **65**(1): 73-79.

Cao, B., B. Zheng, et al. (2003). "Muscle stem cells differentiate into haematopoietic lineages but retain myogenic potential." Nat Cell Biol **5**(7): 640-646.

Caron, N. J., I. Asselin, et al. (1999). "Increased myogenic potential and fusion of matrilysin-expressing myoblasts transplanted in mice." Cell Transplant **8**(5): 465-476.

Carpenter, A. E., T. R. Jones, et al. (2006). "CellProfiler: image analysis software for identifying and quantifying cell phenotypes." Genome Biol **7**(10): R100.

Chan, Y. S., Y. Li, et al. (2005). "The use of suramin, an antifibrotic agent, to improve muscle recovery after strain injury." Am J Sports Med **33**(1): 43-51.

Charge, S. B. and M. A. Rudnicki (2004). "Cellular and molecular regulation of muscle regeneration." Physiol Rev **84**(1): 209-238.

Chavey, C., B. Mari, et al. (2003). "Matrix metalloproteinases are differentially expressed in adipose tissue during obesity and modulate adipocyte differentiation." J Biol Chem **278**(14): 11888-11896.

Chazaud, B., M. Brigitte, et al. (2009). "Dual and beneficial roles of macrophages during skeletal muscle regeneration." Exerc Sport Sci Rev **37**(1): 18-22.

Chazaud, B., C. Sonnet, et al. (2003). "Satellite cells attract monocytes and use macrophages as a support to escape apoptosis and enhance muscle growth." J Cell Biol **163**(5): 1133-1143.

Choi, S. J., K. L. Jung, et al. (2009). "Cervicovaginal matrix metalloproteinase-9 and cervical ripening in human term parturition." Eur J Obstet Gynecol Reprod Biol **142**(1): 43-47.

Chromek, M., K. Tullus, et al. (2003). "Matrix metalloproteinase-9 and tissue inhibitor of metalloproteinases-1 in acute pyelonephritis and renal scarring." Pediatr Res **53**(4): 698-705.

Corsi, K. A., J. B. Pollett, et al. (2007). "Osteogenic potential of postnatal skeletal muscle-derived stem cells is influenced by donor sex." J Bone Miner Res **22**(10): 1592-1602.

Cowan, C. A., J. Atienza, et al. (2005). "Nuclear reprogramming of somatic cells after fusion with human embryonic stem cells." Science **309**(5739): 1369-1373.

Crawford, K. and D. L. Stocum (1988). "Retinoic acid coordinately proximalizes regenerate pattern and blastema differential affinity in axolotl limbs." Development **102**(4): 687-698.

Creemers, E. E., J. N. Davis, et al. (2003). "Deficiency of TIMP-1 exacerbates LV remodeling after myocardial infarction in mice." Am J Physiol Heart Circ Physiol **284**(1): H364-371.

Curran, J. M., F. Pu, et al. (2011). "The use of dynamic surface chemistries to control msc isolation and function." Biomaterials **32**(21): 4753-4760.

Deasy, B. M., B. M. Gharaibeh, et al. (2005). "Long-term self-renewal of postnatal muscle-derived stem cells." Mol Biol Cell **16**(7): 3323-3333.

Deasy, B. M., Y. Li, et al. (2004). "Tissue engineering with muscle-derived stem cells." Curr Opin Biotechnol **15**(5): 419-423.

Decraene, C., R. Benchaouir, et al. (2005). "Global transcriptional characterization of SP and MP cells from the myogenic C2C12 cell line: effect of FGF6." Physiol Genomics **23**(2): 132-149.

Derycke, L. D. and M. E. Bracke (2004). "N-cadherin in the spotlight of cell-cell adhesion, differentiation, embryogenesis, invasion and signalling." Int J Dev Biol **48**(5-6): 463-476.

Ehrhardt, J. and J. Morgan (2005). "Regenerative capacity of skeletal muscle." Curr Opin Neurol **18**(5): 548-553.

El Fahime, E., Y. Torrente, et al. (2000). "In vivo migration of transplanted myoblasts requires matrix metalloproteinase activity." Exp Cell Res **258**(2): 279-287.

Epting, C. L., J. E. Lopez, et al. (2004). "Stem cell antigen-1 is necessary for cell-cycle withdrawal and myoblast differentiation in C2C12 cells." J Cell Sci **117**(Pt 25): 6185-6195.

Fitzgerald, J., C. Rich, et al. (2008). "Evidence for articular cartilage regeneration in MRL/MpJ mice." Osteoarthritis Cartilage **16**(11): 1319-1326.

Foster, W., Y. Li, et al. (2003). "Gamma interferon as an antifibrosis agent in skeletal muscle." J Orthop Res **21**(5): 798-804.

Fujita, H., A. Endo, et al. (2010). "Evaluation of serum-free differentiation conditions for C2C12 myoblast cells assessed as to active tension generation capability." Biotechnol Bioeng **107**(5): 894-901.

Fukushima, K., A. Nakamura, et al. (2007). "Activation and localization of matrix metalloproteinase-2 and -9 in the skeletal muscle of the muscular dystrophy dog (CXMDJ)." BMC Musculoskelet Disord **8**: 54.

Furochi, H., S. Tamura, et al. (2007). "Overexpression of osteoactivin protects skeletal muscle from severe degeneration caused by long-term denervation in mice." J Med Invest **54**(3-4): 248-254.

Gharaibeh, B., A. Lu, et al. (2008). "Isolation of a slowly adhering cell fraction containing stem cells from murine skeletal muscle by the preplate technique." Nat Protoc **3**(9): 1501-1509.

Gill, S. E. and W. C. Parks (2008). "Metalloproteinases and their inhibitors: regulators of wound healing." Int J Biochem Cell Biol **40**(6-7): 1334-1347.

Gomis-Ruth, F. X. (2003). "Structural aspects of the metzincin clan of metalloendopeptidases." Mol Biotechnol **24**(2): 157-202.

Gourevitch, D., L. Clark, et al. (2003). "Matrix metalloproteinase activity correlates with blastema formation in the regenerating MRL mouse ear hole model." Dev Dyn **226**(2): 377-387.

Grefte, S., A. M. Kuijpers-Jagtman, et al. (2007). "Skeletal muscle development and regeneration." Stem Cells Dev **16**(5): 857-868.

Guerin, C. W. and P. C. Holland (1995). "Synthesis and secretion of matrix-degrading metalloproteases by human skeletal muscle satellite cells." Dev Dyn **202**(1): 91-99.

Guo, Z., K. Draheim, et al. (2011). "Isolation and culture of adult epithelial stem cells from human skin." J Vis Exp(49).

Han, M., X. Yang, et al. (2008). "Development and regeneration of the neonatal digit tip in mice." Dev Biol **315**(1): 125-135.

Hazan, R. B., G. R. Phillips, et al. (2000). "Exogenous expression of N-cadherin in breast cancer cells induces cell migration, invasion, and metastasis." J Cell Biol **148**(4): 779-790.

Hnia, K., J. Gayraud, et al. (2008). "L-arginine decreases inflammation and modulates the nuclear factor-kappaB/matrix metalloproteinase cascade in mdx muscle fibers." Am J Pathol **172**(6): 1509-1519.

Huangfu, D., K. Osafune, et al. (2008). "Induction of pluripotent stem cells from primary human fibroblasts with only Oct4 and Sox2." Nat Biotechnol **26**(11): 1269-1275.

Huard, J., B. Gharaibeh, et al. (2010). "Regenerative Medicine Based on Muscle-Derived Stem Cells." Oper Tech Orthop **20**(2): 119-126.

Huard, J., Y. Li, et al. (2002). "Muscle injuries and repair: current trends in research." J Bone Joint Surg Am **84-A**(5): 822-832.

Huard, J., T. Yokoyama, et al. (2002). "Muscle-derived cell-mediated ex vivo gene therapy for urological dysfunction." Gene Ther **9**(23): 1617-1626.

Hurme, T., H. Kalimo, et al. (1991). "Healing of skeletal muscle injury: an ultrastructural and immunohistochemical study." Med Sci Sports Exerc **23**(7): 801-810.

Huxley-Jones, J., T. K. Clarke, et al. (2007). "The evolution of the vertebrate metzincins; insights from Ciona intestinalis and Danio rerio." BMC Evol Biol **7**: 63.

Iimuro, Y., T. Nishio, et al. (2003). "Delivery of matrix metalloproteinase-1 attenuates established liver fibrosis in the rat." Gastroenterology **124**(2): 445-458.

Jacobsen, J., R. Visse, et al. (2008). "Catalytic properties of ADAM12 and its domain deletion mutants." Biochemistry **47**(2): 537-547.

Jankowski, R. J., B. M. Deasy, et al. (2002). "Muscle-derived stem cells." Gene Ther **9**(10): 642-647.

Jankowski, R. J., C. Haluszczak, et al. (2001). "Flow cytometric characterization of myogenic cell populations obtained via the preplate technique: potential for rapid isolation of muscle-derived stem cells." Hum Gene Ther **12**(6): 619-628.

Kaar, J. L., Y. Li, et al. (2008). "Matrix metalloproteinase-1 treatment of muscle fibrosis." Acta Biomater **4**(5): 1411-1420.

Kasper, G., J. D. Glaeser, et al. (2007). "Matrix metalloprotease activity is an essential link between mechanical stimulus and mesenchymal stem cell behavior." Stem Cells **25**(8): 1985-1994.

Kato, T., K. Miyazaki, et al. (2003). "Unique expression patterns of matrix metalloproteinases in regenerating newt limbs." Dev Dyn **226**(2): 366-376.

Kauvar, D. S., D. G. Baer, et al. (2007). "Influence of systemic hypotension on skeletal muscle ischemia-reperfusion injury after 4-hour tourniquet application." J Surg Educ **64**(5): 273-277.

Kim, K. S., J. H. Lee, et al. (2008). "The osteogenic differentiation of rat muscle-derived stem cells in vivo within in situ-forming chitosan scaffolds." Biomaterials **29**(33): 4420-4428.

Kim, Y. J., H. J. Kim, et al. (2008). "PTHrP promotes chondrogenesis and suppresses hypertrophy from both bone marrow-derived and adipose tissue-derived MSCs." Biochem Biophys Res Commun **373**(1): 104-108.

Kubo, S., G. M. Cooper, et al. (2009). "Blocking vascular endothelial growth factor with soluble Flt-1 improves the chondrogenic potential of mouse skeletal muscle-derived stem cells." Arthritis Rheum **60**(1): 155-165.

Kuroda, R., A. Usas, et al. (2006). "Cartilage repair using bone morphogenetic protein 4 and muscle-derived stem cells." Arthritis Rheum **54**(2): 433-442.

Lai, E. C. (2004). "Notch signaling: control of cell communication and cell fate." Development **131**(5): 965-973.

Lavasani, M., A. Lu, et al. (2006). "Nerve growth factor improves the muscle regeneration capacity of muscle stem cells in dystrophic muscle." Hum Gene Ther **17**(2): 180-192.

Lee, J. Y., Z. Qu-Petersen, et al. (2000). "Clonal isolation of muscle-derived cells capable of enhancing muscle regeneration and bone healing." J Cell Biol **150**(5): 1085-1100.

Li, G., K. Corsi-Payne, et al. (2009). "The dose of growth factors influences the synergistic effect of vascular endothelial growth factor on bone morphogenetic protein 4-induced ectopic bone formation." Tissue Eng Part A **15**(8): 2123-2133.

Li, G., H. Peng, et al. (2005). "Differential effect of BMP4 on NIH/3T3 and C2C12 cells: implications for endochondral bone formation." J Bone Miner Res **20**(9): 1611-1623.

Li, Y., W. Foster, et al. (2004). "Transforming growth factor-beta1 induces the differentiation of myogenic cells into fibrotic cells in injured skeletal muscle: a key event in muscle fibrogenesis." Am J Pathol **164**(3): 1007-1019.

Li, Y., F. H. Fu, et al. (2005). "Cutting-edge muscle recovery: using antifibrosis agents to improve healing." Phys Sportsmed **33**(5): 44-50.

Li, Y. and J. Huard (2002). "Differentiation of muscle-derived cells into myofibroblasts in injured skeletal muscle." Am J Pathol **161**(3): 895-907.

Li, Y., J. Li, et al. (2007). "Decorin gene transfer promotes muscle cell differentiation and muscle regeneration." Mol Ther **15**(9): 1616-1622.

Li, Y., H. Pan, et al. (2010). "Isolating stem cells from soft musculoskeletal tissues." J Vis Exp(41).

Luo, D., V. M. Renault, et al. (2005). "The regulation of Notch signaling in muscle stem cell activation and postnatal myogenesis." Semin Cell Dev Biol **16**(4-5): 612-622.

Lyon, C. A., E. Koutsouki, et al. (2010). "Inhibition of N-cadherin retards smooth muscle cell migration and intimal thickening via induction of apoptosis." J Vasc Surg **52**(5): 1301-1309.

Marongiu, F., R. Gramignoli, et al. (2010). "Isolation of amniotic mesenchymal stem cells." Curr Protoc Stem Cell Biol **Chapter 1**: Unit 1E 5.

Matsumoto, T., S. Kubo, et al. (2008). "The influence of sex on the chondrogenic potential of muscle-derived stem cells: implications for cartilage regeneration and repair." Arthritis Rheum **58**(12): 3809-3819.

Mauritz, C., A. Martens, et al. (2011). "Induced pluripotent stem cell (iPSC)-derived Flk-1 progenitor cells engraft, differentiate, and improve heart function in a mouse model of acute myocardial infarction." Eur Heart J.

McCawley, L. J. and L. M. Matrisian (2001). "Matrix metalloproteinases: they're not just for matrix anymore!" Curr Opin Cell Biol **13**(5): 534-540.

McCawley, L. J., J. Wright, et al. (2008). "Keratinocyte expression of MMP3 enhances differentiation and prevents tumor establishment." Am J Pathol **173**(5): 1528-1539.

McClure, K. D., A. Sustar, et al. (2008). "Three genes control the timing, the site and the size of blastema formation in Drosophila." Dev Biol **319**(1): 68-77.

Melendez-Zajgla, J., L. Del Pozo, et al. (2008). "Tissue inhibitor of metalloproteinases-4. The road less traveled." Mol Cancer **7**: 85.

Menon, B., M. Singh, et al. (2005). "Matrix metalloproteinases mediate beta-adrenergic receptor-stimulated apoptosis in adult rat ventricular myocytes." Am J Physiol Cell Physiol **289**(1): C168-176.

Miki, T., F. Marongiu, et al. (2010). "Isolation of amniotic epithelial stem cells." Curr Protoc Stem Cell Biol **Chapter 1**: Unit 1E 3.

Miyazaki, K., K. Uchiyama, et al. (1996). "Cloning and characterization of cDNAs for matrix metalloproteinases of regenerating newt limbs." Proc Natl Acad Sci U S A **93**(13): 6819-6824.

Mu, X., M. L. Urso, et al. (2010). "Relaxin regulates MMP expression and promotes satellite cell mobilization during muscle healing in both young and aged mice." Am J Pathol **177**(5): 2399-2410.

Nakagawa, M., M. Koyanagi, et al. (2008). "Generation of induced pluripotent stem cells without Myc from mouse and human fibroblasts." Nat Biotechnol **26**(1): 101-106.

Nath, M., M. Offers, et al. (2011). "Isolation and in vitro expansion of Lgr6-positive multipotent hair follicle stem cells." Cell Tissue Res.

Nishimura, T., K. Nakamura, et al. (2008). "Inhibition of matrix metalloproteinases suppresses the migration of skeletal muscle cells." J Muscle Res Cell Motil **29**(1): 37-44.

Nishita, M., C. Tomizawa, et al. (2005). "Spatial and temporal regulation of cofilin activity by LIM kinase and Slingshot is critical for directional cell migration." J Cell Biol **171**(2): 349-359.

Nozaki, M., Y. Li, et al. (2008). "Improved muscle healing after contusion injury by the inhibitory effect of suramin on myostatin, a negative regulator of muscle growth." Am J Sports Med **36**(12): 2354-2362.

Ohtake, Y., H. Tojo, et al. (2006). "Multifunctional roles of MT1-MMP in myofiber formation and morphostatic maintenance of skeletal muscle." J Cell Sci **119**(Pt 18): 3822-3832.

Okita, K., M. Nakagawa, et al. (2008). "Generation of mouse induced pluripotent stem cells without viral vectors." Science **322**(5903): 949-953.

Owens, B. D., J. F. Kragh, Jr., et al. (2007). "Characterization of extremity wounds in Operation Iraqi Freedom and Operation Enduring Freedom." J Orthop Trauma **21**(4): 254-257.

Page-McCaw, A., A. J. Ewald, et al. (2007). "Matrix metalloproteinases and the regulation of tissue remodelling." Nat Rev Mol Cell Biol **8**(3): 221-233.

Pardo, A. and M. Selman (2005). "MMP-1: the elder of the family." Int J Biochem Cell Biol **37**(2): 283-288.

Parks, W. C., C. L. Wilson, et al. (2004). "Matrix metalloproteinases as modulators of inflammation and innate immunity." Nat Rev Immunol **4**(8): 617-629.

Parsons, S. L., S. A. Watson, et al. (1997). "Matrix metalloproteinases." Br J Surg **84**(2): 160-166.

Paul, S., A. V. Sharma, et al. (2008). "Role of melatonin in regulating matrix metalloproteinase-9 via tissue inhibitors of metalloproteinase-1 during protection against endometriosis." J Pineal Res **44**(4): 439-449.

Pawlikowski, B., L. Lee, et al. (2009). "Analysis of human muscle stem cells reveals a differentiation-resistant progenitor cell population expressing Pax7 capable of self-renewal." Dev Dyn **238**(1): 138-149.

Payne, K. A., L. B. Meszaros, et al. (2010). "Effect of phosphatidyl inositol 3-kinase, extracellular signal-regulated kinases 1/2, and p38 mitogen-activated protein kinase inhibition on osteogenic differentiation of muscle-derived stem cells." Tissue Eng Part A **16**(12): 3647-3655.

Peault, B., M. Rudnicki, et al. (2007). "Stem and progenitor cells in skeletal muscle development, maintenance, and therapy." Mol Ther **15**(5): 867-877.

Peister, A., J. A. Mellad, et al. (2004). "Adult stem cells from bone marrow (MSCs) isolated from different strains of inbred mice vary in surface epitopes, rates of proliferation, and differentiation potential." Blood **103**(5): 1662-1668.

Pereira, A. M., M. Strasberg-Rieber, et al. (2005). "Invasion-associated MMP-2 and MMP-9 are up-regulated intracellularly in concert with apoptosis linked to melanoma cell detachment." Clin Exp Metastasis **22**(4): 285-295.

Pittenger, M. F., A. M. Mackay, et al. (1999). "Multilineage potential of adult human mesenchymal stem cells." Science **284**(5411): 143-147.

Prag, S., E. A. Lepekhin, et al. (2002). "NCAM regulates cell motility." J Cell Sci **115**(Pt 2): 283-292.

Qu-Petersen, Z., B. Deasy, et al. (2002). "Identification of a novel population of muscle stem cells in mice: potential for muscle regeneration." J Cell Biol **157**(5): 851-864.

Ra, H. J. and W. C. Parks (2007). "Control of matrix metalloproteinase catalytic activity." Matrix Biol **26**(8): 587-596.

Ritenour, A. E., R. J. Christy, et al. (2010). "The Effect of a Hypobaric, Hypoxic Environment on Acute Skeletal Muscle Edema after Ischemia-Reperfusion Injury in Rats." Journal of Surgical Research **160**(2): 253-259.

Romero-Ramos, M., P. Vourc'h, et al. (2002). "Neuronal differentiation of stem cells isolated from adult muscle." J Neurosci Res **69**(6): 894-907.

Rui, Y. F., P. P. Lui, et al. (2010). "Isolation and characterization of multipotent rat tendon-derived stem cells." Tissue Eng Part A **16**(5): 1549-1558.

Sato, K., Y. Li, et al. (2003). "Improvement of muscle healing through enhancement of muscle regeneration and prevention of fibrosis." Muscle Nerve **28**(3): 365-372.

Satoh, A., S. V. Bryant, et al. (2008). "Regulation of dermal fibroblast dedifferentiation and redifferentiation during wound healing and limb regeneration in the Axolotl." Dev Growth Differ **50**(9): 743-754.

Scott, M. A., V. T. Nguyen, et al. (2011). "Current Methods of Adipogenic Differentiation of Mesenchymal Stem Cells." Stem Cells Dev.

Seeberger, K. L., A. Eshpeter, et al. (2011). "Isolation and culture of human multipotent stromal cells from the pancreas." Methods Mol Biol **698**: 123-140.

Serrano, A. L. and P. Munoz-Canoves (2010). "Regulation and dysregulation of fibrosis in skeletal muscle." Exp Cell Res **316**(18): 3050-3058.

Shan, B., C. A. Morris, et al. (2007). "Activation of proMMP-2 and Src by HHV8 vGPCR in human pulmonary arterial endothelial cells." J Mol Cell Cardiol **42**(3): 517-525.

Sharifiaghdas, F., M. Taheri, et al. (2011). "Isolation of human adult stem cells from muscle biopsy for future treatment of urinary incontinence." Urol J **8**(1): 54-59.

Shen, W., Y. Li, et al. (2008). "Interaction between macrophages, TGF-beta1, and the COX-2 pathway during the inflammatory phase of skeletal muscle healing after injury." J Cell Physiol **214**(2): 405-412.

Shi, Y., C. Desponts, et al. (2008). "Induction of pluripotent stem cells from mouse embryonic fibroblasts by Oct4 and Klf4 with small-molecule compounds." Cell Stem Cell **3**(5): 568-574.

Sicinski, P., Y. Geng, et al. (1989). "The molecular basis of muscular dystrophy in the mdx mouse: a point mutation." Science **244**(4912): 1578-1580.

Smaldone, M. C. and M. B. Chancellor (2008). "Muscle derived stem cell therapy for stress urinary incontinence." World J Urol **26**(4): 327-332.

Somerville, R. P., S. A. Oblander, et al. (2003). "Matrix metalloproteinases: old dogs with new tricks." Genome Biol **4**(6): 216.

Stadtfeld, M., M. Nagaya, et al. (2008). "Induced pluripotent stem cells generated without viral integration." Science **322**(5903): 945-949.

Stetler-Stevenson, W. G. (2008). "Tissue inhibitors of metalloproteinases in cell signaling: metalloproteinase-independent biological activities." Sci Signal **1**(27): re6.

Stevenson, T. J., V. Vinarsky, et al. (2006). "Tissue inhibitor of metalloproteinase 1 regulates matrix metalloproteinase activity during newt limb regeneration." Dev Dyn **235**(3): 606-616.

Stojkovic, M., M. Lako, et al. (2004). "Derivation of human embryonic stem cells from day-8 blastocysts recovered after three-step in vitro culture." Stem Cells **22**(5): 790-797.

Sung, L. Y., S. Gao, et al. (2006). "Differentiated cells are more efficient than adult stem cells for cloning by somatic cell nuclear transfer." Nat Genet **38**(11): 1323-1328.

Takahashi, K., K. Tanabe, et al. (2007). "Induction of pluripotent stem cells from adult human fibroblasts by defined factors." Cell **131**(5): 861-872.

Takahashi, K. and S. Yamanaka (2006). "Induction of pluripotent stem cells from mouse embryonic and adult fibroblast cultures by defined factors." Cell **126**(4): 663-676.

Ten Broek, R. W., S. Grefte, et al. (2010). "Regulatory factors and cell populations involved in skeletal muscle regeneration." J Cell Physiol **224**(1): 7-16.

Thomson, J. A., J. Itskovitz-Eldor, et al. (1998). "Embryonic stem cell lines derived from human blastocysts." Science **282**(5391): 1145-1147.

Urish, K. L., J. B. Vella, et al. (2009). "Antioxidant levels represent a major determinant in the regenerative capacity of muscle stem cells." Mol Biol Cell **20**(1): 509-520.

Vidal, P. and M. G. Dickson (1993). "Regeneration of the distal phalanx. A case report." J Hand Surg [Br] **18**(2): 230-233.

Vinarsky, V., D. L. Atkinson, et al. (2005). "Normal newt limb regeneration requires matrix metalloproteinase function." Dev Biol **279**(1): 86-98.

Visse, R. and H. Nagase (2003). "Matrix metalloproteinases and tissue inhibitors of metalloproteinases: structure, function, and biochemistry." Circ Res **92**(8): 827-839.

Vu, T. D., F. Yun, et al. (2008). "Placental matrix metalloproteinase--1 expression is increased in labor." Reprod Sci **15**(4): 420-424.

Wang, W., H. Pan, et al. (2009). "Matrix metalloproteinase-1 promotes muscle cell migration and differentiation." Am J Pathol **174**(2): 541-549.

Wilby, M. J., E. M. Muir, et al. (1999). "N-Cadherin inhibits Schwann cell migration on astrocytes." Mol Cell Neurosci **14**(1): 66-84.

Wright, V., H. Peng, et al. (2002). "BMP4-expressing muscle-derived stem cells differentiate into osteogenic lineage and improve bone healing in immunocompetent mice." Mol Ther **6**(2): 169-178.

Wu, X., S. E. Wolf, et al. (2010). "Muscle contractile properties in severely burned rats." Burns **36**(6): 905-911.

Yamada, M., R. Tatsumi, et al. (2006). "Matrix metalloproteinases are involved in mechanical stretch-induced activation of skeletal muscle satellite cells." Muscle Nerve **34**(3): 313-319.

Yang, E. V., D. M. Gardiner, et al. (1999). "Expression of Mmp-9 and related matrix metalloproteinase genes during axolotl limb regeneration." Dev Dyn **216**(1): 2-9.

Yang, P., Z. Liu, et al. (2009). "Enhanced activity of very low density lipoprotein receptor II promotes SGC7901 cell proliferation and migration." Life Sci **84**(13-14): 402-408.

Yazawa, M., B. Hsueh, et al. (2011). "Using induced pluripotent stem cells to investigate cardiac phenotypes in Timothy syndrome." Nature **471**(7337): 230-234.

Yokoyama, H. (2008). "Initiation of limb regeneration: the critical steps for regenerative capacity." Dev Growth Differ **50**(1): 13-22.

Yu, F., H. Kamada, et al. (2008). "Induction of mmp-9 expression and endothelial injury by oxidative stress after spinal cord injury." J Neurotrauma **25**(3): 184-195.

Yu, J., M. A. Vodyanik, et al. (2007). "Induced pluripotent stem cell lines derived from human somatic cells." Science **318**(5858): 1917-1920.

Zammit, P. S., F. Relaix, et al. (2006). "Pax7 and myogenic progression in skeletal muscle satellite cells." J Cell Sci **119**(Pt 9): 1824-1832.

Zeng, Z. Z., H. Yao, et al. (2009). "alpha(5)beta(1) Integrin Ligand PHSRN Induces Invasion and alpha(5) mRNA in Endothelial Cells to Stimulate Angiogenesis." Transl Oncol **2**(1): 8-20.

Zheng, B., B. Cao, et al. (2006). "Mouse adipose-derived stem cells undergo multilineage differentiation in vitro but primarily osteogenic and chondrogenic differentiation in vivo." Tissue Eng **12**(7): 1891-1901.

Zimowska, M., E. Brzoska, et al. (2008). "Distinct patterns of MMP-9 and MMP-2 activity in slow and fast twitch skeletal muscle regeneration in vivo." Int J Dev Biol **52**(2-3): 307-314.

Zuk, P. A., M. Zhu, et al. (2002). "Human adipose tissue is a source of multipotent stem cells." Mol Biol Cell **13**(12): 4279-4295.